Hydrological Snowmelt Modelling in Snow Covered River Basins By Means of Geographic Information System and Remote Sensing

Case Study -- Latyan Catchment in Iran

Dissertation

zur Erlangung des akademischen Grades doctor rerum naturalium
(Dr. rer.nat.)

vorgelegt dem Rat der Chemisch-Geowissenschaftlichen Fakultät der
Friedrich-Schiller-Universität Jena

von Master-Geographer Houshang Behrawan
geboren am 20. März 1972 in Mahabad, Iran

1. Gutachter: Prof. Dr. rer. nat. Wolfgang-Albert Flügel, Jena

2. Gutachter: Univ. Prof. Dr. rer. nat. Volker Hochschild, Tübingen

Tag der öffentlichen Verteidigung: 08.07.2010

To my dears, Snoor and Chawan and to those who are always in my mind.

Contents

Acknowledgment

At this point, I want to take the chance to thank all those people who have directly or indirectly contributed to the successful fulfilment of this work. Without the support, guidance and patience of the following people this work would not have been possible.

First of all, I would like to express my deepest gratefulness to my supervisor and doctor father Prof. Dr. Wolfgang-Albert Flügel who gave me the opportunity to write this dissertation in Jena and for his guidance, support and advice over the last years. Again thank you so much in advance for all. I am also grateful to Prof. Dr. Volker Hochschild who supported this work. The discussions with him lead to the ideas that are presented in this work.

My cordial thanks go to Dr. Peter Krause, which every time his office was open for my solving problems and discussions with him helped me a lot to work through the technical as well as some challenging argumentative problems with my study. His constructive criticism helped me to focus my ideas and to describe them more clearly. I am also thankful to him for reading the some part of thesis draft within a short time period.

I appreciate the support of the Ministry of Science, Research and Technology of Iran and Ministry of Agriculture of Iran, without whose support I could not have done my PhD in Germany.

I am very grateful to all my colleagues of the Department for Geoinformatics, Hydrology and Modelling, especially, Dr. Manfred Fink, Dr. Sven Kralisch, Dr. Jörg Helmschrot, Björn Pfennig, Markus Wolf, Markus Reinhold, Christian Fischer, Franziska Zander, Christian Schwartze, Marcel Wetzel, Daniel Varga, Frank Bäse, Hannes Müller Schmied who have given their time to discuss pieces of my work with me and who have also offered valuable advice. Special thanks also go to Rainer Hoffmann, the system administrator, who helped with any occurring technical problem.

I am grateful to my friends and colleagues, Markus Reinhold, Dr. Shamsuddin Shahid, Dr. Timothy Steele and Amanpreet Singh for proofreading and their constructive comments to improve this dissertation.

Thanks to all agencies and institutes providing data and various support for this study: to the AREEO staffs, in particular, Prof. Dr. Ali Ahoonmanesh, Dr. Bahram Saghafian, Dr. Kazemi, Mr. Akbarpour, to the Iran Water Resource Management Company (IWRMCO), in particular to Mr. Babaee, to the Iranian Revenue Operation of Dams, in particular Mr. Engineer

LISTS OF FIGURES

LISTS OF TABLES

ABBREVIATIONS

ABBREVIATION	DESCRIPTION
AC	Air Capacity
AET	Actual Evapotranspiration
Alb	Albedo
ASA	Aggregated Simulation Area
AVE	Absolute Volume Error
AVG	Average
D	Depth
DHI	Danish Hydraulic Institute
E	East
FAO	Food and Agriculture Organization of the United Nations
FCA	Field Capacity Adaption
GCM	General Circulation Model
GIS	Geographical Information System
GSI	Geological Survey Organization Iran
HRU	Hyrological Response Units
HBV	Hydrologiska Byråns Vattenbalansavdelning model
HEC-1	Hydrologic Engineering Center
HSPF	Hydrological Simulation Program - FORTRAN
ICSI	International Commission on Snow and Ice
IDW	Inverse Distance Weighting
IPCC	Intergovernmental Panel on Climate Change
ISRIC	International Soil Reference and Information Centre
IWRMCO	Iran Water Resource Management Company
JAMS	Jena Adaptable Modeling System
LAI	Leaf Area Index
LAT	Latitude
Log.NSE	Logarithmic Nash-Sutcliffe Efficiency
LON	Longitude
LSS	Land cover Soil Sets

MAP	Mean Annual Precipitation
MAR	Mean Annual Runoff
MASL	Meter Above See Level
MCM	Million Cubic Meter
MMS	Modular Modeling System
N	North
NCC	National Cartographic Center
NSE	Nash Sutclif
OBS	Observation
P	Precipitation
PBIAS	relative percentage volume error
PET	Potential Evapotranspiration
PRMS	Precipitation-Runoff Modeling System
Q	Discharge
R²	coefficient of determination
Rd	Roothing Depth
Rhum	Relative Humidity
RS	Remote Sensing
RU	Response Unit
S	South
SC	Soil Class
SIM	Simulation
SLURP	Semi-distributed Land Use-based Runoff Processes
SMHI	Swedish Meteorological and Hydrological Institute
SRTM	Shuttle Radar Topography Mission
SRM	Snow Runoff Model
STDEVP	Standard Deviation Population
SUN	Sunshine duration
SVAT	Soil-Vegetation-Atmosphere-Transfer
SWE	Snow Water Equivalent
SWRI	Soil Water Research Institute
TIN	triangulated irregular network

TS	Topography Sets
TWRCO	Tehran Water Regional Company
USGS	US Geological Survey
UTM	Universal Transverse Mercator
VSC	Vegetation Soil Complex
W	West
WASIM	Water balance Simulation Model
WEI	Water and Energy Institute
WMO	World Meteorological Organization
WRB	World Reference Base for Soil Resources
WSIMO	Weather Service Iran Meteorological Organization

Abstract

In mountainous watersheds snow melt can have a significant impact on the water balance and at certain times of the year it could be the most important contribution to runoff. In many parts of the world snow act as natural reservoirs that can play an important role for water supply. Alas, despite its importance, many of snow driven basins suffer from a lack of hydrological infrastructure and equipment so they cannot be described adequately in terms of snow hydrological dynamics. Because of limited accessibility are the few observation stations in such areas very rarely located in the higher elevations but are concentrated mostly in the middle and low elevation resulting in an underrepresentation in data availability of the high altitudes which are important for the process dynamics. Thus the modelling of snow hydrological dynamics in mountainous regions such as the Latyan catchment is often difficult. Reasons for this are in addition to the aforementioned data availability, topographic effects and gradients that can make a spatial interpolation of the input data and the model states a complicated task.

Especially in semi-arid regions, high-altitude headwater basins with a significant snow component have a large potential by balancing and distributing scarce water resources. Particular here, a quantitative assessment of the spatial distribution of snow cover and snow processes are an important basis for a sound water management and for the hydrological forecasting and risk prevention. Therefore, the water management in such regions could benefit from reliable predictions of the hydrological dynamics derived from model based studies. Suitable models should represent the physical basis and hydrological processes that simulate the system's response, fairly well.

In this study the spatially distributed process-oriented hydrological model J2000g was used for the 700 km² large Latyan catchment in Iran. The target was to derive spatially distributed estimates of the quantity and timing of hydrological balance terms and state variables like rainfall, actual evapotranspiration (AET), runoff, snow water equivalent (SWE) and snow melt. The model uses the distribution concept of Hydrological Response Units (HRU) to take the spatial variability in the basin into account. The model simulates for each HRU and each time step snow accumulation and snow melt, soil water content, the actual evapotranspiration, groundwater recharge and runoff generation distributed into two components – direct runoff and ground water runoff. The fact that J2000g cannot account for anthropogenetic influences

and natural water losses as they occur in karsts regions made the selection of suitable sub-basin for model calibration a difficult task. However, three sub-basins Roodak, Najarkola and Naran could be identified which underground is characterized mainly by impervious bed rock and which have only minimal anthropogenic influences. The sizes of the three sub-basins are between 31 to 430 km². For each of these sub-basins, the model parameters were calibrated automatically by means of Monte-Carlo analysis and the Shuffled Complex Evolution (SCE-UA) calibration procedure. The calibration was done by the comparison with measured runoff values for the period from October 1990 to September 2001 in monthly time steps using the Nash-Sutcliffe efficiency as the objective function. In addition, for each sub-basin the spatial distribution of rainfall, runoff, actual evapotranspiration, snow melt and snow water equivalent was analysed and compared with corresponding measurements.

The snow module of the J2000g model was developed and checked against measured values of nine snow observation stations, which were located within the test basins. For each of the observation stations the corresponding HRUs were extracted and separate models calibrated were calibrated using the measured SWE. The model quality was quantified by using the Nash-Sutcliffe efficiency (NSE) and the coefficient of determination (r²) as objective functions. The comparison with the calibrated catchment models showed that accumulation and melting of the snowpack could be simulated reasonably well at all stations but the results were less good than those of the separately calibrated catchment models.

The comparison of the separate SWE models resulted in values between 0.28 - 0.68 for NSE and values between 0.53 - 0.83 for r². For the catchment models the comparison of the simulated runoff with measured data showed NSE values between 0.78 and 0.82. By these values it can be stated that the hydrological dynamics and the snow processes of the three sub-basins within the Latyan catchment could be simulated sufficiently well with J2000g. Finally, a "global" parameter set for whole the Latyan catchment was generated by an area-weighted mean of the parameters from the calibrated sub-basin models. With this parameter set Nash-Sutcliffe efficiencies between 0.68 and 0.79 could be obtained for Latyan.

It can be summarized that the single modules and in particular the snow components of J2000g along with the HRU distribution approach can be considered as suitable for the given project objectives i.e. the assessment of the hydrological dynamics of the Latyan catchment.

Hereby, the model can be used to elaborate important hydrological information for a sustainable management of the water resources.

Kurzfassung

In gebirgigen Einzugsgebieten kann die Schneeschmelze einen entscheidenden Einfluss auf die Wasserbilanz haben und zu gewissen Zeiten im Jahr der wichtigste Beitrag zur Abflussbildung sein. In vielen Teilen der Welt stellen Schneedecken natürliche Speicher dar, die eine wichtige Rolle für die Wasserversorgung einnehmen können. Trotz ihrer großen Bedeutung leiden aber viele dieser schneebeeinflussten Einzugsgebiete an einer mangelhaften hydrologischen Infrastruktur und Ausstattung wodurch sie hinsichtlich der schneehydrologischen Dynamik nur unzureichend beschrieben werden können. Aus Gründen der Erreichbarkeit sind die wenigen Beobachtungsstationen in solchen Gebieten nur sehr selten in den höheren Lagen lokalisiert sondern meist in den mittleren und geriengeren Höhen konzentriert wodurch die für die Dynamik wichtigen Hochlagen hinsichtlich der Datenverfügbarkeit unterrepräsentiert sind. Hierdurch ist die Modellierung der schneehydrologischen Dynamik in gebirgigen Regionen wie dem Latyan Einzugsgebiet oft schwierig. Gründe hierfür sind neben der bereits angesprochenen Datenverfügbarkeit auch topographische Effekte und Gradienten, die eine räumliche Interpolation der Eingangsdaten und der Modellzustände deutlich erschweren können.

Besonders in semi-ariden Regionen besitzen hoch gelegene Quelleinzugsgebiete mit einer deutlich ausgeprägten Schneekomponente aufgrund ihres Potentials, als Ausgleich und Verteiler von knappen Wasserressourcen zu wirken, eine große Bedeutung. Hier ist aber ganz besonders eine quantitative Erfassung der räumlichen Ausprägung von Schneedecken und der Schneeprozesse eine wichtige Grundlage für ein fundiertes Wassermanagement und für die hydrologische Vorhersage und die Risikovorbeugung von großer Bedeutung. Insbesondere das Wassermanagement könnte von einer verlässlichen Vorhersage der hydrologischen Dynamik basierend auf Modellstudien in solchen Gebieten deutlich profitieren. Hierzu werden Modelle benötigt, die die physikalischen Grundlagen und die hydrologischen Prozesse, die die Gebietsantwort kontrollieren, hinreichend genau abbilden können.

In dieser Studie wurde das räumlich distributive, prozessorientierte hydrologische Modell J2000g für das ca. 700 km² große Latyan Einzugsgebiet im Iran angewendet. Das Ziel war eine räumlich verteilte Abschätzungen bezüglich der Menge und der zeitlichen Verteilung der hydrologischen Bilanzglieder und Zustandsgrößen Niederschlag, aktuelle Verdunstung (AET), Abflussbildung, Schneewasseräquivalent (SWÄ) und Schneeschmelze zu liefern. Das Modell nutzt das Distributionskonzept der Hydrological Response Units (HRU) um die

räumliche Variabilität im Einzugsgebiet zu berücksichtigen. Das Modell berechnet für jede HRU und jeden Zeitschritt die Schneeakkumulation und Schneeschmelze, den Bodenwassergehalt, die aktuelle Verdunstung, die Grundwasserneubildung und die Abflussbildung in zwei Komponenten – Direktabfluss und Grundwasserabfluss. Die Tatsache, dass J2000g keine anthropogenen Einflüsse und auch natürliche Wasserverluste, wie sie z.B. in Karstregionen auftreten können, berücksichtigt, erschwerte die Auswahl an Teileinzugsgebieten für die Modellkalibrierung. Dennoch konnten drei Teileinzugsgebiete Roodak, Najarkola und Naran identifiziert werden deren Untergrund weitestgehend durch undurchlässige Gesteine geprägt sind und die nur minimale anthropogene Einflüsse aufweisen. Die Größen der drei Gebiete liegen zwischen 31 und 430 km². Für jedes dieser Gebiete wurden die Modellparameter automatisch mit Hilfe der Monte-Carlo-Analyse und dem Shuffled-Complex-Evolution (SCE-UA) Verfahren kalibriert. Die Kalibrierung erfolgte anhand gemessener monatlicher Werte für die Periode von Oktober 1990 bis September 2001 wobei die Nash-Sutcliffe Effizienz als Gütekriterium eingesetzt wurde. Zusätzlich wurde für jedes Einzugsgebiet die räumliche Verteilung von Niederschlag, Abfluss, aktueller Verdunstung, Schneeschmelze und Schneewasseräquivalent analysiert und mit entsprechenden Messwerten verglichen.

Die Schneewasseräquivalentmodellierung wurde mit Messwerten von neun Schneebeobachtungsstationen, die innerhalb der Testeinzugsgebiete lagen überprüft. Hierzu wurden diejenigen HRU, die der Lokalisierung der Beobachtungsstationen entsprachen, extrahiert und separate Modelle für diese HRU anhand der SWÄ Messwerte kalibriert. Die Modellqualität wurde mit der Nash-Sutcliffe Effizienz (NSE) und dem Bestimmtheitsmaß (r²) quantifiziert. Der Vergleich mit den kalibrierten Einzugsgebietsmodellen zeigte, dass diese den Schneedeckenauf- und –abbau an den Vergleichsstationen hinreichend gut simulieren können, dass sie aber schlechtere Ergebnisse als die separat kalibrierten Modelle ergaben.

Der Vergleich der separaten Modelle ergab Werte zwischen 0.28 – 0.68 für NSE und Werte zwischen 0.53 – 0.83 für r². Für die Einzugsgebietsmodelle und dem Vergleich des simulierten Abfluss mit Messwerten ergab NSE Werte zwischen 0.78 und 0.82. Hierdurch konnte belegt werden, dass die hydrologische Dynamik und auch die Schneeprozesse in den Latyan Teileinzugsgebiet mit J2000g hinreichend gut wiedergegeben werden können. Schließlich wurde mit Hilfe einer flächenbasierten Gewichtung aus den Parametern der kalibrierten Teileinzugsgebiete ein „globaler" Parametersatz für das gesamte Latyan

Einzugsgebiet erzeugt. Mit diesem Parametersatz wurden Nash-Sutcliffe Effizienzen zwischen 0.68 und 0.79 für das Latyan Einzugsgebiet erzielt.

Es kann zusammenfassend festgestellt werden, dass die einzelnen Module und insbesondere die Schneekomponenten des J2000g sowie das HRU Konzept für die erzielte Fragestellung der Erfassung der hydrologischen Dynamik des Latyan Einzugsgebiet als sehr gut geeignet betrachtet werden können. Hierdurch können mit dem Modell wichtige hydrologische Grundlagen für eine nachhaltige Bewirtschaftung der Wasserressourcen erarbeitet werden.

1.   Introduction

Iran receives a total precipitation of about 416 billion cubic-meter, of which 140 billion can be recycled. So far 82 billion cubic-meter of total precipitation water has been made usable in Iran. However, even if the figure reaches to 162 billion, it would not suffice the burgeoning population of the country (http://www.shanatelex.ir/archive-2003_09_26-en.html). Per capita water index of Iran has decreased by fivefold during past six decades. In addition, unsuitable distribution of rainfall and social tensions incur heavy costs on the country. At present, in some parts of the country the water is being transferred from a distance of about 30 km. Water supply situation of Tehran much more severe compared to many other parts of the country. Average precipitation of Tehran region is about 25 percent lower than other parts of the country, while it hosts about 30 percent of the country's population. At the same time, per capita water consumption in Tehran region is 800 cubic-meters which comprise 38% of the country's total. The global index has set water crisis threshold at 1,000 cubic-meters, with absolute crisis limit standing at 500 cubic-meters (SHANATELEX, 2003). Therefore, Tehran is rapidly approaching the crisis threshold. At present, due to excessive uptake from ground waters and a two-year drought, the volume of ground waters is decreasing at the annual rate of about 1.3 billion cubic-meter (SHANATELEX, 2003). On the other, Tehran is suffering from burgeoning population, immigration and excessive constructions. Therefore, comprehensive plan is essential for sustainable supply of water to Tehran.

At present, about 70% of Tehran water comes from surface waters, while 30% is from ground waters. Surface waters are supplied from Latyan, Karaj and Lar dams while ground waters come from wells dug at various places (SHANATELEX, 2003). The inputs from Latyan, Karaj and Lar dams are estimated as 95, 205, and 960 million cubic meters (MCM), respectively (JAHANI AND REYHANI, 2006). Accoring the Urban Development Council of Iran, the population of Tehran will reach about 15.1 million in the most optimistic state and 15.8 percent in the most pessimistic state. On this basis, three scenarios can be considered, that is, wet years, normal years and dry years. If we consider the average to be normal years - which is true in 50 percent of cases - water requirements of Tehran would stand at about 1,233 MCM by 2021, which would be supplied from the following sources: 186 MCM from Lar Dam; 135 million cubic-meter from Latyan Dam; 137 MCM from Taleqan Dam; 240 million cubic-meter from Karaj Dam and 233 MCM from ground waters, which totals 931 MCM. It is about 302 MCM less than of the forecasting for normal years and would have to

reduce agricultural water supply in favour of drinking water (SHANATELEX, 2003). Scarcity of water is a common problem especially in the urban areas of Iran because of the dry conditions, which prevail in most of the country. There is a need for continuous drinking, household and industrial water supply in the large cities for economic development and urban livelihood. In addition, there can be a flooding problem in some years due to huge precipitation. Because of these needs, it is important to manage the water resources, which require an understanding of the hydrological processes in the catchments. This knowledge is also required for hydrologic modelling and for transposing data from gauged catchments to ungauged ones. Traditionally hydrological studies in Iran have been made from an engineering point of view, whereby no or little attempt was made to relate the discharges to the catchment characteristics (KARAMOUZ ET AL., 2001; ZARGHAAMI AND SALAVITABAR, 2006; ZEINIVAND AND DE SMEDT, 2008).
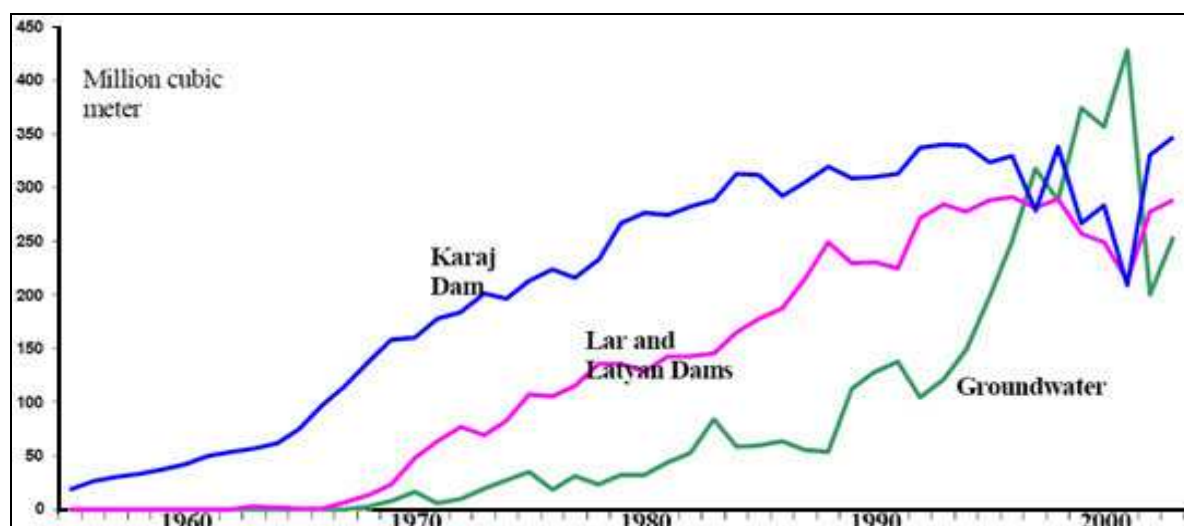
Figure 1.1: Increasing pattern of water extraction from various catchments including the Latyan for water supply to the Tehran (Source: Zargaami and Salavitabar, 2006:P.5)

Snow accumulation and melt is an important hydrological process for the hydrological dynamics of catchments at higher altitudes. Snowmelt is a vital source of water in many parts of the world for public supply, hydropower, irrigated agriculture and other uses and may significantly contribute to river floods (FERGUSON, 1999; SINGH AND SINGH, 2001; PARAJKA ET AL., 2001). At the same time the seasonal snow cover affects also biotic components and water quality in river basins. Distributed modelling of snow accumulation and snowmelt is therefore an important issue. Recent advances in geographical information

system (GIS) and remote sensing (RS) technology allow powerful integration of GIS and RS analytical and visualization tools with physically based hydrological models. In the field of snowmelt modelling, such integration provides a valuable basis for better understanding of snow accumulation and snowmelt runoff processes within the catchment, as well as for incorporating the spatial variability of hydrological and geographical variables and their impacts on catchment response (FERGUSON, 1999; PARAJKA ET AL., 2001). Application and studies in terms of snow modelling by means of GIS and RS for Iranian catchments are only sparsely available (MORID, 2004).

1.1 OBJECTIVE

One common problem that scientists encounter in developing countries is the lack of informative data for the related study. Even if the data exist, quick on-line and timely access to the data may be problematic and in particular the quick access to snow data, which is a must be in operational snow melt forecasting, is not possible yet. Ground based snow measurements are mostly gathered in form of snow courses by governmental organisations mostly in 2-3 week periods. In such snow courses, snow water equivalent and snow depths are measured along defined track. Most of the courses are started mainly in November or December and they are abandoned by mid or end of March, when the snow ripens and starts to melt, even if a reasonable amount of snow may still remain in upper mountainous areas. For an assessment of the impact of snow processes on Iranian catchments, by the analysis of snow pack development and the estimation of snowmelt, snow cover data as well as hydro-meteorological parameters in the higher altitudes of the watersheds are needed. Unfortunately such parameters are not available in the higher altitudes because precipitation and temperature data are generally measured in the lower or moderate altitudes of the catchments only. Because of this lack of data only very few studies using models are available for the area of interest. The number of snowmelt models which was applied in various catchments in the Iran is limited to the snow runoff model (SRM) which was used in the very rare simulation of snowmelt runoff in Iranian mountainous catchments. To overcome that lack of data and to enforce modelling activities in such data remote areas globally available data sets from regionalization, using Hydrological Response Units approach as well as RS availability like Shuttle Radar Topography Mission SRTM for Digital Elevation Model (DEM) could be available. To make most out use such data it should be used as drivers for hydrological models to allow a simulation of the complex processes and hereby a quantification of the hydrological dynamics.

Therefore, the main objective of the present study is Develop better understanding of hydrological process interaction in Iranian catchments by means of GIS and process-oriented modelling

The detail objectives of the research are:

- Providing scientific basis for sustainable water resource management in the Latyan catchment

  - To analyze the hydro-meteorological data in terms of areal extent, frequencies and intensities

  - Delineation of Hydrological Response Units (HRUs) using GIS and RS

- Improvement of the understanding of snow driven hydrological dynamics in the Latyan catchment

  - Spatial distributed hydrological modelling of snow driven catchments using J2000g

## 2.	Research Review

Snow is an important component of the hydrological cycle. A reasonable snowmelt estimate is essential for the regional planning of water resources. To achieve this objective, data such as the snow cover, snow depth, and water equivalent are necessary. Snow cover is an important index for predicting the spring melt, and it is interpreted better than the other snow parameters. Snowpack are the drinking water source for many communities. Snowpack are also studied in relation to climate change and global warming. Snowpack modelling is done for flood forecasting, water resource management, and climate studies.

In hydrology, snowmelt is surface runoff produced from melting snow. It can also be used to describe the period or season during which such runoff is produced. Water produced by snowmelt is an important part of the annual water cycle in many parts of the world and in some cases contributing high fractions of the annual runoff in a watershed. Predicting snowmelt runoff from a drainage basin can be a part of designing water control projects. Recent development in snow hydrology has continued to emphasize the temporal and spatial variability in snow sublimation and melt and, therefore, the spatial heterogeneity in surface energy fluxes. There is also a rising interest in modelling snow hydrology and snow ecology (WOO and MARSH, 2005).

2.1 Snow in the hydrological cycle

The global water cycle is the process by which our freshwater is produced and as illustrated in figures 2-1 and 2-2, snow has a big role in this process as a vital source of produce freshwater. Only 1.74 % of the world total water storages which accounts for 68.7 % of the fresh water reserves (SEIDEL AND MARTINEC, 2004:P. 5) are stored as snowpack. Snow plays a vital role in distributing the natural water resource.
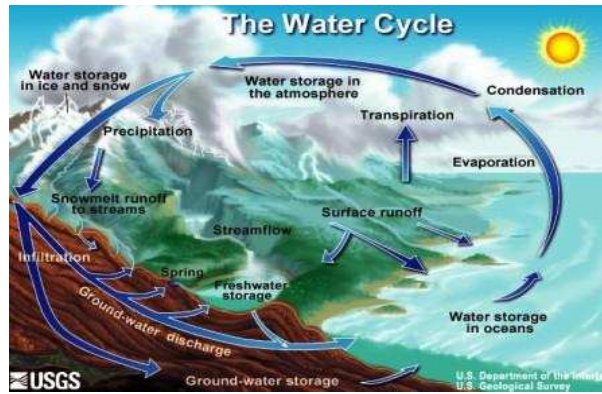
Figure2-1:The Global Water Cycle,(Source:http://ga.water.usgs.gov/edu/watercyclegraphichi)
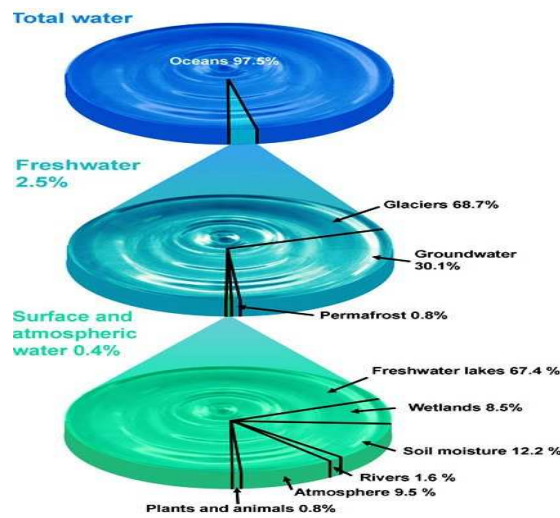
Figure 2-2: The Global freshwater and role of snow (Source: UNESCO, UN-WATER WWAP, (2006:p.121)

One of the most obvious and direct consequences on the hydrological cycle is snow accumulation and snowmelt runoff. The timing and magnitude of snowmelt derived runoff events are important for several reasons: (1) in the earth climate system, via energy exchange among the surface snow and the atmosphere for example albedo and latent heat (ARMSTRONG AND BRUN, 2008) as well as is considered as sensitive indicator of climate change and controlling monsoon activity(SINGH AND SINGH, 2001); (2) in high and middle latitude areas, snowmelt constitutes a major source of river runoff and groundwater recharge (EDWARDS ET AL., 2007); (3) in water resources management, for flood control, drought mitigation and water supply; (4) in regional planning like energy and agriculture, tourism, and sport development (SINGH AND SINGH, 2001);; and (5) in ecology, snowpack impact of animal habitats and plant succession (SANTEFORD, 1974).

An understanding of snow characteristics, physical, optical and thermal is important to hydrological-snow modelling and also in many practical applications of snowpacks. From viewpoint of hydrological modelling, physical characteristics of snow are between the most significant properties, and hence, are reviewed here (SINGH and SINGH, 2001).

2.1.1   Defintion of Snow

"Snow is a mixture of ice water and air; and forms from crystallization of ice molecules in the atmosphere during precipitation. When they are in the atmosphere, snow crystals grow and can take on a large size, although smaller sizes are more common. Snow is a very porous medium. Sometimes snowpacks also contain liquid water" (SINGH and SINGH: P.104, 2001).

The snow texture represents the shape, size and bond structure of snow grains. By visual examination, snow can be classified as crystalline, powdery, granular, pellet and mixtures. As per grain size, it can be classified as fine medium and coarse, whereas per moisture content it may be classified as dry, damp or wet. The primary distinction among various snow covers can be made on the basis of the physical characteristics. The special gravity of snow can vary from 0.05 to 0.85, but normally it is confined between 0.1 and 0.6. Long slender forms are more fragile than compact forms. (SINGH and SINGH, 2001)

2.1.2   Snow density

Density, defined as the mass per unit volume, is the fundamental parameter of snow (SINGH and SINGH, 2001). The snow density, ρs, describes the compaction of a snow cover and can be considered as the relationship of air-filled pores to the total volume of a snow package or as the ratio of mass of a snow sample and its volume (in g/cm³ or kg/m³) (BAUMGARTNER AND LIEBSCHER 1996; MANIAK 1993). Neglecting the proportion of air pores in the snow body, the snow density for hydrologic applications, can also be expressed as the ratio of the total water equivalent of snow to the snow depth.

The density of snow increases with its age. This process can be accelerated by strong winds, warm temperature and intermittent melting of snow cover. According to Martinec (1977), time appears to be a dominant factor so that it is possible to derive a simple relationship between density of new snow and snow density after n days (SINGH and SINGH, 2001).

$$\rho n = \rho 0 \, (n + 1)^{0.3} \qquad\qquad \text{Equation 2-1}$$

Where, $\rho 0$ is the average density of new snow (0.1 gm/cc) and ρn is the snow density after n days. Or,

$$\rho s = HS / HWE \, [cm] \qquad\qquad \text{Equation 2-2}$$

Where, ρs is the snow density, HS is the Height snow and HWE is height or snow water equivalent.

When the deposition of snow crystals begins their transformation, dynamic process of compaction and metamorphism of the snow takes place (RANGO ET AL., 1996a/b). Accordingly, in many studies and model approaches, the initial density of snowfall dynamically modified by the density of snow during the snow period differed (BRAUN 1985; VEHVILÄINEN 1992; GRAY AND PROWSE 1993; RANGO AND MARTINEC 1995; BAUMGARTNER AND LIEBSCHER 1996).

The initials snow density e.g. depends on a number of climatic factors during the deposit such as air temperature, humidity or wind speed. So, it can be assumed that wet snow deposits, which developed at temperatures around the freezing point, are set higher snow densities than cold dry deposits (COLBECK ET AL., 1990). KUCHMENT et al. (1983) derived initial snow density as a function of air temperature. He found an exponential relationship between the increase of temperature and snow density. Due to the high variability and complexity of the factors of influence in some snow-hydrological modelling approaches, the initials snow density is accepted an average value of 0.1 g/cm³ for simplification (MARTINEC AND RANGO, 1991).

In the further process of the snowpack formation, strong compaction processes that are complex meteorological, seasonal and local contexts can be determined (BRAUN 1985; ROHRER 1992; NAKAWO AND HAYAKAWA 1998). DINGMAN (1994) reported a strong relationship between snow compaction and wind. On the other hand, BRAUN (1985) found no clear causal relationship between the snow density and individual factors such as elevation or snow depth.

On the basis of the wide range of variation for observed snow density values between deposit and ablation, a high variability of snow density has been described in the literature. BRAUN (1985) found a variation ranges from 0.1-0.4 g/cm³ for 50 cm snow cover. MANIAK (1993)

indicated a density of 0.05-0.13 g/cm ³ for new powder snow. For granular powder snow (0.25 g/cm³) and granular snow (0.33-0.4 g/cm³), he found an increase in snow density (0.5-0.6 g/cm³). Furthermore, BAUMGARTNER AND LIEBSCHER (1996) found that new snow which depends upon humidity and packing condition, can exhibit densities between 0.01 and 0.2 g/cm ³. They identified first depletion product of new snow as snowfall with densities between 0.15 and 0.25 g/cm³. With the passage of time, ongoing transformation of snow structure by grain melting or regulation processes leads to the development of old snow, which exhibits densities up to 0.6 g/cm³. DUNN AND COLOHAN (1999) quoted various empirical investigations. According to him, the density of fresh snow already lies between 0.05 and 0.3 g/cm³. In case of a gradual compaction, it lies between 0.3 and 0.7 g/cm³for older snow deposits.

2.1.3 Snow depth

The snow depth or snow cover thickness means the vertical height of a snow cover (BAUMGARTNER AND LIEBSCHER 1996). It is recorded also in standard measuring programs regularly in cm (International Commission on Snow and Ice (ICSI)-classification, NAKAWO/HAYAKAWA 1998). Snow depth is considered as snow-hydrologic size, which varies like the other physical characteristics and can be detected easily in dependence of different climatic, topographic and vegetative factors which influence strongly in space and time. Generally, snow precipitation ensures for an increase, and evaporation and melts causes a dynamic reduction of the snow height during compaction processes. The snow depth, HS, must be understood as secondary size and can be determined by the relationship of snow water equivalent (HWE) and snow density (ρs) (DINGMAN, 1994; BAUMGARTNER AND LIEBSCHER, 1996):

$$HS = \rho s \ / \ HWE \ [cm] \qquad\qquad \text{Equation 2-3}$$

2.2   Snow water equivalent (SWE)

The snow water equivalent, SWE, is considered to be the most important hydrological snow-related variable. It is defined as the snow cover both in solid and liquid form, containing a

certain quantity of water, measured in mm, L/m² or kg/m². Alternatively, SWE is defined as the vertical depth of water which is obtained by the melting of snow (WOHLRAB ET AL., 1992; BAUMGARTNER AND LIEBSCHER, 1996; SINGH and SINGH, 2001).

According to Singh and Singh (2001) the water equivalent of a snow cover, HSW, of thickness D is given by:

$$HSW = \sum_{i=1}^{n} d_i \rho_i = \bar{\rho} D$$

Equation 2-4

Where the snow cover of thickness D has been divided in to n homogeneous thicknesses d1, d2… dn having densities ρ1, ρ2… ρn, respectively, and ρ is mean density of snow cover and may be defined by the following relation:

$$\bar{\rho} = 1/D \sum_{i=1}^{n} d_i \rho_i$$

Equation 2-5

The amount of snow water equivalent varies greatly, depending on various regional and local factors. A linear empirical relationship between the increase of the terrain and the height of the water equivalent has been indicated (MARTINEC 1991). Martinec (1991) found no more increase in snow water equivalent above 2800 meter above see level (m.a.s.l) elevation. If the influence of the terrain elevation is described as dominant, other regional factors such as the latitude, topography and vegetation does not affect much. Thus, the influence of high dense forest particularly with the snow floor system proves as strongly reducing factor for the height of the water equivalent. In contrast, the exposure strengthened during the ablation by modifying melt rates on the development of water-equivalent (ISHII AND FUKUSHIMA, 1994).

In the standard measurement programs, the water equivalent is rarely determined. Generally, in the European stations, point measurements are error-prone values. So, regionalization is required to obtain best possible values (MARTINEC AND RANGO, 1981). In the USA, the

snow telemetry (SNOTEL) network is used for determining snow water equivalent (SIMPSON ET AL., 1998; FERGUSON, 1999). Based upon recent remote sensing and radar techniques, it is possible to obtain spatial images of the water equivalent (MARTINEC ET AL., 1991; LUNDBERG AND THUNEHED, 2000). With the help of passive microwave data for terrain, water equivalent can be calculated. However, Rango et al., (1996a/b) described that the assessment of values are somewhat negated by the variability of size and shape of snow crystals. Depending on the recording technology, the thin and waterlogged snow is expected to be falsely measured, as reflections of the underlying soil surface and high liquid water contents in the snow provide distortion (LUNDBERG AND THUNEHED, 2000). Also, forest areas provide distortion of the recorded signals (FERGUSON 1999). Moreover, image resolution, surface cover and frequency recording of most remote sensing techniques are still very limited (BRAUN 1985; BLÖSCHL AND KINBAUER, 1992; NAKAWO AND HAYAKAWA, 1998). However, an exception is made regarding the resolution from active microwaves, which are not able to detect the water equivalent of dry snow cover (FERGUSON, 1999).

Frequently, the snow water equivalent is calculated from the measured rainfall depth. Besides, a simple mass relationship between snow water equivalent, snow density and snow height can be set up. In many investigations and applications of models to derive and describe the snow storage variable, water equivalent is used (VEHVILÄINEN, 1992; WOHLRAB ET AL., 1992; DINGMAN, 1994; MARTINEC, ET AL., 1994b). This relationship is as follows:

HWE= HS * ρs [mm]   Equation 2-6

Where, HWE is height or snow water equivalent [mm], HS is snow depth [cm], and ρs is snow density [g / cm³].

2.3   Snowmelt

The snowmelt process is defined as the phase transition of solid snow ingredients parts (ice crystals, Ice grains) into liquid water, for which about 340 joules per gram (j/g) of energy are needed. Snowmelt processes is determined by the energy balance of the snowpack. The

energy balance of the snow is predominantly determined by atmospheric and microclimatic variables (BAUMGARTNER AND LIEBSCHER, 1996). The necessary energy quantity, in order to raise the snow temperature to the melting point, corresponds to the cooling content of snow pack. After reaching isothermal conditions within the regarded snow pack at 0°C, each further energy input causes melt. The two primary factors of the energy balance for using melt are the short-wave net radiation and the perceptible heat flow (KUHN 1984; RACHNER AND MATTHÄUS, 1986; DINGMAN, 1994; RACHNER ET AL., 1997).

The respective importance of the individual energy components for the melt is a function of weather processes (BLÖSCHL ET AL., 1987). For instance, with open land snow covers in the alpine and polar areas, the sun light is considered as main influencing factor for melting processes. Higher influence of sun increases the further melting process in the spring (BRAUN 1985). According to Baumgartner and Liebscher (1996) the radiation supplies approximately 80 percent of the melting energy for mountain snow covers. However, in lowland snow covers, where often wet weather conditions predominate, 50 percent of the heat of melting comes out from perceptible and latent heat flows. Rachner et al. (1997) emphasized the importance of heat transfer of flowing air for melting mountain snow covers because of heat transport by moisture exchange. On the other hand, turbulent heat flows as a function of the wind speed. Generally, in the lowlands and the low mountain area, high air temperatures, high humidity and strong wind is considered as crucial determinants of melting processes aforementioned (HERRMANN AND RAU, 1984; KUHN, 1984; BLÖSCHL ET AL., 1987; BAUMGARTNER AND LIEBSCHER, 1996).

Due to the storage capability of snow for liquid water, the snowmelt rate and water loss rate from snow cover are not particularly identical at the beginning of a melting period. If the retention capacity of the snowpack for liquid water is exceeded, melt water percolated by the snowpack occurs only at the base of the snowpack (FERGUSON, 1986; BLÖSCHL AND KIRNBAUER, 1992; SINGH ET AL., 1998; KATTELMANN, 1998).

Over logging related crystal transformations in forest areas and compactions, the dynamic melting process itself induced a sustained increase in melting of snowpack. Besides water-saturated snow covers in recent melt or rain entry, a direct translation of the stored liquid water leads to direct discharges from snowpack (FERGUSON, 1986; SINGH ET AL., 1998). Accordingly, the condition of the snow package at the time of entering melting conditions from snowpack is of crucial importance for causing melt and the water discharge (RACHNER AND MATTHÄUS 1984; RANGO AND MARTINEC 1995; SINGH ET AL., 1998).

2.3.1 Effect of rainfall, topography and landcover on snowmelt

Depending on the amount, intensity and duration of the precipitation, snow cover thickness and snowpack logging will significantly increase the melting process. On thin snow cover, moderate rainfall can contribute to complete-melt (KUUSISTO, 1980; BAUMGARTNER AND LIEBSCHER 1996; SINGH ET AL., 1998).

Singh et al., (1998) emphasized that the melting snow and runoff response of snowpack due to heavy rain is significantly higher than melt alone. Thus, in particular, the destructuring effect and registered transmitted rainwater have high importance for the melting and release of water attached. Especially, in areas with variable winter conditions, various authors described the influence of rain as the most important determinant of ablation process (KUUSISTO, 1980; WOHLRAB ET AL., 1992; RACHNER ET AL., 1997). In contrast, the energetic contribution of rain to melt described as very low (BAUMGARTNER AND LIEBSCHER 1996; SINGH ET AL., 1998).

The snow cover depletion also varies spatially and temporally depending on the level terrain, the slope exposure, tilt, and the forest area. As the name of the location factors influence is very specific and variable, only qualitative statements can be made. On the contrary, generalized quantification of the degree of influence is not possible (HERRMANN AND RAU, 1984; BRAUN, 1985; BLÖSCHL AND KIRNBAUER, 1992; ISHII AND FUKUSHIMA, 1994; BAUMGARTNER AND LIEBSCHER, 1996; RACHNER ET AL., 1997; KATTELMANN, 1998).

The influence of the ground level can be explained mainly by the decrease in temperature and increase of radiation energy with increasing altitude, as well as the prevailing weather conditions (BAUMGARTNER AND LIEBSCHER, 1996; RACHNER ET AL., 1997). Generally, powerful radiation dominated melting snow in high mountain passes gradually. However, it often comes in lower layers by turbulent weather conditions rapidly due to ablation of the most thin snow covers (HERRMANN AND RAU 1984; BAUMGARTNER AND LIEBSCHER, 1996).

The importance of slope and exposure in melting process can be felt especially in radiative weather conditions, where north-facing slopes received significantly lower energy than south-

facing slopes. Accordingly, it resulted in delayed melting in northern side and accelerated melting in the southern side (BRAUN, 1985; BLÖSCHL AND KIRNBAUER, 1992).

Depending on the density of the canopy, most of the evergreen forest may be expected to have reduced and delayed melt as compare to open areas. In contrast, winter bare deciduous forest is not significantly different from open areas in terms of melt. Often, reduction in melting takes place by the already smaller accumulation of snow, for example, due to high interception values and higher evaporation losses under forest. Melting delays are mainly due to shading effects of the crowns, the days of radiation, if the melt is mainly due to sun exposure, are effective. In addition, lower melt rates may be caused by the attenuation of wind speeds, which resulted in reduction of turbulent heat exchange (DICKISON ET AL., 1984; BUTTLE AND MCDONNELL, 1987; ISHII AND FUKUSHIMA, 1994; BENGTSSON AND SINGH, 2000).

2.4   Implications of snow-hydrological process dynamics

Snow cover and depletion in many places characterizes the winter and spring runoff dynamics. This leads to fundamental regional differences in flow regime influenced by snow reserves, based on the regularity of outflows, their temporal distribution and volume effects. Regional characteristics of the discharge events are also influenced by local factors and typical meteorological conditions. In particular, the influence of rain is mentioned in sub-alpine, mid-mountain and lowland climatic conditions during the ablation process (HERRMANN AND RAU, 1984; BAUMGARTNER AND LIEBSCHER, 1996; SINGH ET AL., 1998). High intensity rain events can thereby lead to a short-term release of significant volumes of melt (SINGH ET AL., 1998). Accordingly, rainfall on similar level surfaces with thin snow cover is one of the main factors for the flood generation (BAUMGARTNER AND LIEBSCHER 1996). An investigation followed by HERRMANN AND RAU (1984), described the flow regime in Figure 2.4.5, which also shows the characteristic course of snowmelt runoff in various regions of Central Europe.
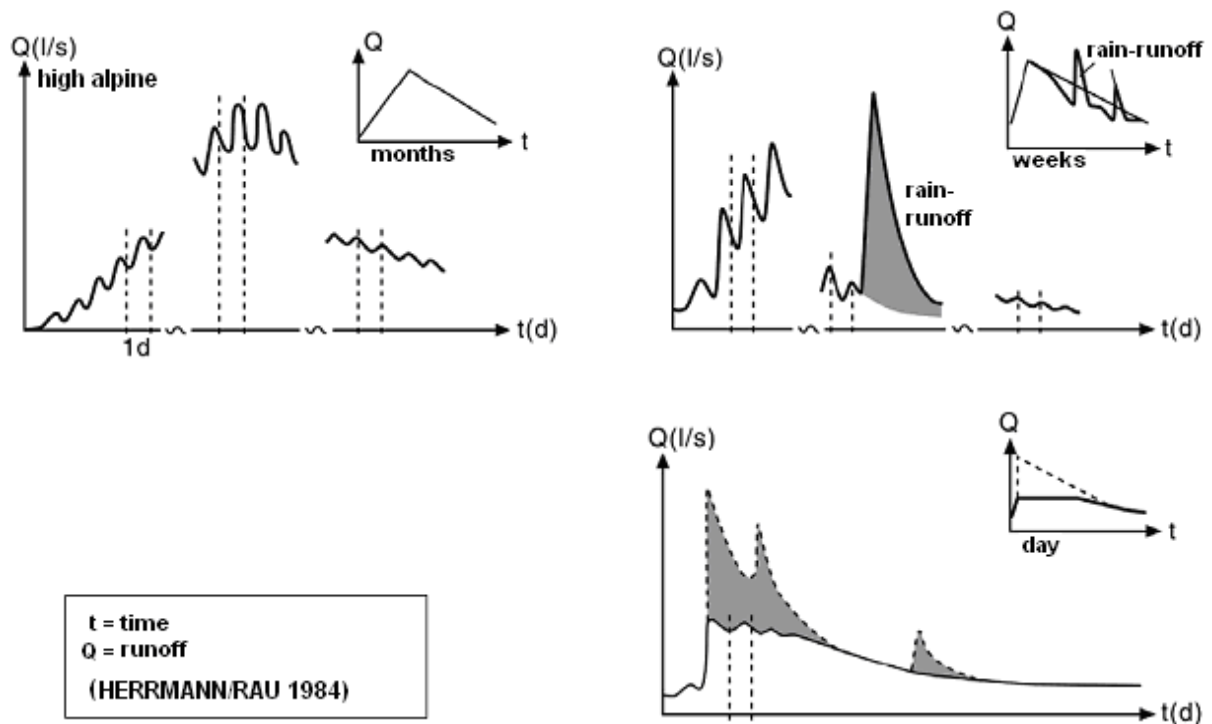
Figure 2-3: Schematic representation of typical hydrograph curves of melt runoff in selected Central European region (HERRMANN AND RAU 1984). (Source: HERPERTZ, 2006:P. 30)

Figure 2-3 shows that in the high-alps during one period of months (usually between late spring and summer) melt runoff can occur. The predominantly radiation-induced reduction of the seasonal thick snow covers determines the runoff regime. During the ablation, the runoff is characterized as a function of the radiation due to more or less pronounced diurnal variations. With reduced snow depth and snow cover at the end of ablation, the regular runoff development is modified increasingly. In the outside alpine regions of central Europe, thin snowpack combined with an unstable weather condition in principle is the case of a lower regularity of snow-induced runoff than alpine areas. In sub-alpine basins, extending ablation can be seen at the start of weekly, daily variations of the hydro-graphs is still significant, which are dissolved but increases also by weather conditions. The snow-affected outflows of the mountain regions are characterized by changing climatic conditions. At any time during winter or spring, there may be sporadic snow cover up and depletion that controls the runoff. Characteristic of the lower regions are also secondary rain induced melting peak runoff, prevent the development of regular outflow. During ablation of a snow cover, the effective

16

runoff extends only for a period of days (HERRMANN AND RAU, 1984; BAUMGARTNER AND LIEBSCHER 1996)

2.5   Snow modelling

Core of snow-hydrological modelling approaches is simulation of snowmelt. The main processes in snow accumulation and ablation models are: accumulation of new snow, snow settlement, snowmelt caused by heat transfer from air and rain, water holding capacity, refreezing of water in the snow pack, temperature changes of snow, and water percolation through snow. There are two fundamental approaches of snow modelling: the energy balance method and the temperature index method (TURČAN, 1990).

The energy balance method simulates the physical processes that affect the thermal energy content of the snow pack such as sensible, latent and ground heat fluxes, heat conduction between layers, and energy released from phase changes. This type of model requires a number of inputs including incoming and reflected solar radiation, incoming long wave radiation, temperature, precipitation, relative humidity, and wind. Normally, data for determination of long-wave and short-wave radiation balance as well as sensible and latent heat flows are needed. Because of their nature, physically-based models typically require less calibration because their parameters are assumed to represent measurable characteristics. These data are available but limited. As a result, relatively insignificant elements of the balance are neglected and more important factors like net short wave radiation and albedo as their determinant are either measured or derived. FERGUSON, (1999) described the extrapolation of this estimation to be very error-prone. Moreover, BLÖSCHL, (1991) indicated that temporal and spatial albedo variation strongly varies and is difficult to estimate. He also described a high sensitivity of the most energy balance procedures for the albedo, which can lead to much larger misidentifications of the melting volume, for example, inaccuracies in estimating the air temperature. FERGUSON, (1999) focussed on the high variability of the particular balance in terms of temporal (daily, seasonal and synoptic scale) and spatial attributes.

In particular, the energy model approaches usually need very high data, but in the applied hydrology, preferred temperature index or degree-day factor methods can be used to simulate snowmelt (BERGSTRÖM, 1975; KUUSISTO, 1980; BRAUN, 1985; WMO 1986; VEHVILÄINEN, 1992; GRAY AND PROWSE 1993; MARTINEC ET AL., 1994b;

RANGO AND MARTINEC, 1995; DUNN AND COLOHAN 1999). Temperature index methods are based on empirically-derived relationships between air temperatures and melt rates and require calibration of a number of parameters to represent the regional characteristic of this relationship. Air temperature is assumed to integrate the effects of advection, convection, radiation, and latent heat changes on the energy balance of the snowpack (LANG AND BRAUN, 1990). In this method, snowmelt ($\Delta\omega$) is estimated as a linear function of the difference between the air temperature (Ta) and a base temperature (Tbase) (DINGMAN, 2002):

$$\Delta\omega = M \times (Ta - T\,base), \qquad Ta \geq T\,base; \qquad \text{Equation 2-7}$$

$$\Delta\omega = 0, \qquad\qquad Ta < T\,base$$

Where, M is the melt factor or degree-day factor (DDF). In the traditional temperature index method, the DDF typically remains constant because the method assumes a constant relative contribution of all the components of the energy balance.

In basic approach, for determination of the melt volume per time interval, the difference of a defined limit value of the air temperature and the mean air temperature is formed over a time step and correlated to a constant melting coefficient. Generally, the procedure is used in the daily or multi-hourly scale. Therefore, this method can be described for furthest common snowmelt calculation (BRAUN, 1985; RANGO AND MARTINEC, 1995):

$$M = a * (T0 - Tlimit) * \Delta t / 24 \qquad\qquad \text{Equation 2-8}$$

Where, M is as melt volume [mm/time interval], A is melt coefficient [°C/mm* time interval], T0 is mean temperature over the defined time interval [°C], T limit is defined limit temperature for the use (usually 0°) [°C] and Δt = time interval, to which the melt volume refers.

The air temperature is the best available meteorological factor, which is to be determined relatively reliable for area surfaces (BLÖSCHL, 1991). It is also an important influencing

factor for all energy balance terms except net radiation. RANGO AND MARTINEC (1995) showed that temperature-based methods at lower data requirements can provide comparable good results as energy balance model approaches. Thus, in addition to SRM, the snow module of HBV model (BERGSTRÖM, 1975; VEHVILÄINEN 1992) and J2000g model (http://jena.de/jamswiki/index.php/Hydrologcal_Model_J2000g) are based on variants of the temperature index procedure.

KUHN (1984) considered a constant melt factor during longer periods (days and months), in which fluctuations of the parameter can be compensated (RANGO AND MARTINEC, 1995). In the SRM, the melt factor is not a static parameter, but identified as variable time series over the entire season (MARTINEC ET AL., 1994b). In this way, the change of the sun position with the season is included into the melt computations. According to VEHVILÄINEN (1992), the melt factor varies in forest surfaces and opens areas, but time remains constant. GRAY AND MALE (1981) developed an empirical relation of the melting factor for different slope angles and exposures. At one index, the ratio of solar radiation received by a slope with a given inclination and orientation described a horizontal surface.

The temperature index method has been found to be adequate under most circumstances; however, it cannot account for changes in the surface energy balance caused by diurnal and annual changes in the incoming solar radiation, albedo, and turbulent energy exchanges (LANG AND BRAUN, 1990). ANDERSON (1973) gave two basic reasons for using a temperature index model in operational forecasting: (1) air temperature data are readily available throughout the all regions in real-time, and (2) tests conducted on two experimental watersheds showed that the temperature index method (SNOW17) produces results "at least as good as" those from using the energy-aerodynamic method (HYDRO19). The similar quality of output between the two models was attributed to the errors involved in determining input values for the energy method due to the difficulty in measuring the required variables (ANDERSON, 1973). ANDERSON (1976) showed that the temperature index process became unreliable when factors other than temperature (such as solar radiation or turbulent energy exchanges) dominated the melt process. The energy balance model, conversely, gave good snowmelt estimates for all meteorological conditions in this study.

More recent studies can be found to support either the use of the temperature index method or the energy balance methods for snowmelt prediction. Arguments for the use of temperature-based methods continue because of the simple data requirements and comparable performance to energy balance methods (LANG, 1986; WMO, 1986; KUSTAS ET AL., 1994; RANGO

AND MARTINEC, 1995; DALY ET AL., 2000). Reasons for using more complex snow modelling methods include the increased accuracy of energy balance models at time steps less than 1 day, appropriateness for modelling spatial processes, the ability to use a variety of remote sensing observations, and the easy transferability between basins of varying climate conditions (LANG, 1986; WILLIAMS AND TARBOTON, 1999; STRASSER ET AL., 2002; SIMPSON ET AL., 2004; WALTER ET AL., 2005). The standard in snow hydrology is that when only one meteorological variable is available, temperature is the best predictor of snowmelt (Anderson, 1976). However, regression analysis from ZUZEL AND COX (1975) showed that when vapour pressure, net radiation, and wind data was available, temperature was relatively unimportant(Anderson, 1976). But on the other hand, the above mentioned data can increase the capability of temperature index method in snow hydrological models like J2000g model.

2.5.1 Snow-hydrological modelling approaches

In many regions of the earth, the melt water discharge from snow covers plays a substantial role for the water supply and flood development especially in areas with more regular seasonal snowpack like the alpine or polar area or some mountains located in high latitude situations. Therefore, a set of modelling tools for the forecast of melt runoff was developed 30 year ago (BERGSTRÖM, 1975; MARTINEC, 1975; WMO 1986; SINGH, 1995). Among the still most common snow hydrological modelling approaches in the early 70's, MARTINEC (1975) developed the SRM and the Swedish Meteorological and Hydrological Institute (SMHI) developed HBV-model for the Alpine region (BERGSTRÖM, 1975; FERGUSON, 1999). Both approaches operate on the daily scale (HBV, shorter time steps) and have a semi-distributive structure. For other regions, the increasing importance of snow for the winter runoff dynamics has been identified (HERRMANN AND RAU 1984; BRAUN AND LANG, 1986; RACHNER AND MATTHÄUS, 1986; RACHNER AND SCHNEIDER 1992). Extensions of the existing approaches and new developments of snow-hydrologic models are based partially on new scientific realizations (DUNN AND COLOHAN, 1999; FERGUSON, 1999).

Defined objectives, target application space and data availability determine the extent and structure of snow-hydrologic modelling tools. As in all environmental locations, preferred modelling approaches, even involving snow-hydrologic modelling components, tried to find a

suitable balance between the scientific complexity and a practicable simplicity (FERGUSON, 1999).

2.5.1.1 Conceptual outlines of snow-hydrologic modelling approaches

On one hand, snow-hydrological modelling tells the description of a winter process dynamics in terms of scientific questions (descriptive approach). Here, usually small-scale process analyses are the centre of attention, which are to be made possible by deterministic physically based computation approaches (BLÖSCHL ET AL., 1987; BLÖSCHL AND KIRNBAUER, 1991). On the other hand, predictions of snow water equivalent as well as the temporal process and the volume of the melting water runoff from snowpack are needed for water-economical purposes (prescriptive approach). The prescriptive approaches need to be designed for larger territorial units, such as mesoscale river basins, which require a conceptual model and technical view of the physical process structure (BRAUN AND LANG 1984; BRAUN AND LANG 1986; BLÖSCHL ET AL. 1991a). In snow-hydrological modelling, it distinguished deterministic, conceptual, and also stochastic approaches for the simulation of complex natural system. In the snow-hydrological modelling, there is distinction between deterministic, conceptual, and stochastic approaches for the simulation of complex natural system. When statistical modelling used in conjunction with physically based modelling, it serves as a valuable tool for addressing important issues (OBLED AND ROSSE, 1977; VEHVILÄINEN, 1992; FERGUSON, 1999).

In general, hydrologic-snow model approaches accounted for the mass budget and heat flow of a snow cover. This heat flow is determined either on temperature or on energy-based methods. The structure of snow routine integrated into the SHE model enables the use of both the methods. Depending on objective and data availability, methods to be used can be determined by the user (SINGH, 1995).

The extent of snow-hydrological modelling approaches based primarily on their objectives. Some models include only the removal of snow, as they were developed as an independent tool specifically for the prediction of the melting volume and outflow from seasonal snow cover. Thus, the SRM includes a set of a melting and runoff routine. The accumulation process itself is not simulated. Rather, measured dataset of snow water equivalent and the spatial distribution of snow are required as a model input (MARTINEC ET AL., 1994b).

21

SRM model calculates the resulting melt water streams and converts the results together with the input of rainfall runoff coefficients in daily field outflows. In addition, the effects of climate changes are involved in applications of the SRM (RANGO 1992, 1995). Other snow-hydrological modelling approaches are not developed as separate models. It forms a component of rainfall-runoff and water balance models, and contributes to complete the system representation. These models include approaches of varying complexity on the processes of snow accumulation, snow cover and snowmelt (e.g., HBV, HSPF, NASIM, PRMS / MMS, SHE; WASIM-ETH).

The snow evaporation and sublimation is often considered only in energy-based or detailed descriptive model approaches, as it is classified as a loss in negligible amount of water (BRAUN, 1985; DHI 1986; BLÖSCHL AND KIRNBAUER 1991; MARTINEC ET AL., 1994b; SINGH 1995).

Meteorological data, especially, measurements of air temperature are considered as the minimum requirement for all snow simulation approaches. Energy based model approaches require usually at least solar radiation, including albedo data (LEAVESLEY et al. 1983; DHI 1986; BLÖSCHL 1991; SINGH 1995). In addition, often point measured values of the snow depth or snow water equivalent is required. In order to obtain an approximate spatial representation, these input data via interpolation and regionalization methods must be extrapolated at the local area surfaces. The data requirements of the different models often are based on available regional or national monitoring network of the study area. Especially in the U.S.A., higher-resolution data are available than in Europe and other countries (LEAVESLEY, 1989; JAMES, 1991; KUSTAS ET AL., 1994; RANGO, 1996). Switzerland also has more strongly snow-hydrologic measuring and monitoring networks than other regions of the Europe (BRAUN, 1985; ROHRER, 1992). In Iran, the collection of snow-related hydrological data in some parts of Tehran and a few representative mountains close to some big cities are more intensively operated than another parts of country.

Point measured values of snow parameters are also used to compare the random simulation results. However, the model calibration must be undertaken in all models by runoff measurements. First, the spatial-temporal data available from snow parameters is low; on the other hand, extrapolation of the extremely variable quantities of water equivalent, snow depth or density on the surface represents a significant failure rate (FERGUSON, 1999). According

to KIRNBAUER ET AL. (1994), the combination of modelling with geographic information systems (GIS) and remote sensing techniques are new possibilities for regionalization and calibration of snow models (NAKAWO AND HAYAKAWA, 1998). The overall objective, for example, in newer versions of the SRM by a raster-based remote sensing data coupled with a direct areal coverage of snow water equivalent and snow distribution. Remote sensing images can be consulted for the verification of the identified values (RANGO, 1992; MARTINEC ET AL., 1994b; RANGO AND MARTINEC, 1995). In addition, there are also opportunities for advanced radar-based determination of rain and snow precipitation, which require terrestrial measurements (RICHTER, 1995). The practical application of modern remote sensing and radar techniques is still very limited to describe. This is mainly due to a low availability of enough temporal-spatial resolution data and more error recording in snow cover data (RANGO, 1996; NAKAWO AND HAYAKAWA, 1998; DUNN AND COLOHAN, 1999; LUNDBERG AND THUNEHED, 2000).

2.5.1.2 Spatial differentiation in the snow- hydrological modelling

BLÖSCHL AND KIRNBAUER (1992) considered the area subdivisions and model technical characteristics in regard to surface area of snow hydrological modelling as an essential methodological tool (BENGTSSON AND SINGH, 2000). Through the use of available new technologies (multi-capacity computer, GIS, elevation models, KIRNBAUER ET AL., (1994) foresee the future of the dawn of a new era in snow hydrological models. Also FERGUSON (1999) described a trend for distributives modelling, by taking meteorological input data and different model parameters.

The discretization of the snow-hydrological model approach is based on the usual methods of general regionalization of hydrological models (e.g., grid, hydrological response units (HRU), catchment areas, zones, triangulated irregular network (TIN)). Accordingly, the same problem occurs in the transmission of point values to the surface and the designation of sub-areas of similar hydrologic response (BLÖSCHL 1996). Most approaches have at least a limited subdivision of the study areas to reflect the physical heterogeneity of catchments. In particular, the dominant influence of the ground level to the snow hydrology is determined by taking levels of terrain into account. Based on the height of the temperature measuring station, a temperature adjustment amount per level will be carried out, which is considered substantial

for snow hydrological simulations (e.g. BERGSTRÖM, 1975; LEAVESLEY ET AL., 1983; RACHNER AND MATTHÄUS, 1984; BRAUN AND LANG, 1986; BLÖSCHL AND KIRNBAUER, 1992; MARTINEC ET AL., 1994b; SINGH, 1995; RACHNER ET AL., 1997). While SRM allowed vertical zoning of any other area subdivisions but, the HBV-model based on subdivision zones separated simulation of snow dynamics in forest and field areas (BERGSTRÖM 1975; MARTINEC ET AL., 1994b; FERGUSON, 1999). According to BENGTSSON AND SINGH (2000) an area division both following topography and landuse for snow-hydrologic modelling approaches is essential. They described in particularly the importance of different land covers for the melting dynamics and temporal distribution of melting induced peak flows. VEHVILÄINEN (1992) reported no distinctions in his approaches to model the ground level, mainly due to the low relief energy of its test sites in Finland. However, he highlighted the importance of forests for the snow distribution and considered the site-specific forest influence by reduction algorithms for the simulation of accumulation and melt (BERGSTRÖM, 1975; DINGMAN, 1994; POMEROY ET AL., 1998b). CALDER (1990) represented one of the few model approaches to take in to account the snow interception (POMEROY ET AL., 1998a).

If the effect of slope exposure and gradient involved in snow hydrological simulations, its influence can be seen on accumulation and melting process. RACHNER ET AL., (1997) considered the project SNOW-D is a modification of the terrain height prescribed snow deposition and distribution as a function of exposure and redistribution of wind. DUNN AND COLOHAN, (1999) developed a function for the wind-conditional snow redistribution, in order to determine small-scale snow accumulations, which proved in their Scottish highlands test areas as significant for the base flow. In many more different approaches, the radiation at southern and northern slopes in the modelling of the melting process is taken into account (GRAY AND MALE 1981; LEAVESLEY ET AL., 1983; BRAUN 1985; BLÖSCHL AND KIRNBAUER 1992). Small-scale topographic factors (valleys, summits and slopes) having influence on the snow distribution in the modelling in catchment gauges are generally neglected.

2.5.1.3 Model-technical coverage of the snow accumulation

Regardless of the discretization of the catchment area, the extensive snow accumulation process in hydrological modelling approaches is derived directly from the rainfall input

(BERGSTRÖM, 1975; LEAVESLEY ET AL., 1983; RACHNER AND MATTHÄUS, 1984; BRAUN, 1985; VEHVILÄINEN, 1992; RACHNER ET AL., 1997). The determination of precipitation type is of crucial importance in snow modelling. In most models, they used the temperature in near-surface air layers as a dominant factor which influences the composition of precipitation at the ground. For determination of the transition of rain to snow, precipitation is often accepted as simplifying individual temperature threshold value (RACHNER AND MATTHÄUS, 1984; BRAUN, 1985; VEHVILÄINEN, 1992). In order to involve mixed precipitation, which occurs frequently, especially in lower layers, LEAVESLEY ET AL., (1983) used a temperature interval for the PRMS. At temperatures within the interval limits, it comes to the creation of mixed precipitation (BERGSTRÖM, 1975). Amount of new or additional water equivalent of a snow cover is measured finally by amount of area precipitation fallen in solid or mixed form (BERGSTRÖM, 1975; LEAVESLEY ET AL., 1983; BRAUN, 1985; VEHVILÄINEN, 1992; RACHNER ET AL., 1997). In other approaches, for example in SRM, at least point measured values of the water equivalents or snow depth are required (MARTINEC ET AL., 1994b).

2.6   Snow modelling and water resources

Snowpack act as water reservoirs during the winter months, storing precipitation until spring and early summer when melt occurs. Water managers rely on this storage effect to better manage reservoir releases, water deliveries, and water needs throughout the rest of the year (SINGH AND SINGH, 2001). Snowmelt currently makes up 75% of all the streamflow in some part of north hemisphere like the west U.S. where surface water resources meet about 90% of the water needs for the regions (FRANZ, 2006).
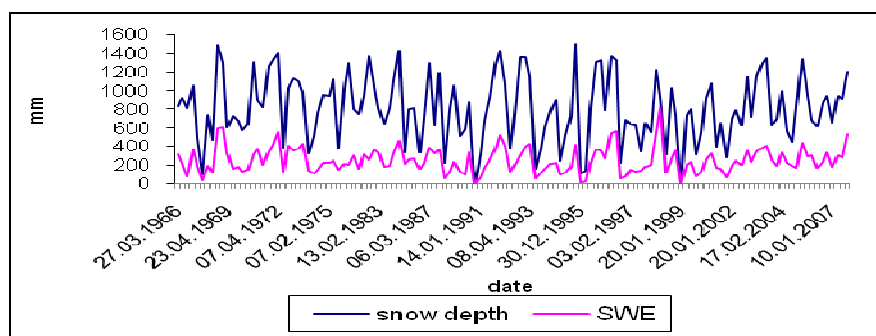
Figure 2-4: The Long-Term of Snow depth and SWE in Shemshak station, Latyan Catchment (Data source: Iranian Water Resource Management Company (IWRMCO))
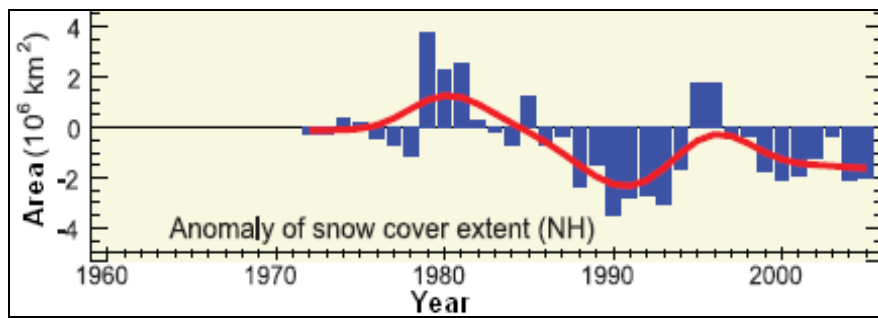
Figure 2-5: Anomaly of snow cover extent in North Hemisphere (Source: http://www.ipcc.ch/pdf/assessment-report/ar4/wg1/ar4-wg1-chapter4, 2007:P.376)

Peak snow accumulation and SWE in the mountains of the Iran can show big variations from 1966-2007(Figure 2-4). Analyses of satellite images snowpack collected over the past decades indicate that accumulation levels have dropped considerably throughout the high latitude and mountainous regions and that packs are melting earlier in the year (Figure 2-5) (LEMKE; REN, ET AL., 2006). Climate impact studies have indicated that even if the most moderate level of a predicted warming occurs over the next 50 years, snowpack in some regions could be reduced by up to 60%. This would reduce the spring streamflow volume by an estimated 20-50% (Service, 2004). As the storage effects of snow diminished, there will be less water available to meet the needs of agriculture, hydropower production, and environmental protection. The balance between maintaining low flow requirements and maintaining reservoir storage to meet future water demands will become even more delicate. Because snow is important as a natural resource and is also extremely variable, accurate estimates of the volume of water within the snowpack and the rate of release of the water from snow is required for efficient management (SINGH AND SINGH, 2001).

There is a great deal of uncertainty over whether increased climate variability will cause more floods, droughts, or significant changes in water supplies (IPCC, 2001). If the changes in the timing and amount of snow runoff indicated by recent climate studies continue, as well as continue of growth urban population as a big crisis of 21th Century, accurate hydrologic predictions will become increasingly important as water managers and hazard response groups will have to make decision under conditions not previously experienced. It is necessary that hydrologic predictions systems be able to adapt to and assure reliability in the face of uncertain future conditions.

2.7   Previous Researches in the Latyan catchment

As Tehran is the capital of the country, its water security implies to have a clear vision of the future. Simulation of the balance of the supply source of the city is very important for supporting decision makers. Though the hydrological process of Latyan catchment is very important for water supply and economy of Tehran, the capital of Iran, only few studies have been carried out so far on the hydrology and water balance of Latyan catchment. Previous works related to hydrological balance modeling of Latyan catchment are discussed below.

Most important works on precipitation-runoff modeling in Latyan catchment is carried out by HOSSEIN (1997), FATTAHI (1998), Morid ET AL. (2004) and ZEINIVAND and De SMEDT(2008). HOSSEIN (1997) analyzed the hydrological behavior of the Roodak sub-catchment and evaluated the flood simulation by means of HEC-1(Hydrologic Engineering Center) model. He found that the most runoff in catchment depend on snowmelt during March to July. Moreover, heterogeneity in rainfall with lack data, seasonal difference snowmelt, variable channel conditions, inaccurate estimate of routing coefficients and inaccuracy in hydrological soil groups increased the difference between observed and predicted peakflows, but finally the differences are not big, therefore HEC-1 model can be used for design of peak discharge in Roodak and another ungauged catchments. FATTAHI (1998) also used an Iranian model (SNOW) for analysis and quantification of snowmelt in Latyan dam catchment. He found that the 64% of all annual precipitation of catchment is snow. He determined the temperature threshold, and predicted runoff input to the dam during April to June. Moreover, he noted that in such catchments as Latyan, due to simplicity and data accessible like temperature, the degree- day method is preferable to predict the snowmelt runoff.   MORID ET AL., (2004) used SWAT (Soil and Water Assessment Tool) for runoff simulation of Ammameh Sub-catchment of Latyan catchment using different snowmelt algorithm such as Degree-Day, SRM, and SNOW17. They found better performance of the energy budget method using synthesized data, compared with solely simple temperature-based method. ZEINIVAND AND DE SMEDT (2008), modelled snow accumulation and melt using a distributed hydrological model known as water and energy transfer between soil, plant and atmosphere (WetSpa) with two different snowmelt simulation modules namely degree day and energy balance methods for simulating river discharge in the Roodak subcatchment, in the Latyan dam watershed. They used data of three years of observed daily precipitation, air temperature, potential evaporation, and wind speed. The discharge data is used for model calibration. They found that the model performance is satisfactory for both methods with

efficiencies of more than 80%. They concluded that the WetSpa model for snow accumulation and melt has great potentiality to predict the impact of snow accumulation and melt on the hydrological behaviour of a river basin.

NOURANI ET AL., (2008) and ROSHAN ET AL. (2007) studied the hydrological process in Ammameh sub-catchment of Latyan. NOURANI ET AL., (2008) developed a geomorphologic hydrologic model based on distributed flow routing and linear reservoirs cascade to simulate the runoff of the Ammameh watershed. They proposed that combination of a non-linear distributed routing model and a linear lumped rainfall-runoff model causes the proposed model to be a proper runoff routing model. ROSHAN ET AL. (2007) used Smirnov-Kolmogorov method to optimize the relationship between water and sediment discharge rates in the Ammameh watershed.

A number of researches related to various hydrological issues to Latyan catchment and water supply of Tehran can also be found in POURABDULLAH (2006), ZARGHAAMI AND SALAVITABAR (2006), JAHANI AND REYHANI (2006), GOLTERMAN (2005), MICAELLI (2007), VALLES ET AL., (1990), KARAMOUZ ET AL., (1999), KARAMOUZ ET AL., (2001), Bureau of Soil Conservation and Watershed Management (1975), HYDARIAN (1994), AQIQI (1995), KHOSROSHAHI (1989). Soil Conservation and Watershed Management (1975) carried out the comprehensive plan of Latyan dam in Latyan catchment. KHOSROSHAHI (1989) carried out a unit hydrograph study for floods prediction in Roodak sub-catchment of Latyan. HYDARIAN (1994) evaluates the performance of different models in predicting soil erosion of Latyan catchment. AQIQI (1995) calculated depth area duration (DAD) curves in Jajrood area of Latyan catchment for different days. POURABDULLAH (2006) used RUSLE model, for estimating the amount of erosion Latyan catchment. The results of modeling showed that the degree of erosion of Latyan catchment was high because of steep slopes, lack of plant coverage and the quality of soil. VALLES ET AL., (1990) studied the soil alkalinization and salinization in some parts of Latyan catchment. A system approach to water resources management of Latyan catchment is discussed by KARAMOUZ ET AL., (1999). ZARGHAAMI AND SALAVITABAR (2006) used system dynamics which considered the water supply sources, demand sources (as domestic, irrigation and industry uses) and management tools (demand reduction, inter-basin water transfer) for

urban water management of Tehran. They predicted water shortage in the future years in the capital of Iran. KARAMOUZ ET AL., (2001) used a system approach to water resources development in Tehran considering its complex system of water supply and demands.

3. METHODICAL APPROACH

3.1 Hydrological System Analysis and Delineation of Hydrological Response Units

3.1.1 Hydrological System Analysis

The hydrological system analysis is the base for the delineation of the Hydrological response units (HRUs) and the calibration of the spatially distributed conceptual hydrological model J2000g. Initially, the hydrological system analysis studies the interactions of the landscape parameters soil, water, vegetation and climate in order to understand the system response to rainfall and therefore the generation of the respective hydrological response. Also, the examination of the hydro-meteorological time series using data analysis methods for changes in hydrological system response is an important preparation for the rainfall-runoff modeling of the catchment.

3.1.1.1 Data Analysis of Hydro-Climatological Time Series

The quality of the model output is directly depending on the input data (BEVEN, 2001). Hydrological models are driven, in part, by hydrometeorological data, which contains hourly, daily, or monthly field observations. The resulting time series are never perfect and the data contains data errors (BEVEN, 2001). The data errors are divided into systematic errors and random errors. The first group contains errors which affect the measuring instrument systematically (BEVEN, 2001) and result in a constant measurement bias. These errors can be caused, for instance, by false calibration of the instrument. Random errors, on the other hand, are caused by randomly occurring factors, such as interference of the automatic recording by animals. To achieve good modeling results it is crucial to control for data quality.

- *Rainfall Data*

Rainfall data are measured as point observations and there are several potential sources of data errors associated with those measurements (DINGMAN, 2002:P.114). The design of rain gauges can lead to a standard error between 3 to 30 % of the total annual measured rainfall sum (DINGMAN, 2002:P.115). These data errors can be corrected using an approach presented by RICHTER (1995). Rainfall time series might also include missing values. Here,

DINGMAN (2002:P.115-117) suggests the following methods for data filling: station average method, normal ratio method, inverse distance weighting, regression analysis or the most common technique: the double mass curve between two stations.

- ***Runoff Data***

The discharge observed at the runoff station is an integrated value over the entire catchment. In a hydrological model, the data is used for calibration of simulated runoff against observed runoff. Therefore, it is necessary to check runoff data for homogeneity and inconsistency (BEVEN, 2001). The most common technique, in case of available data at a nearby station, is the double mass curve (BEVEN, 2001). The double mass analysis compares two neighbouring measuring stations by the plotting of accumulated volumes. Changes in the runoff records will be visible in slope changes compared to the reference line.

This analysis gives information on missing values or changes in the catchment affecting the measured runoff. The resulting data was used to compute the annual and monthly average runoff and to establish the rainfall runoff relationship.

- ***Additional Datasets***

The time series data on wind speed, humidity, and temperature as well as snow depth and snow water equivalent (SWE) time series was checked for homogeneity and consistence using the aforesaid methods for rainfall and runoff data analysis. Missing values were filled by using regression analysis.

3.1.1.2 Spatial Data Modelling

Hydrological models require spatial information of the hydrometeorological information. The hydro-meteorological time series used, however, contain measurements at point scale. For a spatial representation of these parameters the missing information has to be interpolated. Here, several methods exist such as Thiessen Polygons, linear regression and inverse distance weighting (IDW) (WACKERNAGEL, 1995; KITANIDIS, 1997; WEBSTER AND OLIVER, 2001).

The regionalization of the hydro-meteorological datasets is used for the transfer of punctual values to the model units. The procedure was taken from the hydrological Model J2000

without any changes and is based on the inverse distance weighting (IDW) approach. The regionalization consists of several steps (KRAUSE, 2001; JAMSWIKI, 2010): First, the linear regression is applied to determine the relationship between station measurements and the respective station elevation. In the second step, the numbers of stations next to each HRU is determined, whereas the user defines the number of stations necessary to take into account. Then the distance between the found stations and each HRU is computed. To account for the difference in the distance between HRU and station, the application of a user defined weighting factor weightings the distances. In the third step, the final weighting factor for the hydrometric station is computed applying an inverse distance weighting method (. In the last step, the actual data values were calculated under consideration of the weighted values of stage 3 and the elevation factors of stage 1. For more detailed information on the regionalization algorithm in J2000g refer to JAMS (http://jams.uni-jena.de/jamswiki/index.php/J2000g) and KRAUSE (2001).

Another important stage in this framework is to check the spatial data for missing values. Particularly important is the digital elevation model (DEM), which is one of the most important datasets, because it will be used for the delineation of the stream network, catchment boundaries and topographic parameters such as slope, aspect, flow direction and flow accumulation. The DEM can be derived from remote sensing imagery, such as synthetic aperture radar (SAR) Interferometry (LUDWIG, HELLWICH ET AL., 2000) or from the Shuttle Radar Topography Mission (SRTM) (U.S. GEOLOGICAL SURVEY EROS DATA CENTER AND NASA, 2007). The SRTM-DEM, especially, often contains voids, which have to be filled for a hydrological application (KÄÄB, 2005; GROHMAN ET AL., 2006; WOLF, 2009).

3.1.2 Delineation of Hydrological Response Units

The relationship between rainfall-runoff of a catchment is determined by the following a wide variety characteristics: geology, topography, land use, soils, climate and vegetation cover (BEVEN, 2001:P.179). To account for a realistic representation of the catchment characteristics, the model used should be fully distributed. This type of model is difficult to apply because the model needs high spatially distributed input information of the landscape parameters, which cannot be measured at the requested resolution (BEVEN, 2001; BLÖSCHL, 2005). Therefore, the attempt has been made to define model entities that show a

"hydrological similarity" (BEVEN, 2001:P.179), which can be defined using one of the following three approaches. The first, the concept of Aggregated Simulation Area (ASA) has been applied in the SLURP (Semi-distributed Land Use-based Runoff Processes) model (KITE, 1995). This concept involves aggregating simulation areas which are heterogeneous in their land cover and elevation; however, the distribution of these parameters within the respective entity is known. These ASAs have the requirement of contributing runoff to a stream channel and, therefore, act as sub catchments (KITE, 1995). The second approach, the Representative Elementary Area (REA) (WOOD, ET AL., 1990) defines minimal areas in which the spatial heterogeneity of hydrological variables such as infiltration, evaporation, and runoff are unimportant. The distribution of these variables within the areas is represented by a probability function. The third concept, the Hydrological Response Unit (HRU), was introduced by LEAVESLEY, LICHTY ET AL. (1983) as model entities in the Precipitation Runoff Modelling System (PRMS). HRUs are characterized as homogenous areas with respect to their hydrological response (LEAVESLEY ET AL., 1983:P.9). This approach was extent by FLÜGEL (1995, 1996) who defined HRUs as areas with common in "climate, land use and underlying pedo-topo-geological associations controlling their hydrological dynamics" (FLÜGEL, 1995:P.426). The delineation of HRUs involves the definition of classification criteria, which are based on hydrological system analysis (FLÜGEL, 2000). The concept of HRUs has been tested and applied in several studies as an integrated regionalization tool (BONGARTZ, 2001; KRAUSE, 2001; KRAUSE, 2002; SCHEFFLER ET AL., 2007; SCHEFFLER 2008, KRAUSE AND HANISCH., 2009).

It can be concluded that the concepts of HRUs are the only modeling entities that consider all landscape parameters important in hydrological processes. Therefore, the HRU-approach has been applied in this study and is explained in the following section.

3.1.2.1 Concept Approach of Hydrological Response Units

The HRU concept, according to FLÜGEL (1995; 1996), is based on the representation of the catchment heterogeneity in the form of entities showing a similar or equal system response.

The climate and other landscape parameters of geology, soil, and vegetation are strongly interacting to each other. The natural vegetation depends on climate, relief and soil type. The soil is formed from bedrock material through various weathering and erosion processes.

Climate conditions determine the intensity of these various processes and, therefore, the types of soil formed. Distribution and formation of soil is also determined by the topography controlling the accumulation of soil material and the water movement within and on top of the soil column. A specific combination of geology, soil, relief, vegetation and climate characteristics, therefore, generates a specific system response (SCHEFFLER, 2008).

The HRUs divide the catchment into areas with similar or equal geology, soil-relief-vegetation and climate combinations. These entities are delineated based on detailed hydrological system analyses in a Geographical Information System (GIS) (FLÜGEL, 1995; 1996). The general object of using HRUs is to reduce the data inside each grid cell to unit information per layer. That means after applying this discretisation inside each grid cell, just one value for each landuse, soil, geology, slope, aspect, etc. exists. Based on the results of the hydrological system analysis the GIS datasets are reclassified, aggregated and overlaid in a step-by-step procedure. These entities act as model input for the rainfall-runoff simulation of the study area.

3.2 Water Balance and snowmelt-Runoff Modelling with J2000g Model

To obtain the above stated study goal, the snowmelt contains in the catchment has to be estimated. Due to importance of snowmelt-runoff in the catchment, spatial distribution of the SWE and snowmelt is simulated. For this purpose, the spatially distributed conceptual hydrological model has been applied. The delineated HRUs serve as spatial modelling entities in the model. The following section gives an introduction in the model design but also the steps of the modeling process such as preparation of input data (Section 3.2.2), parameterization and calibration (Section 3.2.3) are described.

3.2.1 The Structure of Modelling System of the J2000G Model

The model used for this study was the spatially distributed conceptual hydrological model J2000g model, which was adapted from the J2000 model (KRAUSE, 2001; KRAUSE, 2002) within the Modelling framework system JAMS (KRALISCH AND KRAUSE, 2006). The structure of the model is shown in Figure3-1. The model has been successfully applied in catchments of between 100 to 16000 km² in Thuringia, Germany for impact of climate change

(KRAUSE and HANISCH, 2009). Additionally the model was applied successfully in the Nam Co basin (about 20,000 km²) in Tibet (KRAUSE ET AL., 2010 in review). The other version of implemented models like, J2000 and J2000s successfully applied in various spatial scale and area ranges from basic scientific investigations in small catchments in Germany (2 - 13 km²), and in the processing of basic and applied research in mesoscale (about 50-1000 km²) catchment Germany, South Africa, Tasmania and the USA to macroscale modelling in the headwaters of the Brahmaputra (about 500 000 km²) under the Brahmatwinn project (KRAUSE, 2001; BÄSE ET AL., 2006;SCHEFFLER ET AL., 2007; SCHEFFLER, 2008; KRAUSE ET AL., 2009; http://www.brahmatwinn.uni-jena.de).
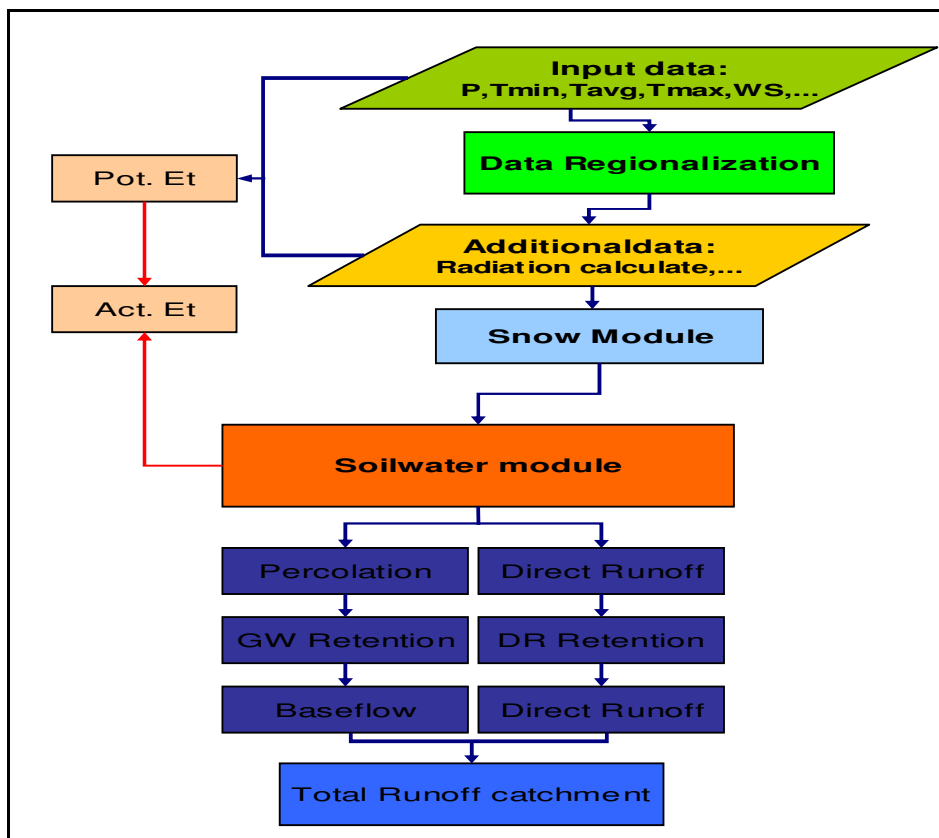
Figure 3-1: The Concept of Modelling System of the J2000g Model

As shown in the figure, the modelling system is divided into process modules such as the snow, soil water, and ground water recharge modules.

For each modelling unit (HRU), in the snow module, rainfall is computed as snow or rain based on temperature and precipitation input and degree day factor. Then the surface runoff and subsurface runoff are calculated in the soil module, but because the J2000g model is defined as simplified model, the surface runoff and subsurface runoff computed together as

direct runoff. In addition, base flow components are calculated in the groundwater recharge module. Afterwards, the simulated values of all the runoff components are added to the respective storages. This process is repeated until the water is transported to the catchment outlet.

The 2000g was developed for historical simulations as well as for snow hydrological modelling. The development was guided by the following requirements: (1) continuous and distributed simulation of important hydrologic characteristics in monthly time steps; (2) applicability of the model to the Iranian mesosclee catchments (Latyan, 700 km²); (3) process oriented and spatially distributed modelling; and (4) robust predictive ability with a small number of calibration parameters in areas with poor data.

The model J2000g requires spatially distributed information related to topography, landuse, soil type and hydrogeology to estimate specific attribute values for each modelling unit. A modelling unit can be a raster cell, a process unit, or a subbasin provided that spatial information is available for each attribute within each unit. J2000g also requires meteorological inputs (precipitation; minimum, average and maximum temperature; sunshine duration; wind speed and relative humidity) from one or more observation stations. The measured point data are transferred to each model unit using the spatial interpolation approach available in J2000 which is a combination of an optional elevation correction and an inverse-distance-weighting (IDW) interpolation. The elevation correction is made when the degree of correlation (calculated with a linear regression for each time step) between the variable values and the respective station elevation shows a coefficient of determination ($r2$) of equal or greater 0.7. In this case, the specific elevation dependent lapse rate, calculated from the regression, is used for the further processing along with IDW. If the $r2$ is smaller than 0.7 then only IDW is used. Next, net radiation (needed within the potential evapotranspiration (PET) module) is calculated from climate input data using the methods presented in ALLEN ET AL., (1998). Then potential evapotranspiration (PET) is computed according to the Penman-Monteith approach for various vegetation and land-use types (JAMS WIKI, 2010).

Snow accumulation and snowmelt are simulated with a simple approach that estimates snow accumulation is related on a base temperature (Tbase) and snowmelt with a time-degree-factor (TMF). During time periods when air temperature is above Tbase, precipitation and snow melt is transferred to the soil-water module. This module consists of simple water storage with a capacity defined from the field capacity of the specific soil type within the respective modelling unit. For calibration purposes, the entire distribution of storage capacity

values for all modelling units can be shifted up or down with a multiplier (FCA) that has the same value for all modelling entities. Water stored in the soil-water storage can only be taken out through evapotranspiration. The actual evapotranspiration (AET) is determined by the saturation of the soil water storage, the potential evapotranspiration and a calibration coefficient ETR. The ETR coefficient controls when potential evapotranspiration is reduced due to limited water availability. Runoff is generated only when the soil-water storage reaches saturation. The partitioning of generated runoff into direct runoff and percolation is based on the slope of the modelling unit and a calibration factor LVD. The percolation component is transferred to a groundwater storage component; outflow from this storage is simulated using a linear outflow routine in order to calculate baseflow with the help of a recession parameter GWK. The total runoff at the outlet of a catchment results from the summation of the direct runoff and the baseflow components from each modelling unit. The primary purpose of the J2000g model is to provide spatially distributed long-term estimates of the amount and seasonal distribution of the following hydrological quantities: actual evapotranspiration, runoff generation, and groundwater recharge. In the J2000g model, streamflow is computed by simply summing up the runoff components generated in each modelling unit of the catchment. Because of these simplifications, the model cannot account for losses and transformations during runoff concentration or for specific hydrological conditions such as streamflow and groundwater losses in karst regions or the influence of human activities KRAUSE AND HANISCH, 2009).

3.2.1.1 The Snow Module of the J2000g

In the snow module, snow cover computation is implemented as simple accumulation and snowmelt approach. The method decides on the basis of the air temperature whether water is saved as snow on a model unit or potentially existing snow melts and produces snowmelt runoff. For this purpose, two temperatures are calculated from the minimum temperature (Tmin), average temperature (Tavg) and maximum temperature (Tmax), which is given below:

The accumulation temperature as:

$$T_{acc} = (T_{min} + T_{avg})/2 \quad [°C] \hspace{3cm} \text{Equation 3-1}$$

And,the snowmelt temperature as:

$$T_{melt} = (T_{avg} + T_{max})/2 \quad [°C]$$

Equation 3-2

If the accumulation temperature (Tacc) lies on or below a threshold (Tbase) value that needs to be given by the user, it is assumed that potentially occurring precipitation falls as snow. It is then saved on the model unit. If the snowmelt temperature goes beyond the temperature threshold Tbase, the snowmelt is calculated with the help of a simple snowmelt factor (TMF). Therefore, a potential snowmelt rate is calculated on the basis of the TMF (in mm/d K), the temperature threshold and the snowmelt temperature as shown below:

$$SM_p = TMF \; (T_{melt} - T_{base}) \quad [mm/d]$$

Equation 3-3

This potential snowmelt rate is then compared to the actual saved snow water equivalent which is then partly or fully melted. The resulting snowmelt water is passed on as input to the following module.

A more detailed description of the snow module can be found in (http://jams.uni-jena.de/jamswiki/index.php/Hydrological_Model_J2000g) and KRAUSE (2001).

3.2.2 Preparation of Input Data

The model J2000g requires the following data files. Also after developing model for the SWE; a new snow water equivalent data is added as input data files that, shown in the following table.

Table 3-1:Input Data files of J2000g Model

DESCRIPTION	UNITS
Absolute Humidity	g/cm³
Relative Humidity	%
Observed Runoff	m³/m
Observed Rainfall	mm
Observed Snow Water Equivalent(SWE)*	mm
Sunshine Duration	H
Maximum Monthly Temperature	°C
Minimum Monthly Temperature	°C
Mean Monthly Temperature	°C
Wind Speed	m

The needed monthly mean temperature for some stations was not provided, therefore it was computed as the average of the maximum (Tmax) and minimum (Tmin) monthly temperature.

Also, the model requires the absolute humidity as an input parameter dataset. The dataset, hence, has been calculated in several steps, depicted in the following equations:

1. Computation of the saturation vapor pressure es (DINGMAN, 2002:P.586)

$$e_s(T) = 6.1078 * e^{\frac{17.3*T}{T+237.3}}$$
Equation 3-4

2. Computation of the maximum humidity with T as mean air temperature and the computed values for es

$$R_m(T) = e_s * \frac{216.7}{T+273.15}$$
Equation 3-5

3. Computation of the absolute humidity (Ra) by taking relative humidity Ru and maximum humidity Rm into account.

$$R_a(T) = R_m * \frac{R_u}{100}$$

<div align="right">Equation 3-6</div>

All input data files (Table 3-1) were transformed into ASCII- format. In addition to the actual data values, J2000g requires information on geographical location as well as the elevation of the station. The geographical location for the stations was derived using Arc GIS 9.3 (ESRI, 2008). In case of missing elevation data, that information was taken from the available digital elevation model (SRTM 2007).

3.2.3 Parameterization and Calibration

The model J2000g requires parameter input files in order to describe the natural characteristics. These parameter values were obtained from literature and are described in Section3.2.1. Additionally, the model J2000g contains direct model parameters: 1 parameters in the groundwater recharge, 4 parameters in the soil module, and 2 snow module parameters, shown in Appendix A.

The goal of model calibration is a satisfactory fit between simulated and observed variables (REFSGAARD AND STORM, 1996:P.42). Therefore these parameters have to be adjusted. That is necessary for three reasons as stated in BLÖSCHL (2005): First, the hydrological models are based on empirical equations which are depended on basin properties. Second, model boundaries are mostly poorly defined. The model calibration adjusts input errors such as measurement errors. Third, landscape parameters such as soil, vegetation, geology and topography are highly variable in space, and the knowledge of their real occurrences as well as physical properties is limited. Here, parameter adjustment accounts for unknown parameters and characteristics (SCHEFFLER, 2008).

According to REFSGAARD AND STORM (1996), three approaches can be used to calibrate hydrological models: 1) manual adjustment using "trial and error", 2) automatic model calibration, and 3) a combination of 1) and 2). The "trial and error" method requires expert knowledge about the model structure and involves a lot of time because the manual

assessment it needs a larger number of model runs (REFSGAARD AND STORM, 1996:P.47). The automatic model calibration, however, is much faster and less subjective than the manual method (REFSGAARD AND STORM, 1996:P.47). The drawback of the automatic parameter adjustment is the evaluation of the model fit depending only on the objective function, which can lead to a wrong model solution. In order to account for the catchment characteristics and decrease the time effort, a combination of both methods is recommended (REFSGAARD AND STORM, 1996:P.48). In this study, the automatic parameter adjustment was used to define sensitive parameters and parameter ranges.

3.2.3.1 Automatic Parameter Estimation using Sensitivity Analysis

Sensitivity analysis is a significant tool in hydrological modelling. Particularly during the model design and model calibration, sensitivity analysis provides a better understanding of the relationship between model parameters and model processes (MCCUEN, 1973). It allows the identification of sensitive parameters influencing the model output (BAHREMAND AND DE SMEDT, 2008:P.2).

KRAUSE (2010) estimated the parameter sensitivity in J2000g using various methods like single and the multi parameter Monte Carlo Analysis in the mesoscale catchment (BODE), Germany. The author reported that in single parameter approach the seven model parameters (LVD, GWK, Tbase, TMF, FCA, and ETR) some of the parameters particularly two snow parameters (Tbase and TMF) have influence on the model results only in part of the year whereas others are active all the time, but heir impact was quantified as medium to low for the overall period. KRAUSE (2010) also found that in the temporal domain, by looking at runoff ensembles, Tbase had some higher impact in the middle of the time series, but two parameters LVD and GWK had the larger impact on the all of time series and model results. A more detailed description can be found in KRAUSE (2010).

For the parameter sensitivity estimations and their ranges in the Latyan catchment, single and the multi parameter Monte Carlo Analysis method in the monthly model of J2000g has been applied. Here, first, the analysis of the results was made by visual inspection of parameter values versus single efficiency criteria. Additionally the analysis of the multi-parameter estimation was done by visual inspection of 'dotty-plots' and more analytical method described in KRAUSE, (2010). This method was based on 10000 Monte-Carlo runs computed with the parameter ranges shown in table 3-2.

Table 3-2: J2000g parameters and feasible parameter range for monthly

Name	Process	Range(monthly)	Unit
Tbase	Snow	-10 - 0	C
TMF	Snow	0 - 20	mm/K
FCA	Soil water	1 - 20	-
ETR	Soil water	0 - 1	-
LVD	Soil water	0 - 50	-
DQK	dQ retention	1	-
GWK	bQ retention	0 - 10	-

Reactions were then evaluated using four objective functions: Nash-Sutcliffe-Efficiency (NSE) (NASH AND SUTCLIFFE, 1970), logarithmic Nash Sutcliffe Efficiency (log. NSE), relative percentage volume error (pbias) and the coefficient of determination (R²).

- ***Nash- Sutcliffe Efficiency***

The Nash-Sutcliffe Efficiency (NSE) is the model coefficient of efficiency (Nash and Sutcliffe, 1970), which expresses the fraction of the measured streamflow variance that is reproduced by the model. The NaS is calculated as follows:

$$NSE = 1 - \frac{\sum_{i=1}^{n}((Q_{obs})_i - (Q_{sim})_i)^2}{\sum_{i=1}^{n}((Q_{obs})_i - (\overline{Q}_{obs})_i)^2} \qquad \text{Equation 3-7}$$

With Qobs representing the observed runoff value and Qsim the modeled runoff value at time i, obs Q defines the observed mean runoff for the given time period. The range of the NSE lies between $-\infty$ and 1; a NSE of 1, hence, confirms a perfect fit. As stated in KRAUSE, BOYLE ET AL. (2005:P.90), the disadvantage of the NSE is an insensitivity to model over and under predictions, especially in periods of low flow. The authors suggested using the NSE with logarithmic values.

- ***Logarithmic Nash Sutcliffe Efficiency***

The calculation of the logarithmic Nash-Sutcliffe Efficiency (log. NSE) is carried out as follows:

$$\log.NSE = 1 - \frac{\sum_{i=1}^{n}((Q_{obs})_i - (Q_{sim})_i)^2}{\sum_{i=1}^{n}((Q_{obs})_i - (\overline{Q}_{obs})_i)^2}$$
Equation 3-8

The influence of the low flow values is stronger than in the NSE calculation due to the logarithmic values of obs Q, Qobs and Qsim. This leads to a higher sensitivity to over and under estimation of the observed runoff during low flow conditions (KRAUSE, BOYLE ET AL., 2005:P.91).

- **_Relative percentage volume error_**

The percent bias (Pbias) is a measure of the average tendency of the modeled flows to be larger or smaller than their observed values. The optimal PBIAS value is 0.0; a positive value indicates a model bias toward underestimation, whereas a negative value indicates a bias toward overestimation (GUPTA ET AL., 1999). PBIAS is expressed as:

$$PBIAS = \frac{\sum_{i=1}^{n}(Q_{i,obs} - Q_{i,sim})(100)}{\sum_{i=1}^{n}(Q_{i,obs})}$$
Equation 3-9

Pbias is deviation of streamflow discharge, expressed as a percent, Qi,obs is observed stream flow and Qi,sim is simulated streamflow .

- **_Coefficient of determination r ²_**

The coefficient of determination r ² is defined as the squared value of the coefficient of correlation according to Bravais - Pearson. It is calculated as:

$$r^2 = \left(\frac{\sum_{i=1}^{n}(O_i - \overline{O})(P_i - \overline{P})}{\sqrt{\sum_{i=1}^{n}(O_i - \overline{O})^2}\sqrt{\sum_{i=1}^{n}(P_i - \overline{P})^2}} \right)^2$$
Equation 3-10

With O observed and P predicted values.

R ^{2} estimates the combined dispersion against the single dispersion of the observed and predicted series. The range of r^2 lies between 0 and 1 which describes how much of the observed dispersion is explained by the prediction. A value of zero means no correlation at all whereas a value of 1 means that the dispersion of the prediction is equal to that of the observation.

The vital identification of a well fit between the two outputs was the visual comparison of the observed and simulated runoff. In the second step, the "Automatic" method was used to determine final parameter values which acted as baseline values for the estimation of uncertainty.

4.   STUDY AREA AND DATA BASE

The case study chosen is located in semi-arid mountainous region. Snow and snowmelt is a vital source of water supply system. This catchment is one of the most important source of water supply for population about 13 million. Hence prediction of snowmelt can be help to water resource management and developing of water supply system. Unfortunately data base of catchment is not proper and access to various data, especially hydro-meteorological data, except temperature, is complex due to spatial variability and complex topography. Therefore one spatial distributed hydrological model based on availability of data was used for hydrological snow modelling to development of water resource management of area.

 The Latyan catchment covering an area approximately 700 km² is located in about 35 km of north-eastern Tehran (capital of Iran), between Latitudes 35°, 45' to 36°, 50' N and longitudes 51°, 23' to 51°, 51' E. Figure 4-1 shows the situation of the catchment.
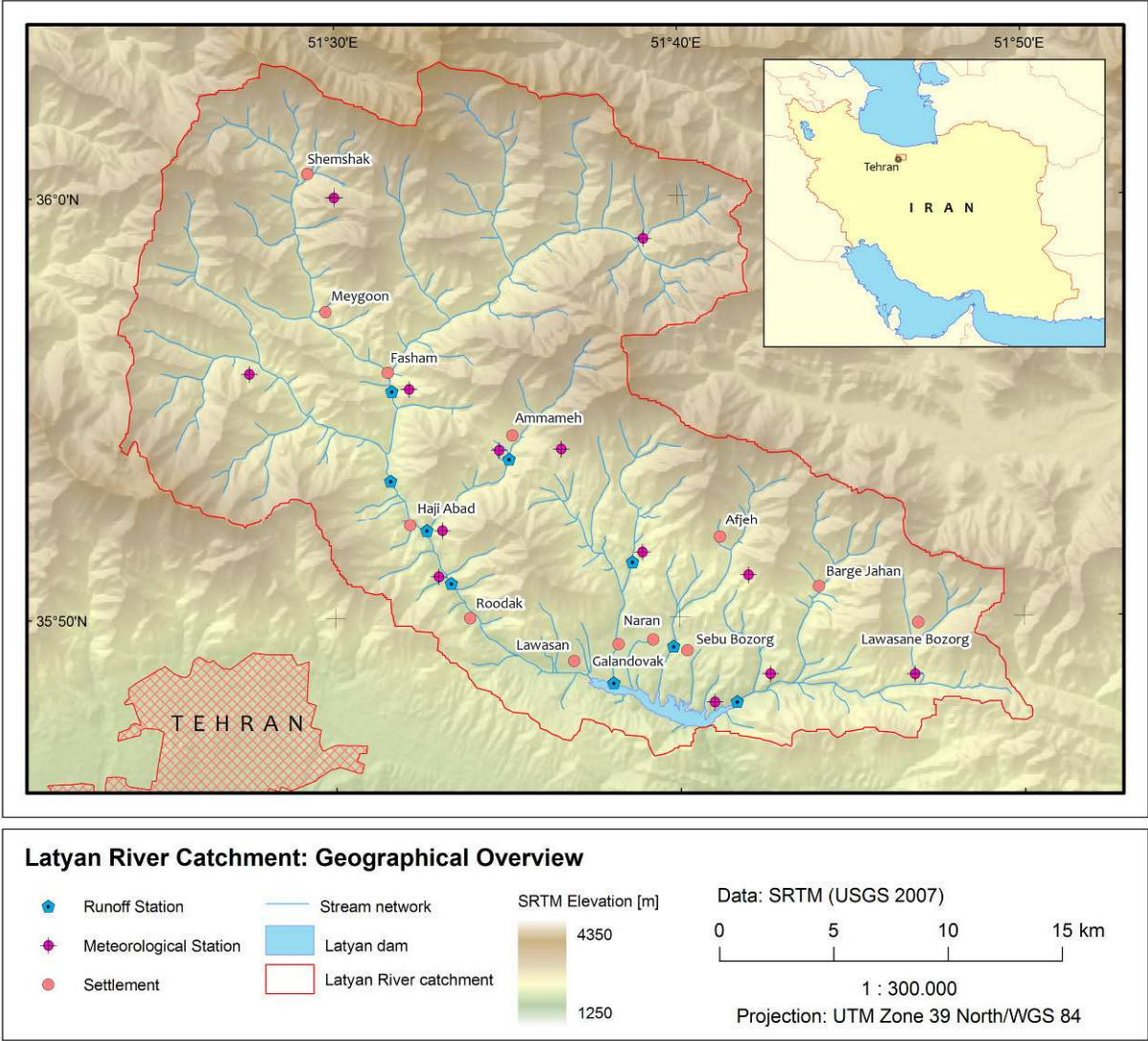
Figure 4-1: Geographical Location of the Latyan catchment

47

The Latyan catchment is located in a mountainous area, and very steep slopes. Elevation difference between the highest and lowest point is about 2825 meters, with the highest point about 4325m.a.s.l at the Valdarbaldar Mountain and the lowest point, at the Latyan dam outlet, about 1500 m.a.s.l..

The main river of this catchment is Jajrood River. North side includes 3 main tributary streams like Garmabdar, Shemshak and Ahar, and joint together with Fasham and Oushan then also in the middle of catchment, Ammameh River and tributary streams of Roodak-Qhuchak joint and then drains in to Lake of Latyan dam. Moreover, in the Eastern part of catchment, streams of Kond, Afjeh, Bargjahan, and Lawasan(north and south Lewarak) with amounts of small tributaries directly drains in to lake dam.

The Latyan dam is one of the primary sources of water supply for the Tehran metropolitan area, with its over 13 million people. From 1988, due to increasing water supply demand of Tehran, yearly about 140 MCM water is transferred to Latyan dam via tunnel from Lar River to Latyan dam. Therefore this extending and transfer water increases the annual volume capability regulation of water dam to 410MCM annually. In addition to its importance for municipal water use, runoff from the Latyan also provides water for agriculture (over 70000 hectares in downstream) and for hydropower generation (45 Megawatt). Besides, this dam, the primary water management structure in the basin, provides water over 95 MCM of storage (http://www.tw.org.ir/dams/selectdam_en.asp).

 Figure of 4-2 illustrates the streams and drainage network of Latyan dam catchment.
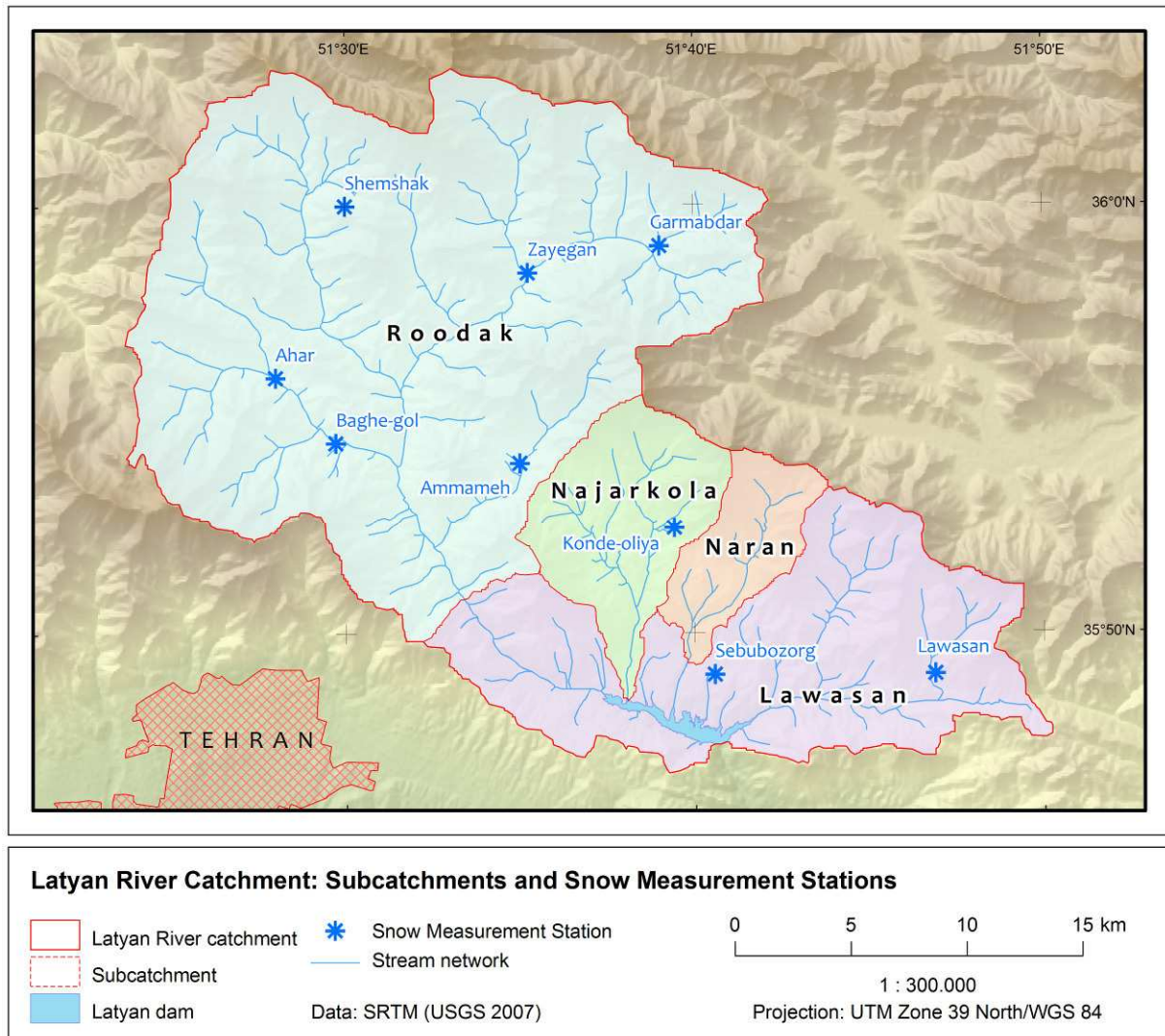
Figure 4-2: Streams and Network and Subcatchments of the Latyan Catchment

4.1 Study Area

4.1.1 Climatic Condition

The Latyan catchment is influenced by Mediterranean and Polar air masses. Distribution of rainfall that belongs to both systems is 27, 39, 30 and 4 for autumn, winter, spring and summer respectively. This distribution rainfall system comparison to distribution of rainfall in Latyan catchment namely 26, 38, 32 and 4 from autumn to summer has very low difference. The characteristic of these air masses is high rainfall in winter and one dry season that continue between 3 to 5 months (WEI, 2004).

Generally can be see an important relationship between rainfall and altitude, namely by increase of altitude, rainfall increase. Normally above 3000 m, rainfall changes to snow.

According to Iranian Water Framework(JAMAB) relation between variability of rainfall to altitude, with due attention to 25 year average of rainfall in 12 rainfall measurement stations Latyan dam catchments is described below:

P = -162.8+0.376Z that,   Equation 3-11

P= annual average precipitation (mm)

Z= altitude of station (m)

According to this function, variability of rainfall to elevation of each 100-meter increase is 37.6mm and correlation coefficient between annual average precipitation and elevation is 0.985(MAHMUDIAN:P.82, 2002). According to Water and Energy Institute(WEI), 2004) reports, based on coefficient correlation between geographical latitude and amount of precipitation at measuring stations of Latyan catchments, variability of rainfall is 10mm. From elevations above 3000 m.a.s.l precipitation form, fallen as snow. After determination of average annual precipitations procedure, average annual precipitation of Latyan catchment is about 573mm.The estimated annual rainfall in Latyan catchment is 406.7 MCM. Minimum of annual rainfall is belong to Qhuchak station with 245mm and annual maximum of rainfall belong to Garmabdar station with 756mm. Out of 39 percent of winter precipitation, about 35% is snowfall that fallen over limestones of high altitude of catchment and make different avalanche forms in tributaries of Shemshak, Ammameh, Laloon, Ahar, and Garmabdar(WEI, 2004). The figure 4-3 shows 40 year mean monthly precipitation in Roodak and Latyan stations. Most of Latyan's precipitation is in winter. It falls at low elevations as rain (winter discharge) and at high elevations as snow, which produces spring discharge as it melts. At intermediate elevations, discharge is a mixture of the two seasons. The maximum of temporal precipitation occur in March and April about 87 and 72 mm for Roodak and Latyan respectively. Additionally minimum of precipitation is occurred in summer especially between August to September about 6 and 3.5 mm for Roodak and Latyan stations.
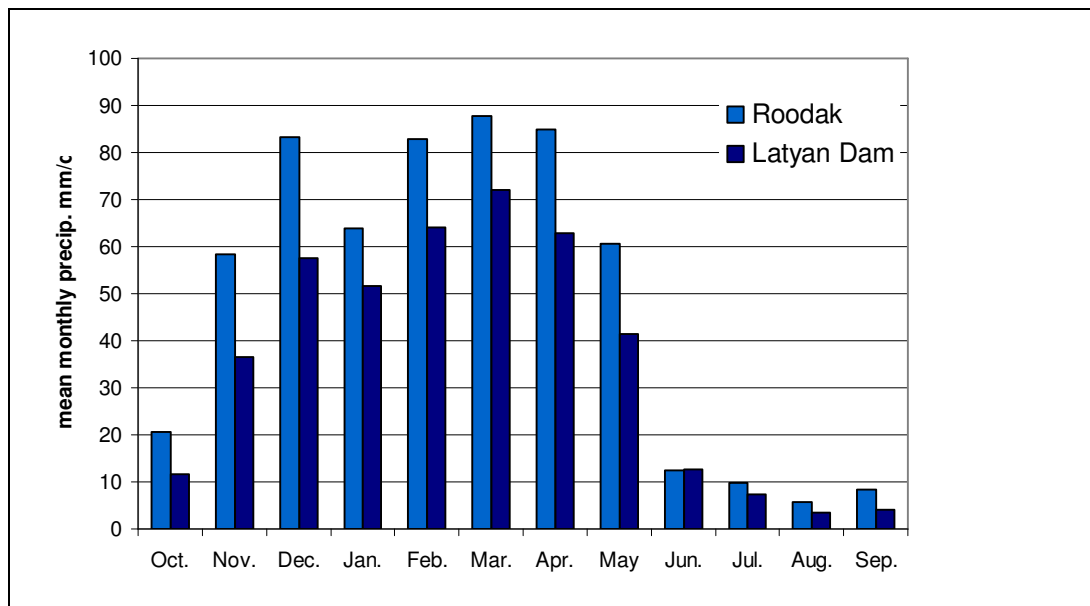
Figure4-3: Mean Annual (1967-2007) Monthly Precipitation in the Latyan Catchment(Latyan and Roodak Station)
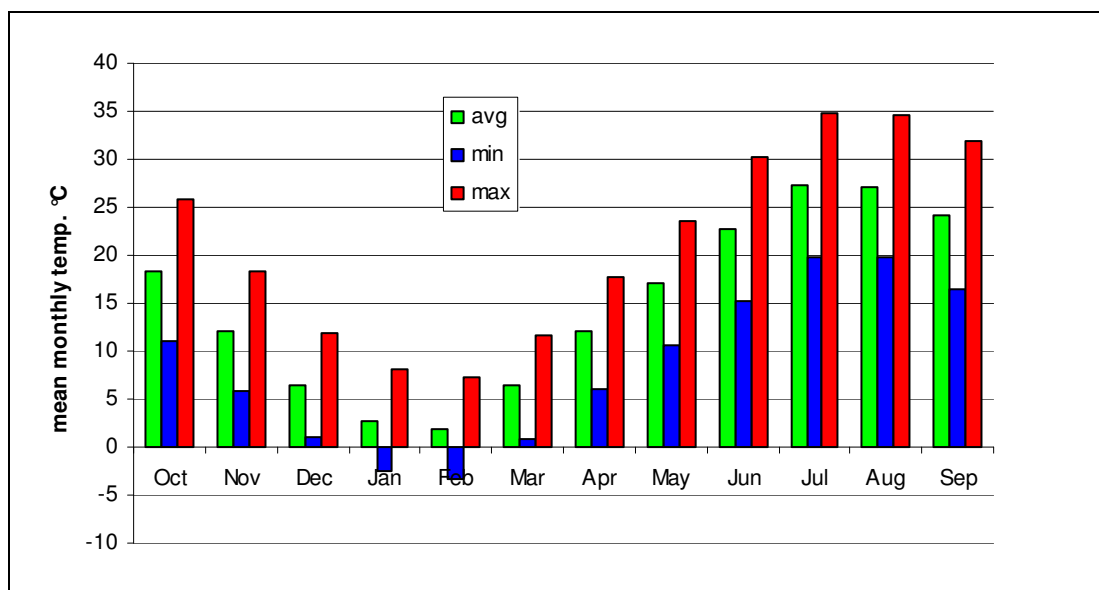
Figure 4-4: Mean Annual (1967-2007) Monthly Precipitation in the Latyan Catchment (Latyan Station)

Generally temperature in months between end of December to middle March fall to below 0°C and this time all the rainfalls fall as snow. Again after March temperature increase to above 0°C and snowmelt start in this time and increasing of temperature will continue and in end of July and August reach to above 30°C (Figure 4-4). Maximum of mean annual temperature of catchment belong to Latyan station with 14 °C and minimum of mean annual temperature with 7 °C belong to Rahatabad station. The absolute minimum temperature belongs to Kamarkhani station is -32°C and absolute maximum of temperature is +38°C in

Latyan station. The mean frozen days is about 75 day and mean dry days are reported about 120 days. According to Amberjeh procedure, can be seen 3 types of climates in Latyan catchment: high elevations, sub humid cold and semi-arid (WEI, 2004).

4.1.2 Geomorphology

4.1.2.1 Slope

The latyan catchment is one of Iranian mountainous catchments and its elevation varies from 1500 meter above see level (m.a.s.l) in Lake Dam to 4300 m.a.s.l in summits. Maximum elevation in this catchment is 4325 m.a.s.l in the Volderbalder Mountain and minimum is 1500 m.a.s.l in outlet of Latyan dam. This catchment is surrounded by Lar dam basin from the north, North Tehran basin from the south, Damavand basin from east and by Karaj basin from west. Base on Hypsometric maps, more than elevations of this catchment are located between 2300-2800 m.a.s.l that is 34% of area catchment. The extent of 44 km² of lands catchment is plateaus and gorge upon alluvial deposits. About 170 km² are geomorphologic unit of hills and 486 km² are mountainous units. Based on gradient maps of Latyan, more than 90% of catchment has gradients above 15% and the higher gradient of catchment located in class of 30-50%. Gradient of above 50% is about 25 percent of all area Latyan catchment. Figure 4-5 shows the slope map of Latyan catchment.
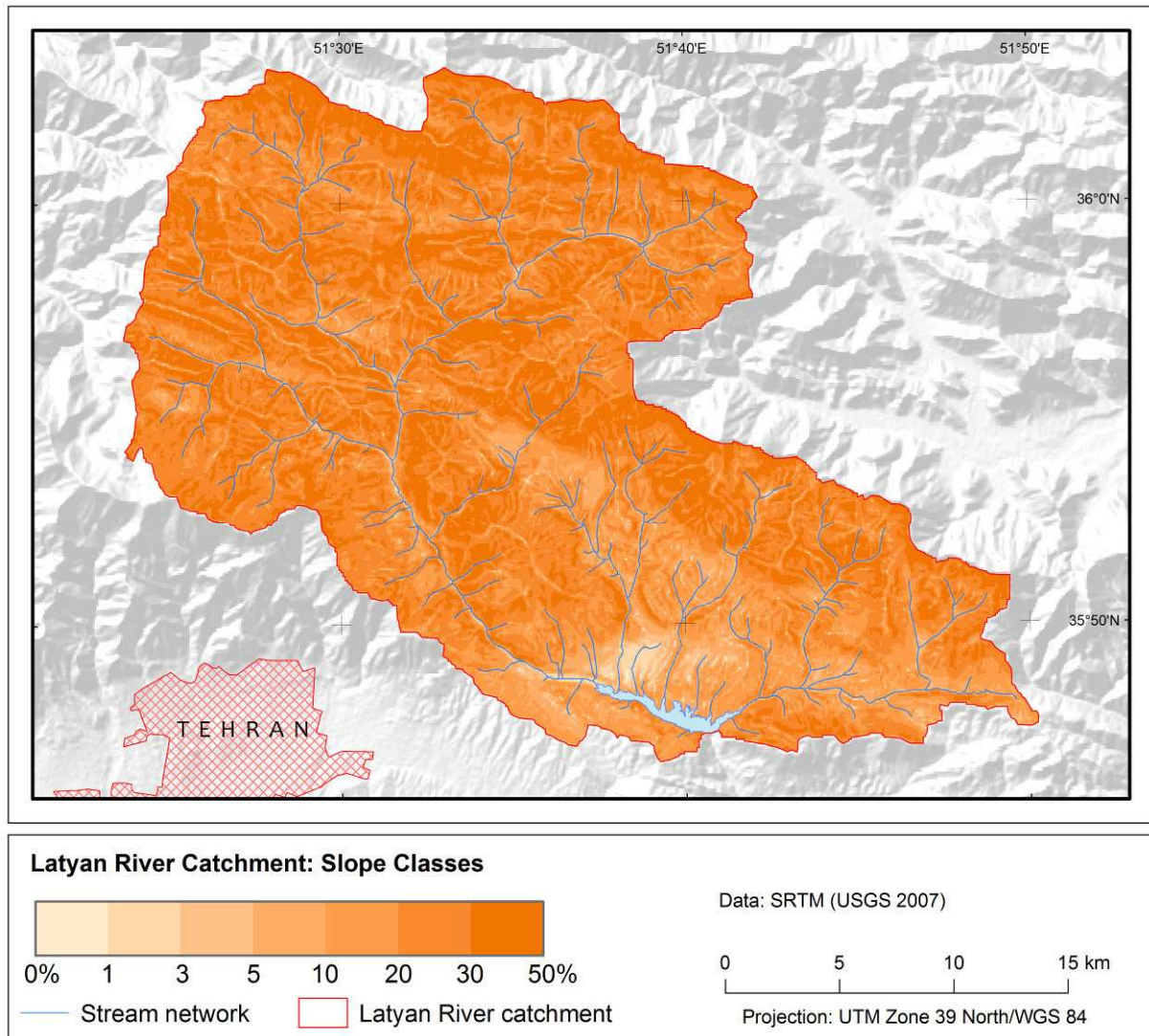
Figure 4-5: Slope Classes in the Latyan Catchment

4.1.2.2 Aspect

Low gradient lands mainly located in south catchment which is around Lake Dam and main tributaries, and high gradient lands are located in limestone elevations of northern catchment. Most of gradient surface (face) is located to direct of south with 33.7% and then with 20% to direct of north. Figure 4-6 illustrates the exposition condition of Latyan catchment.

Latyan River Catchment: Aspect Types

▮ North	— Stream network	Data: SRTM (USGS 2007)	
▮ East	▮ Latyan dam		
▮ South	▭ Latyan River catchment	0 5 10 15 km	
▮ West		Projection: UTM Zone 39 North/WGS 84	
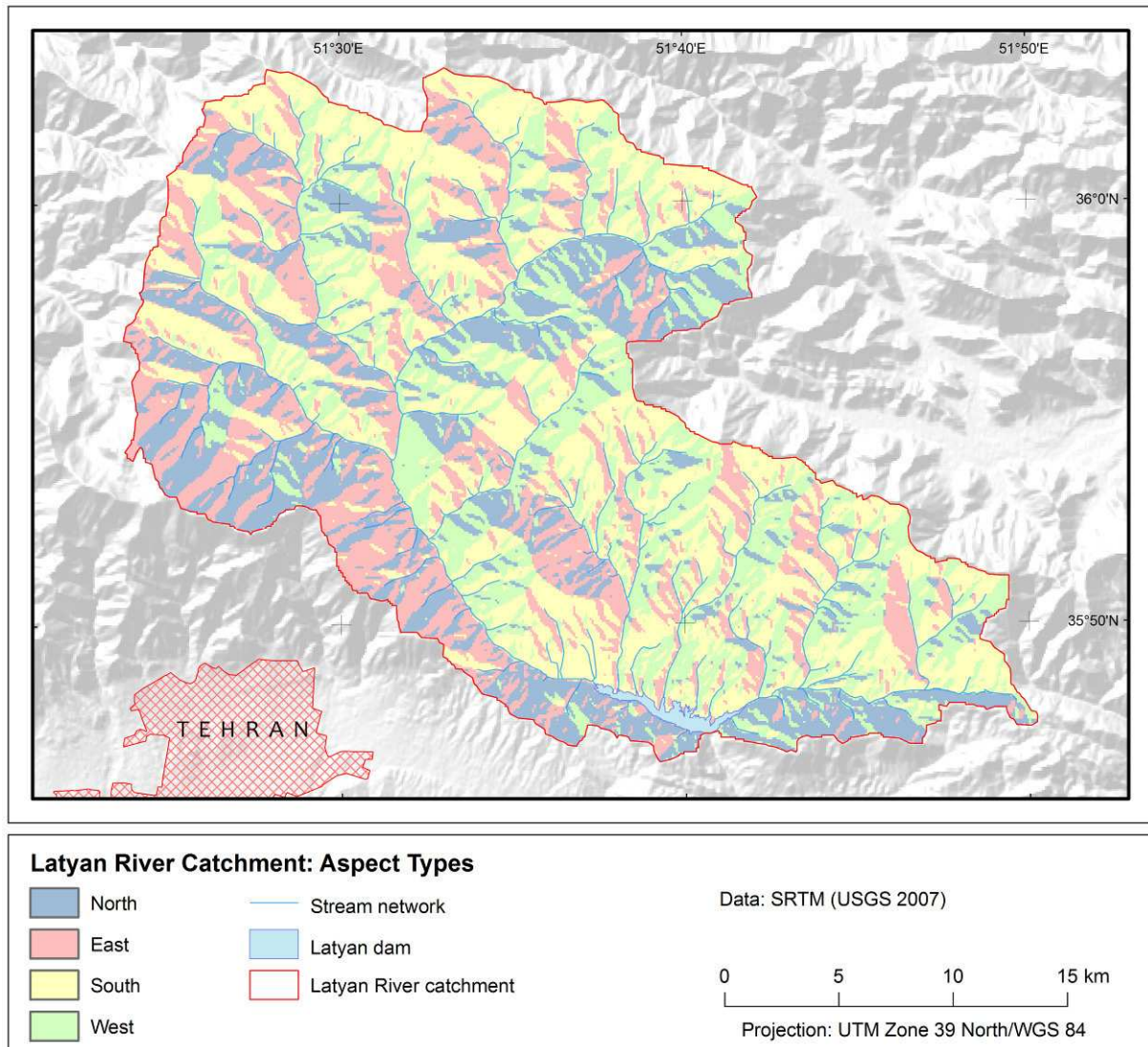
Figure 4-6: exposition condition of the Latyan Catchment

4.1.3 Landcover/Landuse

The land use map for this study with 90 m grid size, showing the land cover for 2005-2006, is depicted in Figure 4-7. The map shows 5 different types of land cover: 81% of the basin is covered by deciduous shrubs, 6% by deciduous broad trees, 2% by short grass, and about 11.0% by agriculture and settlements.

Latyan River Catchment: Landcover

☐ Agriculture	— Stream network	Data: NCC (Iran, 2005)	
☐ Grassland	☐ Latyan dam		
☐ Decidous broadtrees	☐ Latyan River catchment		
☐ Decidious shrubs		0 5 10 15 km	
☐ Settlement		Projection: UTM Zone 39 North/WGS 84	
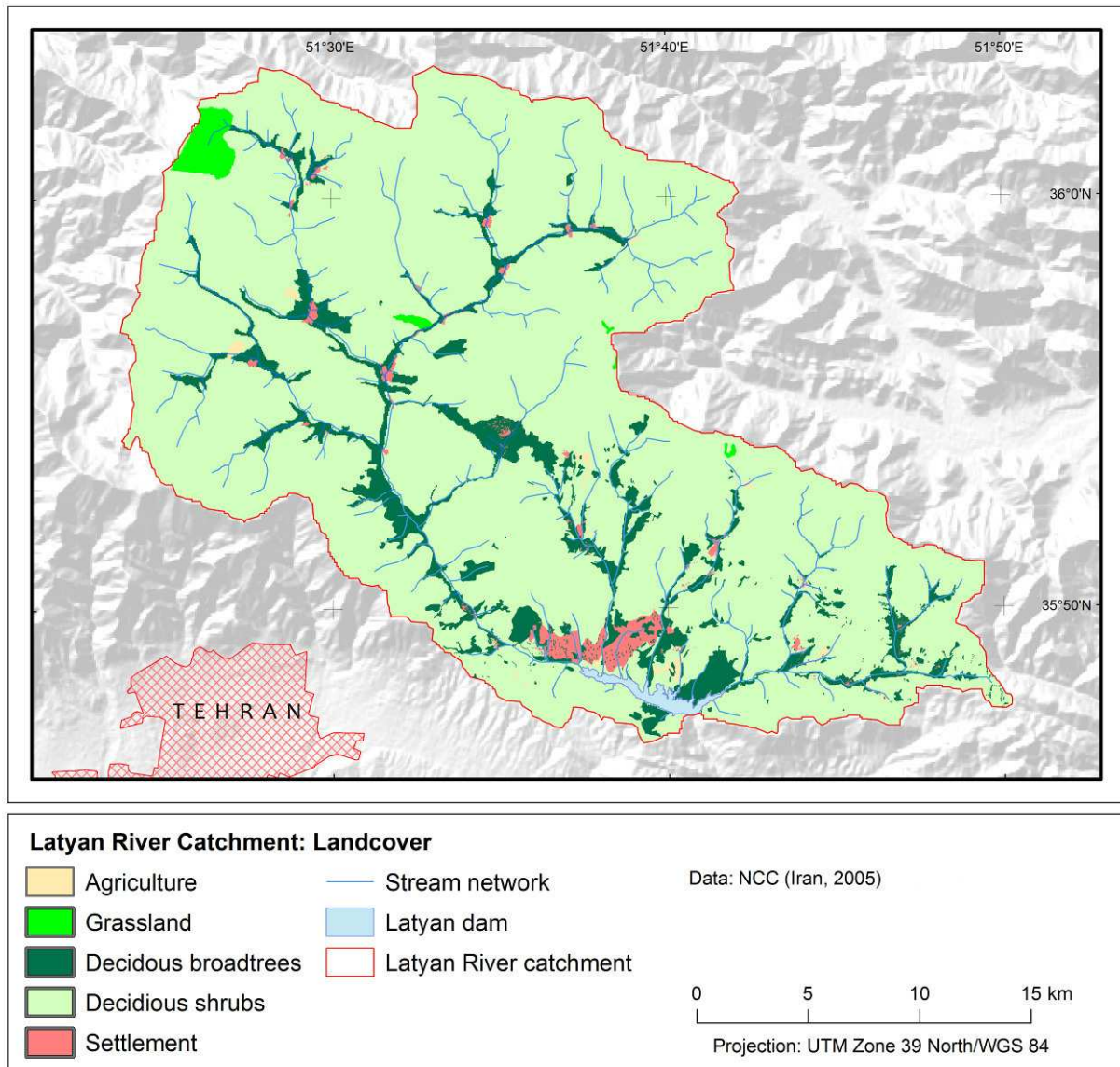
Figure 4-7: Landcover/Landuse of the Latyan Catchment

4.1.4 Geology

The geological characteristic of the Latyan catchment is very complex and is located between zones four and five of the Alborz geological unity and on the middle part of central Alborz Mountains. Therefore, different geological formations from oldest (early Cambrian) to the youngest (Quaternaries sediments) can be found.

In stratigraphy of Latyan catchment, formations of Paleozoic, Mesozoic and Cenozoic has seen. Cambrian, Hiatus of Ordovician, Silurian, Upper Cretaceous, Paleocene and Neocene activities can be seen in the catchment (WEI, 2004, P: 10)

Generally, the northern and central region of the Latyan basin is older than other parts. In this part, different types of tuff (shaly, calcareous and soft), dolomite, limestone, thin layers of

55

sandstone, sandy marl, silt, as well as basaltic-andesitic lava flows and volcanic intrusive screes can be found. In addition, due to mountainous location of catchment, Quaternary activities was limited, but these sediments due to erosion of older formations in long terms deposited in the boarder of the main rivers like Meygoon and Kond River and other tributaries of catchment, especially in the supreme of Latyan lake dam. This part of the catchment is characterized by alluvial fans, scree talus fans as well as terraces and is thereby younger than the rest parts of the catchment and uses by agriculture and farming (WEI, 2004:P.25).

From viewpoints of lithology, Ltyan catchment consists of two parts: first general categories as sedimentary rocks and second, Igneous and Pyroclastics formations.

According to digital geology map of Latyan catchment, the area of igneous and pyroclastics rocks in Latyan dam catchment is about 251 km² and located more in central and southern part of catchment. The area of sedimentary (limestone and dolomite, shale and sandstone,marl) rocks estimated about 102.2 km² and they located more at northern area of catchment. Hence, the northern water tributaries of the Latyan, due to their bedrocks, are carbonated (WEI, 2004:P. 27).

4.1.5 Soil

Soil type of catchment depends on different factors like geological bedrock, climate, overlaying vegetation as well as topographic conditions (SCHEFFLER, 2008).

The following map (Figure 4-8) illustrates the distribution of soil types based on the World Reference Base of Soil (WRB) classification and land capability and resource evaluation map of Tehran province, made by Soil and Water Research Institute of Iran (SWRI, 1991) in the Latyan catchment.
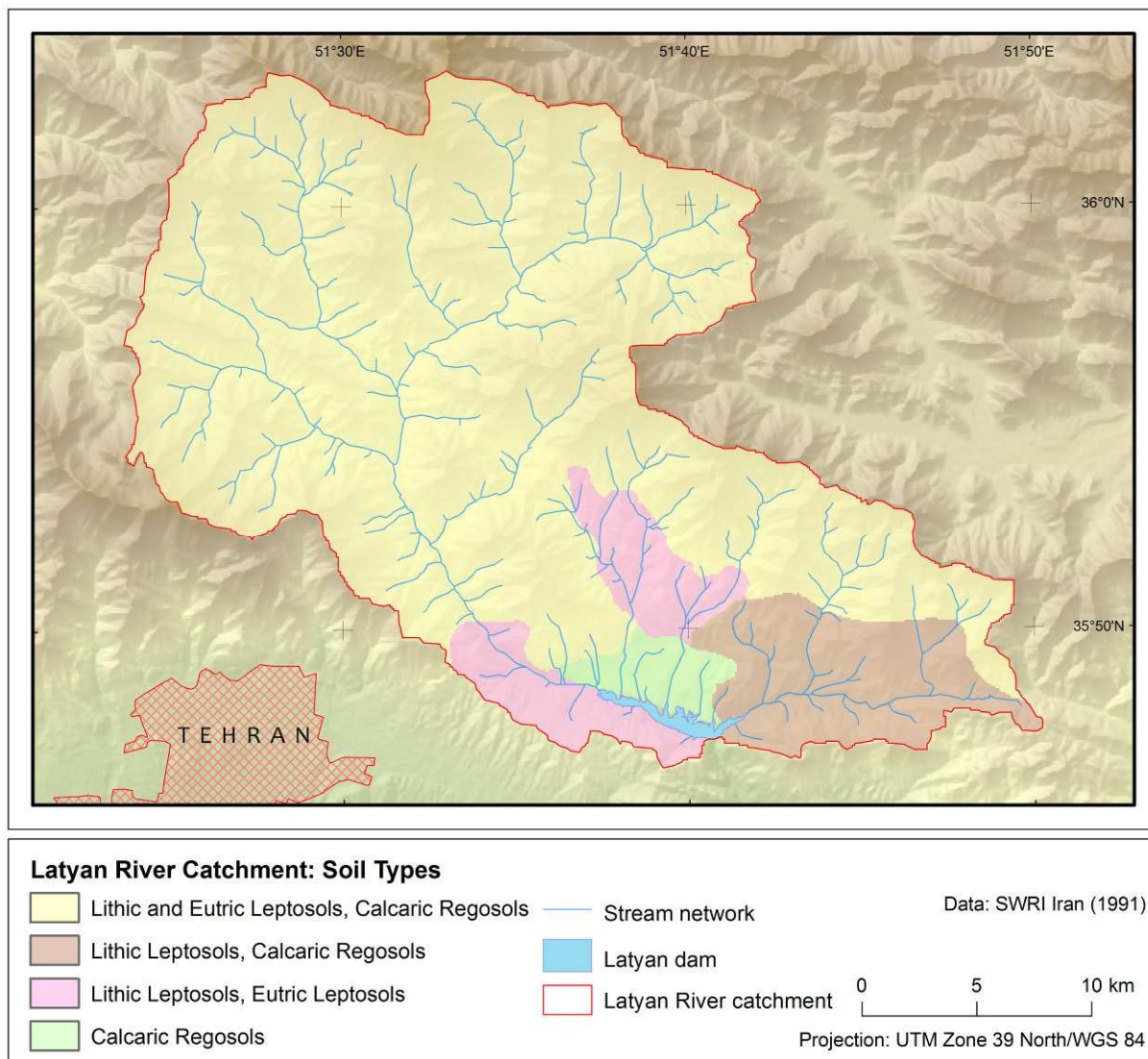
Figure 4-8: Soil Types Map of the Latyan Catchment

Lithic Leptosols, Eutric leptosols as well as Calcaric regosols as independent and combined together with limestone, sandy, shale and conglomerates bedrock are distributed as dominant soil types in Latyan catchment (Jajrood River). This basin is mountainous and characterized by high precipitation as snow in the winter which has formed this weathering soil types in that area. Lithic and Eutric Leptosols with Calcaric Regosols are distributed in upstream and about 80 % area of Latyan catchment (SWRI, 1991). Lithic Leptosols are very shallow, less than 10 cm deep and in mountain areas are the most extensive Leptosols (FAO, ISRIC ET AL., 2006:P. 84, 111). Eutric Leptosols also as second level unit of Leptosols, has a base saturation of 50 percent or more, in a layer, 5 cm or more thick, directly above continuous rock (FAO, ISRIC ET AL., 2006:P. 106). The Leptosols are characterized by weakly developed soils and is a very shallow soil over hard rock or highly calcareous material. This soil type is an azonal

57

soil and particularly common in high mountain regions (FAO, ISRIC ET AL., 2006:P.84). Calcaric Regosols are also found in the catchment, which have similar properties as leptosols. Calcaric soils define as "having calcaric material between 20 and 50 cm from the soil surface or between 20 cm and continuous rock or a cemented or indurated layer, whichever is shallower" (FAO, ISRIC ET AL., 2006:P.103). The Regosols are characterized by "very weakly developed mineral soils in unconsolidated materials" (FAO, ISRIC ET AL., 2006:P.92). These soil types also have a low moisture holding capacity (FAO, ISRIC ET AL., 2006:P.92).

By continuing the river to downstream, Calcaric Regosols developed, which is deeply weathered and characterized by a shallow to deep with fine sand and medium to coarse texture with many lime (SWRI, 1991). According to the same source, on this soil type covered by dry farming and distributed about 2.3 % in the catchment.

In the area of the catchment outlet, the Lithic Leptosols and Eutric Leptosols can be found.These subgroup soiltype are also very poor soil for agricultural use and also are classified as very shallow soils and distributed about 7.6 % area of the Latyan catchment (SWRI, 1991).

4.2   Data Base

4.2.1   Hydro-meteorological datasets

For rainfall-runoff modeling of the Latyan Dam Catchment the following monthly hydro-meteorological time series have been used as input data.

4.2.1.1 Precipitation Data

The rainfall data used were obtained from the Public Weather service of the Iranian Meteorological Organization (WSIMO), Iran Water Resources Management Company (IWRMCO) and Tehran Regional Water Company (TRWCO). This dataset contains rainfall observation between 1967 and 2005 from more than 30 stations. The available stations in the catchment as well as in the surrounding areas were extracted and the proportion of patched values was analyzed. From database of WSIMO, 8 synoptic stations surrounding the catchment were extracted. Figure 4-9 shows the location of meteorological stations

surrounding of the Latyan catchment. For 12 stations within catchment, the rainfall data from the IWRMCO were obtained.
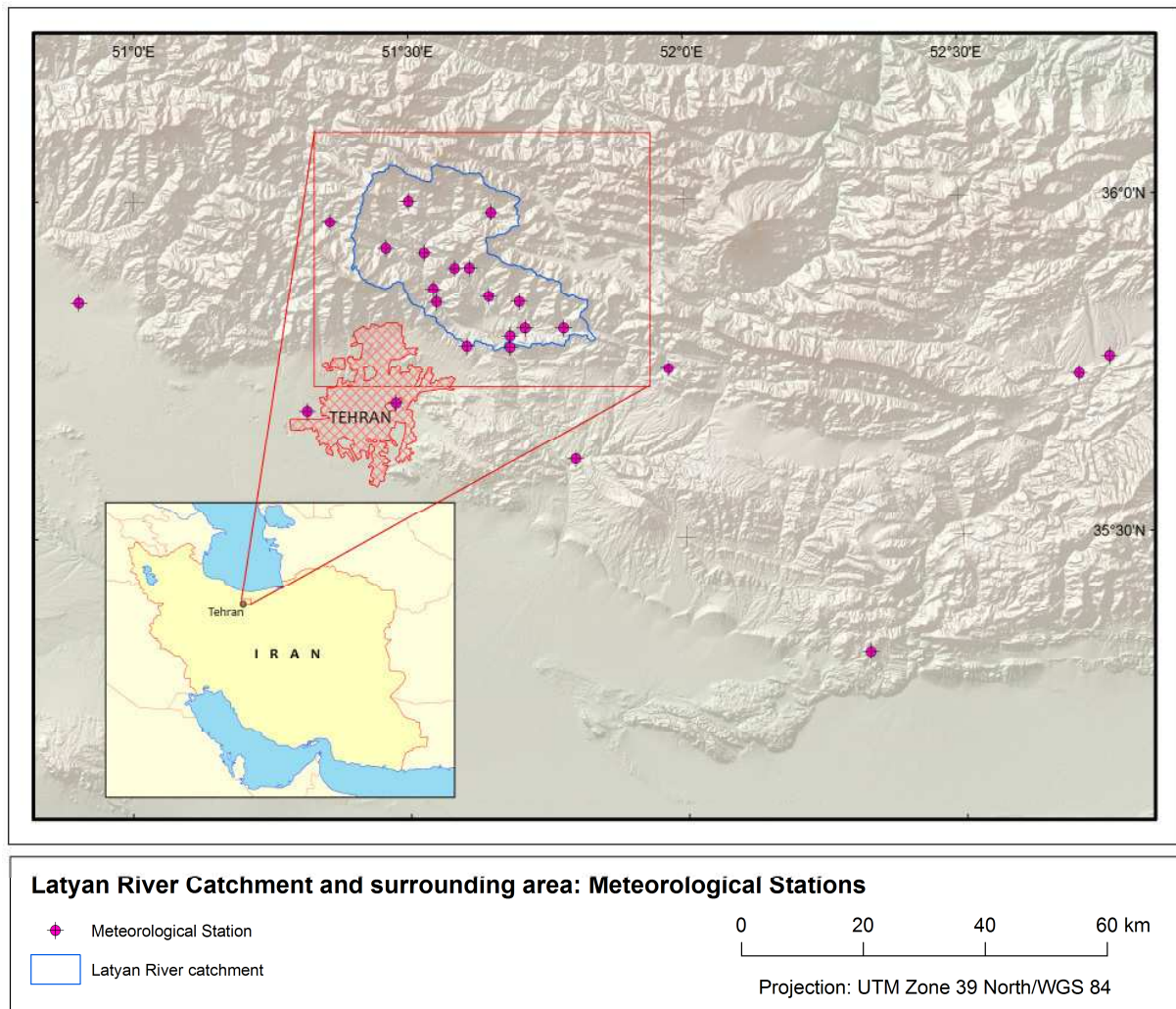
Figure 4-9: The Location of Meteorological Stations inside and around the Latyan Catchment

The data and date format was under text and Persian language. Therefore to better analysis and filling missing data of some stations the format of date and data changed to Excel and standard date. By using linear regression some stations compared together and were filled missing data. Then an experiment to model the catchment with all 20 rainfall data the simulation improved, which indicated that the originally excluded stations were a good source of data. Therefore, it can be assumed that the patched data are a good estimate of the actual rainfall amount and can be used in this study.

4.2.1.2 Temperature Data

There were two data sources used for the temperature data (Table 4-1) data were provided by the WSIMO That includes monthly minimum and maximum temperature data for the time period 1951 to 2003 around of Latyan catchment (Figure 4-9) Data were provided by the IWRMCO and TRWCO which contains daily and monthly of minimum and maximum temperature data for the time period 1967 to 2005 inside of Latyan catchment.

Table 4-1: Temperature Measurement Stations

STATION NUMBER	STATION NAME	START RECORD	END RECORD	LAT	LON	ELEVATION	SOURCE
41-119	Latyan	1967	2005	35.47	51.41	1560	IWRM
41-772	Ammameh	1967	2005	35.54	51.35	2200	IWRM
41-336	Shahrestanak	1967	2002	35.58	51.21	2200	IWRM
41-121	Mamlou	1967	2002	35.37	51.48	1300	IWRM
40-751	Tajrish	1988	2003	35.47	51.37	1548	WSIMO
40-754	Mehrabad airport	1951	2003	35.41	51.19	1191	WSIMO
40-753	Doshantape airport	1972	2003	35.42	51.20	1209	WSIMO
40-752	Karaj	1985	2003	35.55	50.54	1312	WSIMO
40-756	Firozkouh	1993	2003	35.55	52.50	1976	WSIMO
99-370	FirouzkoohPollution	1995	2000	35.43	52.24	2986	WSIMO
40-755	Abali	1983	2003	35.45	51.53	2465	WSIMO

4.2.1.3 Additional Climatic Parameters

The additional climatological parameters (wind speed, sunshine duration and relative humidity) were provided by the WSIMO. Despite the existence of the Latyan, Ammameh,Rahatabad, and Kamarkhani stations, long-term daily and monthly measurements for these parameters within the catchment were not available or incomplete. Therefore, measurements in the area surrounding stations like, the Tajrish, Mehrabad airport, Doshantapeh airport, Abali, Firouzkooh, Firouzkooh pollution, and Karaj synoptic stations, located near and up to 100 km away from the catchment, were taken into account, as shown in the following table.

Table 4-2: Additional Clamatic Parameters

STATION NUMBER	STATION NAME	START RECORD	END RECORD	LAT	LON	ELEVATION	MEASURED PARAMETER
41-119	Latyan	1986	2002	35.47	51.41	1560	Rhum,Wind, Sun
41-772	Ammameh	2000	2002	35.54	51.35	2200	Rhum
41-776	Rahatabad	2000	2002	35.54	51.37	2450	Rhum,Wind
41-115	Kamarkhani	2000	2002	35.52	51.33	1890	Rhum
40-751	Tajrish	1988	2003	35.47	51.37	1548	Rhum, Wind, Sun
40-754	Mehrabad airport	1967	2003	35.41	51.19	1191	Rhum, Wind, Sun
40-753	Doshantape airport	1972	2003	35.42	51.20	1209	Rhum, Wind, Sun
40-752	Karaj	1985	2003	35.55	50.54	1312	Rhum, Wind, Sun
40-756	Firozkouh	1993	2003	35.55	52.50	1976	Rhum,Wind, Sun
99-370	Firouzkooh Pollution	1995	2000	35.43	52.24	2986	Rhum,Wind, Sun
40-755	Abali	1983	2003	35.45	51.53	2465	Rhum,Wind, Sun

The relative humidity was measured at twelve stations but only five stations (Abali, Tajrish, Mehrabad airport, Doshantappeh, and Karaj) had proper data. Eight stations (Latyan, Mehrabad airport, Doshantapeh, Tajrish, Abali, Firouzkooh, Firouzkooh pollution and Karaj) recorded sunshine duration and nine station (Latyan, Rahatabad, Abali, Tajrish, Mehrabad airport, Doshantapeh, Firouzkooh, Firouzkooh pollution and Karaj) provided wind speed measurements.

4.2.1.4 Runoff Data

The discharge data was provided by the Iran Water Resources Management Company (IWRMCO) and Tehran Regional Water Company (TRWCO). Mentioned data are contains daily and monthly runoff data for the time period 1971 to 2005 eight runoff gauges Latyan catchment. The catchment outlet is the hydrometric station 41-119 (Latyan), which went into operation in October 1945 and has been delivering manually and recorder cable since 1945.

4.2.2 Spatial Datasets (GIS-Data)

Hydrogeological investigation over large areas requires assimilation of information from many sites each with a unique geographic location. GIS maintains the spatial location of sampling points, and provides tools to relate the sampling data contained through a relational database. Therefore, it can be used effectively for the analysis of spatially distributed hydrogeological data and modelling (SHAHID AND BEHRAWAN, 2008).

The version of J2000g model uses distributed model entities as input. These entities are based on the concept of the HRUs (FLÜGEL, 1995; FLÜGEL, 1996) using GIS-datasets of land cover, soil, geology as well as a DEM. The datasets used in this study are summarized in Table 4-3. The Shuttle Radar Topography Mission (SRTM) dataset (U.S. GEOLOGICAL SURVEY EROS DATA CENTER AND NASA, 2007) provided information on topography parameters such as elevation, slope and aspect. Additionally, it was used to delineate the stream network, catchment borders and sub catchments. Information on soil type was derived using land capability and resources evaluation map of province Tehran (1991) from the Ministry of Agriculture of Iran, Soil and Water Research Institute (SWRI).The map as mentioned, contains difference datasets of province of Tehran mentioned Latyan Catchment as landtype, soil texture for the soil types, soil classes with (FAO) classification and capability and limits of lands. The geological information was derived form geological map of Iran series 1:100000, Tehran(1996), East of Tehran(1997), Damavand(1997), Baladeh(1993), Marzanabad(2001) sheets from the ministry of Mines and Metals of Iran, Geological Survey Organization of Iran(GSI), and from SHESHANGOSHT ET AL., (2006). The land cover and land use parameters (vegetation type and another utility) were obtained using the National Cartographic Center of Iran (NCC), and from SHESHANGOSHT ET AL., (2006) and ZEINIVAND AND DE SMEDT (2008).

Table 4-3: GIS-dataset for HRU- delineation

Dataset	Description	Format	Resolution	Source	Model - Parameter
DEM	Shuttle Radar Topography Mission(SRTM)	Raster	90m²	US Geological Survey(2007)	Elevation Slope, Aspect Stream network
Geology	Geological maps (Tehran, East Tehran, Damavand, Baladeh)	Vector	1:100.000	Geological Survey Organisation, Iran(GSI), (1993, 1997, 2001)	Bedrock Characteristic, Maximum Perculation
Soil	land capability and resources evaluation map of province Tehran	Vector	1:250.000	Soil and Water Research Institute(SWRI), Iran, 1991	Soiltype, Soil texture
Land Cover	Topographic, Maps Block 15, Tehran Province, 2004	Vector	1:50.000	National Cartographic Center(NCC), Iran, 2004	Vegetation Type, Vegetation height

For the HRU delineation, all datasets should have the same spatial resolution as well as projection. Therefore, all datasets were transformed into the UTM-Projection, Zone 39 North with a spatial resolution of 90 m. Datasets, having a coarser spatial resolution, such as soil information, land cover, and geology have been resampled in ArcGIS 9.3 (ESRI, 2008) using the nearest neighborhood method.

5. RESULTS AND DISCUSSION

In this chapter, the results of the study will be presented. The chapter is divided into three sections. First, in the data analysis section (Section 5.1.1), the input data will be checked for missing values as well as for plausibility. Subsequently, a system analysis will be carried out to investigate the data for indications of an influence on the hydrological response. Second, the conclusion drawn from this analysis will be used for the model calibration and validation (Section 5.2). The modelling outputs will also be investigated for their sensitivity to parameter changes. The conclusions will later be used to assess the snowmelt modelling results. Third, to compare the simulated SWE single HRU stations with the SWE time series, the area under investigation had to be determined (Section 5.3.1). After doing so, the model entities lying in this area of interest are averaged using the area weight, and then compared to the SWE time series (Section 5.3.2). In this step, similarities and variations in long term (trend) and short term (seasonal) SWE will be highlighted. This analysis will give an insight on the evolution of the snowmelt and SWE modelled time series and therefore information on future behavior can be drawn. Based on these results, the capability of the model J2000g for snowmelt modelling will be analyzed.

5.1 System Analysis and Delineation of Hydrological Response Units

5.1.1 Data Analysis and System Analysis

5.1.1.1 Precipitation Data Analysis

As documented in Section 4.2.1.1, the rainfall data needed in this study were collected by WSIMO and IWRMCO. The 24 rainfall stations (Figure 4-9) in and surrounding the catchment area were extracted from this database and used in this study. As discussed in Section 4.2.1.1, the data filled using a combination of algorithms such as inverse distance weighting, linear regression techniques.

For each station the long term monthly and yearly statistical parameters mean, minimum, maximum and standard deviation were calculated for the time frame from 1970 to 2004. The long term mean annual precipitation amounts to between 420 and 563 mm with a standard deviation ranging from 96 mm to 143 mm. The regression analysis reveals a very strong positive relationship between the standard deviation and the mean values ($R^2 = 0.85$). In other words, the year-to-year variability increases with an increasing mean annual rainfall.

5.1.1.2 Discharge Data Analysis

The double mass approach, explained in the Section 3.1.1.1, has been applied to analyze the runoff observation between stations along the Latyan catchment stream. Figure 5-1 shows the double mass–analysis between the runoff stations Latyan and Roodak as well as Naran and Najarkola(Galandoak), whose locations are shown Figure 4-1.

The left hand side of Figure 5-1 shows the double mass curve between the catchment outlet (Latyan) and the Roodak station, located approximately 3km upstream from the Latyan station. On the right hand side of the figure, the double mass curve between the Naran and the Najarkola stations is illustrated. The Naran measuring station records the discharge of the Naran River, a tributary to the Latyan Dam Lake. The Najarkola runoff station lays about 1 km before the Naran River joins the Latyan Dam Lake. The two runoff stations are approximately 1.5 km apart from each other, shown in Figure 4-1.
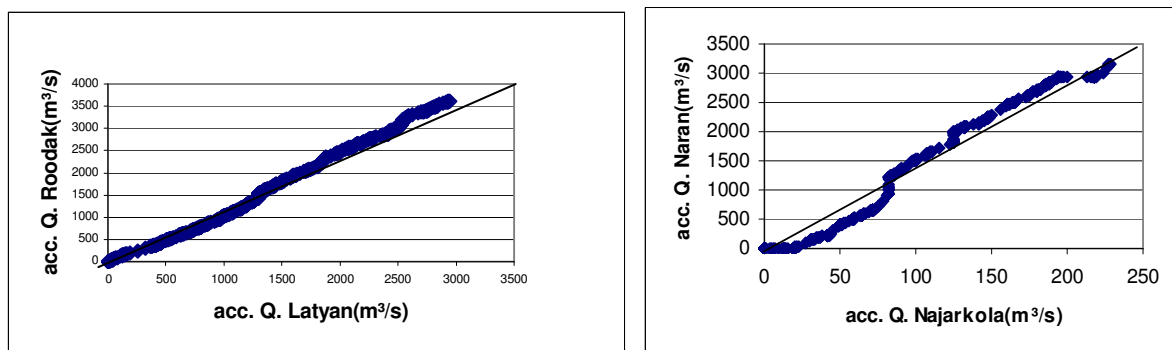
Figure5-1: Dubble Curve Mass Analysis in the Latyan Catchment

The double mass curve on the left side of Figure 5-1, shows that runoff relationship between the two station had been changed, and "more" runoff has been recorded at the outlet station (Latyan) than at the upstream station (Roodak) within the 1970 to 2004 time frame. The comparison of this curve with the mean annual precipitation-data indicates that these characteristics could be explained by anthropogenic influences and natural factors like long time droughton the river discharge. The first section marks the time period until the end of 1982, characterized by an above average mean annual precipitation (MAP) (Figure 5-2). The years from 1980 to 1989, with the exception of one year 1982 are characterized by low precipitation, whereas the years from 1972-78 and 1996-2001 show above average MAP.The changes in slope can be explained by water uptake along the river before the Roodak station or technical measuring problems, especially during the years with low precipitation (1970 to 1992).

This argument of anthropogenic impacts on the stream flow volume is supported by the analysis of the second double mass curve on the right hand with same condition of graph

This double mass analysis indicates intensive anthropogenic regulation of the discharge and natural condition of drought. The discharge in the river stream is especially ruled by the major dams, Latyan dam, located in the outlet of the catchment. To reduce the anthropogenic influence in the rainfall-runoff modeling, the catchment area of the dams was not taken into model calibration.

5.1.1.3 Temporal Relationship between Precipitation and Discharge in the Latyan Catchment

The hydrological modelling of the catchment of Latyan requires an understanding of the natural as well as anthropogenic influences on the runoff generation as shown in the preceding analysis. The rainfall-runoff interaction analysis was carried out for a longer time period (1970-2004) than in the actual study (1990-2001). This was done to gain more information on the system. The investigation focuses on the annual, seasonal and monthly temporal scale.

Figure 5-2 compares the long term mean annual precipitation (blue bars) to the annual runoff sum (blue line), as well as the variation from the 34 years average for rainfall (blue filled bars) and runoff (blue unfilled bars).
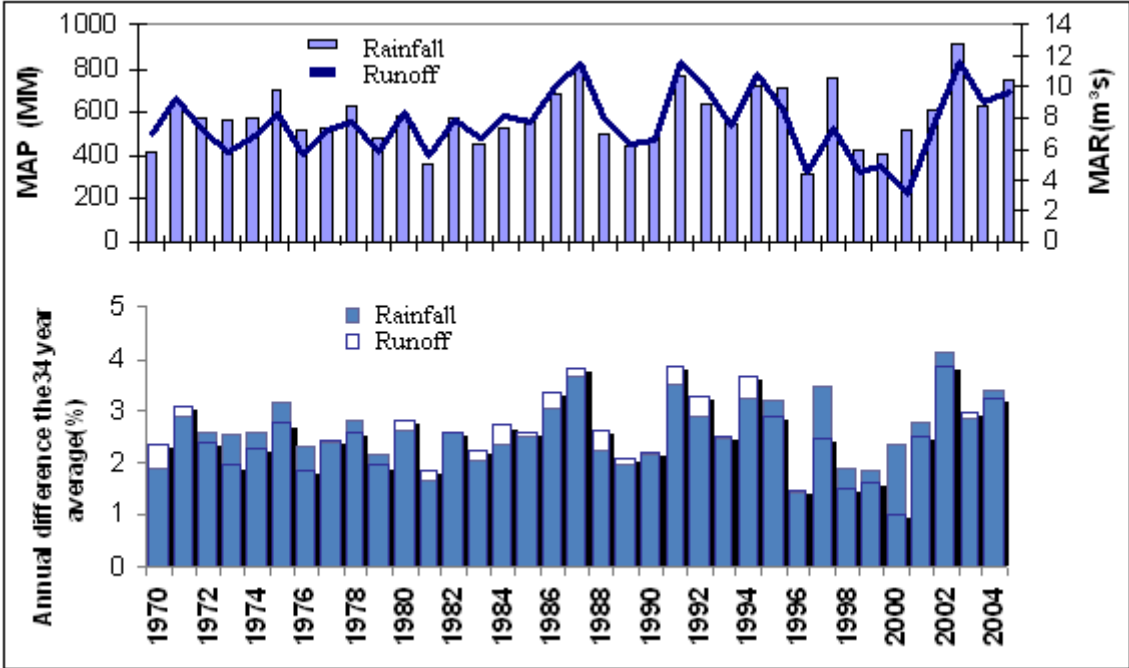
Figure 5-2: The 34 years Evaluations of rainfall and Runoff in the Latyan catchment, (Roodak Station)

The figure shows that the years between 1972 to1979, 1982, 1990 and 1995 to 2002 are characterized with rainfall above the runoff. The rest years runoff was above rainfall. Comparing this with the recorded runoff it is shown that the runoff follows the precipitation dynamics. However, there are some exceptions, which reflect the anthropogenic influence and the high water demand in this region. The double mass curve analysis for 4 stations indicated 2 time duration difference, one time human-made activity from 1980 through 1989, another time from 1995 to 2001. In particular between 1980 to 1989 data analysis showed that the result were influence the human-made activities an data was not correct , because in this time Iran was involve the Iraq war. Increasing water demand and severe drought occurred in the region (JAHANI and REYHANI, 2006).

In the next step, the seasonal variability has been studied. The Latyan catchment lies in the semi-arid climate zone and located at the mountainous area with a difference topography and variability between the dry and wet seasons, as illustrated in Figure 5-3.

Figure 5-3 compares the average monthly values of the runoff rate (blue line) at the outlet of the subcatchment and the observed precipitation (blue bars).

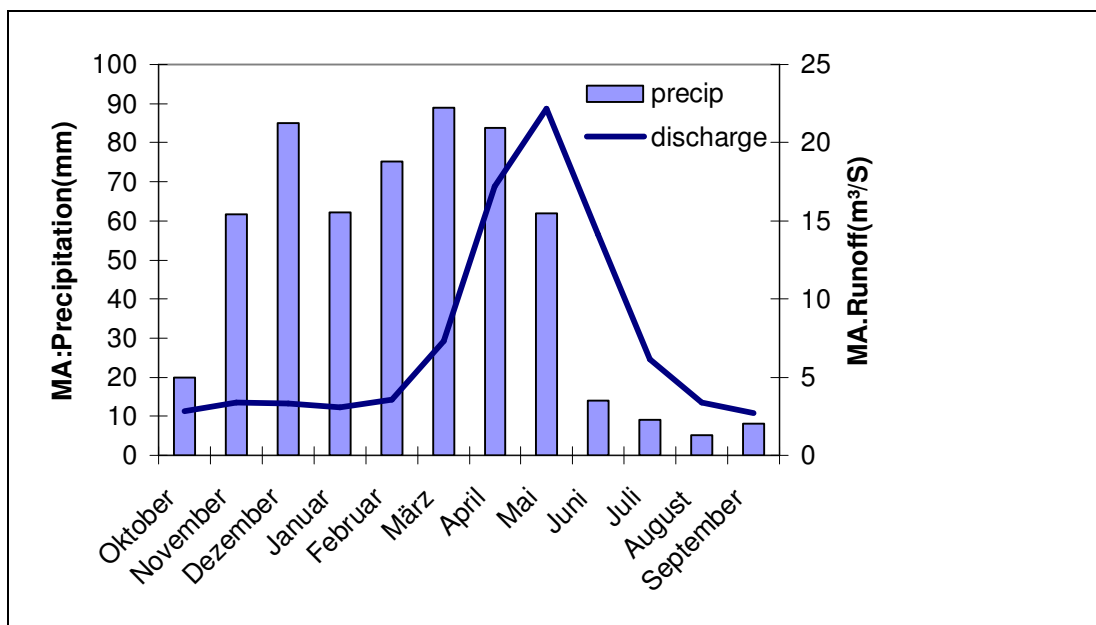Figure 5-3: The34 years Monthly Average of rainfall and runoff in the Latyan Catchment (Roodak station)

The figure is based on data from 1970 to 2004. As shown in the figure, the temporal variability in rainfall amount varies between the dry and wet periods. In the wet period

(November to May) about 518 mm, corresponding to 90 % of the annual rainfall, are recorded. In the dry season (June to September) the measured monthly rainfall amounts to less than 56 mm, whereas during June to August only 13 to 5 mm precipitation are documented. The high temporal variability is also reflected in the runoff, as shown in the differences between the low flow and high flow seasons (Figure 5-3). During the dry season, the average monthly flow rate fall under 2.6 m³/s. It indicated that in dry season catchment rivers are related to snow melt runoff for the river. The wet season, however, is characterized by low discharge values but with a runoff peak in the May and not corresponds to the precipitation peak. It can be concluded that more than precipitation of catchment fall as snow and Runoff River is related to snowmelt.

5.1.2 Spatial Dataset

Table 4-3 shows the datasets used to delineate the HRUs used in the model. In order to achieve a common spatial resolution the raster datasets, land cover and the DEM, were resampled to 90 m. The vector datasets, the soil data and the geology dataset, were converted into raster files with a resolution of 90 m by applying the nearest neighbour method. All GIS-data files were than transformed into the UTM Projection, Zone 39 North.

The DEM delineated from the SRTM-data (U.S. GEOLOGICAL SURVEY EROS DATA CENTER AND NASA, 2007) was used to derive topographical parameters such as aspect and slope. Therefore, the dataset had to first be prepared and sinks had to be filled (WOLF, 2009) with the "fill" routine implemented in ArcInfo within ArcGIS Destop 9.3 (ESRI, 2008). Afterwards, flow direction and flow accumulation were delineated in ArcInfo within ArcGIS Desktop 9.3 (ESRI, 2008). An accumulation threshold of 250 cells was used for the delineation of the stream network. The resulting stream network was compared visually to the available topographic maps and corrected if necessary. Afterwards, the sub catchments were delineated using the Spatial Analyst Tools within ArcGIS Desktop 9.3 (ESRI, 2008). The location of available hydrometric stations was corrected so that the runoff stations were located on the delineated stream network. As a result, 4 sub catchments with areas from 31 to 430 km² were delineated.

The hydro-meteorological time series (Table 4-1, Table 4-2) are representing measurements at point scale. To obtain spatial information for these hydro-meteorological parameters, the measurements had to spatially generalized using the IDW- method implemented in J2000g (KRAUSE, 2001; JAMSWIKI, 2010) described in Section 3.2.1.

5.1.3 Delineation of Hydrological Response Units

The delineation of the HRUs consists of several steps, as shown in Figure 5-4 In the first step the individual GIS-datasets will be reclassified according to their hydrological significance. Then the prepared datasets will be overlaid on one another and, if necessary, reclassified again. Afterwards, small polygons under a certain threshold will be aggregated into neighboring polygons

Finally, the resulting HRUs will act as model entities in the hydrological model. The following sections give a more detailed description of these steps.
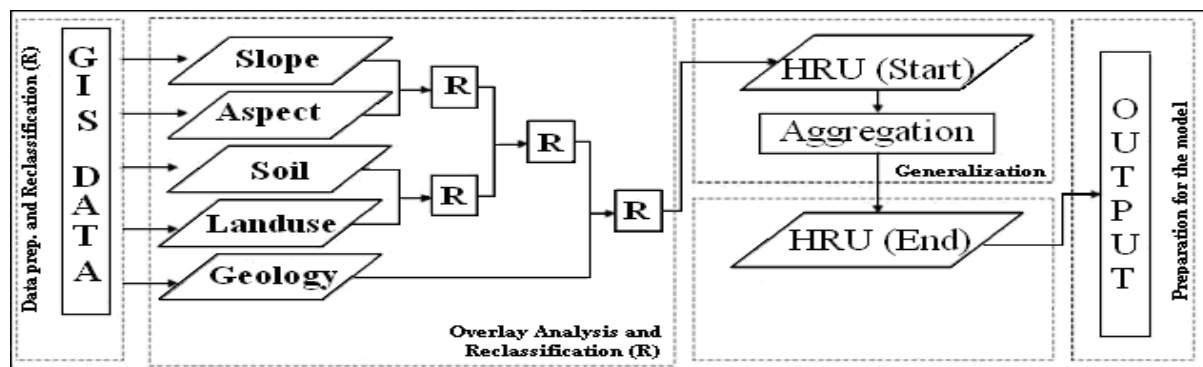
Figure 5-4: Flow-chart of the Delineation of HRUs for the J2000g model (Source: SCHEFFLER, 2008)

5.1.3.1 Data Preparation and Reclassification

The first step of the HRU-delineation involves data preparation and reclassification of the GIS-datasets. This is necessary to meet the requirements for the hydrological model (KRAUSE, 2001:P. 140). The single values of the topography, slope, aspect, geology, and soil and land cover datasets are reclassified according to their hydrological importance to reduce the number of HRUs.

The slope values were grouped into the following classes: low slope areas (0-5°), medium slope areas (5- 15°) and high slope areas (>15°) according to the work of BONGARTZ (2001). For the aspect, classes modified from BONGARTZ (2001) HELMSCHROT (2006) and SCHEFFLER (2008) have been used, as shown in Table 5-1

Table 5-1: Reclassify the aspect

Class	Descrption	Aspect in°
1	North	337.5 – 360; 0 – 22.5
	Northeast	22.5 – 67.5
	Northwest	292.5 – 337.5
2	Southeast	112.5 – 157.5
	South	157.5 – 202.5
	Southwest	202.5 – 247.5
3	West	247.5 – 292.5
	East	67.5 – 112.5

Due to no specific soil data available for the Latyan catchment, a soil map and other information on soil type was derived using land capability and resources evaluation map of province Tehran, Iran from Soil and Water Research Institute (SWRI, 1991). First the soil map of (SWRI) georeferenced using georeferencing tools of ArcMap ArcGIS 9.3(ESRI, 2008), then the boundary of catchment and soil classes were digitized using edit tools of ArcMap ArcGIS 9.3(ESRI, 2008).After analyzing the available soil dataset (SWRI, 1991), the following classes for the catchment were delineated .

Table_5-2 Classification of the Soil Types (Source: SWRI, (1991))

Soil Group	FAO Soil Type	Description
1(11)	Lithic and Eutric Leptosols, Calcaric Regosols	Very shallow to fairly shallow, with coarse sand, medium to coarse texture
2(12)	Lithic Leptosols, Calcaric Regosols	Fairly shallow in peaks, semi shallow with fine sand in slopes
3(21)	Lithic Leptosols, Eutric Leptosols,	Very shallow soils, without soil cover
4(32)	Calcaric Regosols	Fairly shallow to deep, with fine sandy and medium to coarse texture, with many lime

According to SCHEFFLER (2008) all soil groupes mentioned above summarizes soils with clay content between 10 to 25 %, including the Leptosol and Regosol soil types.

Distinction between the major land cover classes was made based on vegetation properties, like leaf area index, vegetation height, rooting depth, and stomata resistance.

The land cover information was grouped into land cover classes, shown in Table 5-3.

Table5-3: Classification of the Land Cover Classes (Source: NCC, (2005))

Land Cover Class	Land Cover Classes	Description
Agriculture	3, 4, 15	Dry farming, Irrigated Farming, Paddy and other agricultural land
Decidous broad trees	13,5,9,10,14	Woodland, A forestation, Orchard, Indigenous Forest, Forest plantation of Plane tree, single trees and others
Decidous shrubs	22,2,1	Shrub, Thicket and Bush, Degraded Land (areas with low vegetation)
Grassland	12,17	Grass, Pasture, Urban Area Grassland
Settlement	8, 25,27	Rural Area(residential), Urban Area(commercial, residential, build up)
Water	6	Water, Lake dam

The available geology information was grouped into only two classes, shown in Table 5-4.

Table 5-4: Stage of Geology Classification

Class	Description	GSI Code
1	Sedimentary Rocks Black limestone, clayey marl intercalation, Light grey massive dolomitic limestone, Black oolitic and intraclastic limestone, Sandstone , shale, limestone, marl, phosphatic layers	Cbj, Ccj, Cdj, Daj
	Sedimentary Rocks Black massive dolomite, green-black shale intercalations, Red arkosic sandstone, Micaceous red siltstone, redsandstone, Trilobite bearing limestone, marl, dolomite and shale, Quartzitic sandstone	Єdbt, Єl, Єz, Єm, Єq
	Sedimentary rocks Calcareous and siliceous dark colored shale, Cream-bedded to massive limestone,dolomite,chertly, Thin-bedded marly limestone,marl,Amonite bearing, Thin-bedded to massive limestone	Eshk, Jl2, Jd, Jl
	Sedimentary rocks Gray,yellow, green,lime.,argilaceus lime.,marl, Light gray,medium-thick bed limestone.,argilaceus limestone, Orbitolina limestone(Aptian- Albian), Miliolids limestone, gypsum, conglomerate, siltstone, sandy marl	K1_M, K1t, Kt M

		Sedimentary rocks Thick-bed to massive polygenetic conglomerate, sandstone, locally limestone beds, Alveolina-nummulitic limestone, conglomerate, gypsum, Sandstone, shale, limestone intercalations, Mudstone intercalations, fusolina limestone, dolomitic limestone	PEcf, PEl, PEz, Pd, PlQcs Pr
		Sedimentary rocks Young-old screeslope, talus, deposit, aluvial fan, Landslide, rockfall, rock stream, Shale, sandstone, siltstone, claystone, coal bearing, Massive dolomite, Thick-bedded to massive limestone	Q, Q1, Ql, TR3Js, TRde, TRle
2		Igneous Rocks Basaltic-andesitic lava flows, White-green tuff breccia, ash tuff, Green thick-bedded tuff, minor lava, pyroclastics, Volcanic rocks locally basic, agglomerate, tuff,	Dvj, Eb, Etk, Evk
		Igneous Rocks Volcanics includ basalt and spilite, Volcanics, pyroclasics, tuffs, Basic and intermediate sills, Mostly syenite and some leucosyenite porphyry	Kv, Pe, PEvf, Tb, Ts

5.1.3.2 Overlay Analysis and Reclassification

The overlay of the GIS-datasets was carried out in successive stages as shown in Figure 5-4. The first overlay (aspect and slope) build Topography-Set (TS) entities.

In second overlay the Landcover-Soil-Set (LSS) were created by overlaying soil and land cover. Afterwards, the resulting LSS was overlaid with the TS. In this step, first the rock classes from deciduous shrubs separately combined as constant classes. Additionally, in forest classes with a slope below 5°, the east / west aspects have been transformed to a north aspect. SCHULZE, MAHARAJ ET AL. (1997:P.29-30 analyzed the solar radiation on different slopes and aspects. They founded that with a slope below 5° the radiation amount for North, NE/NW, as well as E/W facing aspects was comparable, whereas SE/SW and South facing aspects with the same slope showed a much higher radiation input. This has only been applied to areas with dense vegetation, such as forest (SCHEFFLER, 2008:P.88). In the last step of the successive overlay processes the resulting Topography-Soil-Vegetation Complexes were overlaid with the geology groups. As a result of the generalization process 18113 HRUs were defined for the Latyan catchment.

5.1.3.3 Generalization and Delineation

After finishing the knowledge based aggregation, the resulting entities were overlaid with the sub catchments. The smallest polygons with an area below 5 Raster Cells (<0.05 km²), were then eliminated using the Dissolve Adjacent Polygons in Data Management Tools in ArcMap 9.3(ESRI, 2008). The 18113 HRUs were generalized to 5369 HRU-Polygons and used as modelling units for the J2000g model. The physical characteristics were assigned using the majority function for land cover, soil and geology. For elevation, slope and aspect mean values were computed using the Arc Info Arc GIS 9.3 (ESRI, 2008).

5.2 Snowmelt–Runoff Modelling using J2000g model

5.2.1 Model Parameterization

The model requires separate parameter files for land cover, soil and ground water. Each land cover class consists of 5 land use parameters, each soil class of 2 soil parameters and each hydrogeologic class of 1 groundwater recharge parameters. The parameter values were taken from literature values and are explained in more detail in the following sections. (KRAUSE AND HANISCH, 2009)

5.2.1.1 Landuse-Land Cover Information

Because, the advantage of the Penman-Monteith method is the higher physical basis, in this study, the J2000g model calculates the evapotranspiration and potential evaporation rate based on the Penman-Monteith approach (JAMSWIKI, 2010). This approach estimates the evapotranspiration in the canopy layer using several vegetation parameters such as leaf area index (LAI), stomata resistance, rooting depth, and vegetation height. This information was retrieved from literature values, shown in Table 5-4 B in Appendix B for land cover classes.

5.2.1.2 Information on Soil Data

The soil information was extracted from description of land capability and resources evaluation map of Tehran province, Soil and Water Research Institute (SWRI).That description contains difference datasets of province of Tehran mentioned Latyan Catchment as landtype, soil texture for the soil types, soil classes with (FAO) classification and capability and limits of lands. The database did not contain any field probe and more detail of soil within the study area. To achieve representative soil texture characteristics for the soil types found in the study area, the available soil texture information was averaged according to the soil type properties of WRB, and FAO, ISRIC (2006) and later the values for each soil type were averaged according to the soil groups.

The soil water module of the J2000g model has two parameters namely depth of the soil in cm and entire usable field capacity of the soil in mm. For better accuracy of extracting of mentioned soil parameters the land cover and vegetation cover of the Latyan catchment was used. Therefore, in areas with high vegetation cover, the soil parameters were adapted. Namely in the areas with vegetation covers, both depth and FC sum parameters is increased. The soil parameter values shown in the table 5-5

Table 5-5: Parameters of the Soil Classes for the Soil Water Module

Soil Class	Depth [cm]	FC sum [mm]
111	120	73.17
11	60	10.66
112	130	211.5
12	60	21.3
121	60	21.3
21	60	10.66
132	130	211.5
32	130	211.5

5.2.1.3Information on Geology Data

In the geology data, for each hydrogeologic unit the maximum possible ground water recharge rates per time unit are set up. It only contains the following two attributes: GID - a clear numeric ID with which the connection to the model unit table is generated. mxPerc - the maximum possible percolation rate (ground water recharge rate) per time interval in mm per time unit(JAMSWIKI, 2010).

Due to poor information about maximum possible percolation of difference geological classes in the catchment and due to simplify component of ground water recharge in the j2000g model for both hydrogeological classes an constant parameter value about 28 was input to hydrogeology parameter of model(Table 5-6) .

Table 5-6: Parameters of the Geology classes for the Ground Water Module

Geology Class	Max Percolation [mm]
1	28
2	28

5.2.2 Model application, calibration and evaluation

5.2.2.1 Model application

To provide spatially consistent input information for J2000g, the Latyan catchment was partitioned into 5369 modelling units (HRUs) resulting from a GIS overlay of slope, aspect, land-use, soil type and hydrogeology. Slope and aspect were classified into five and three classes in advance. After the GIS overlay, the centroid coordinates, area, mean slope, most frequent aspect, soil type, land-use and hydrogeological type were extracted for each unit and transformed into a J2000g compliant data table. The soil type and the land-use information are correlated to specific tables during model initialisation to derive physical values for field capacity and vegetation-specific parameters such as the stomatal resistances for good water availability and the leaf-area-index. Monthly values of observed climatological input data (temperature, precipitation, relative humidity, sunshine hours, and wind speed) from the meteorological stations shown in figure 4-9 were transferred to each modelling unit using data from the five closest stations. Values of the six J2000g parameters (FCA, Tbase, TMF, LVD, ETR and GWK) had to be estimated through a model calibration procedure. The calibration was done for 3 subbasin within the Latyan catchment boundaries with sufficient streamflow observations. The selection of suitable subbasins was complicated by the fact that J2000g does not explicitly recognize man-made influences on the hydrological processes and does not account for water losses in karst regions both relevant factors for the runoff amount in some parts of the Latyan catchment. As a result, only subcatchments with minimal man-made influence and primarily impermeable bedrock conditions were selected for calibration. Therefore, three subbasins were selected for calibration: Roodak, Najarkola, and Naran. The extent area of these subbasins ranges between 31 to 430 km2 (see figure 4-2). For each subcatchment, values for the six model parameters were calibrated automatically using the Monte-Carlo-Analysis runs and Shuffled Complex Evolution – University of Arizona (SCE-UA) method (Duan et al., 1994). Both methods adapt a selected number of model parameters in order to optimise a single objective function or efficiency criteria. The calibration was done with observed monthly climate values for the time period from October 1990 through September 2001 using the Nash-Sutcliffe efficiency (NSE) measure as main objective function. The calibrated parameter values are shown together with the resulting NSE values in

Table5-7. Table5-7, column CV indicates that the degree of variability among the three subcatchments varies for each parameter. The values for TMF and Tbase vary the least for all subbasins, probably because they are the most "physically based" and are largely independent from other factors in the catchment. The low values of Tbase is caused by the monthly modelling time steps because, Tbase represents the mean monthly temperature which has to be considerably below 0 C° to store precipitation as snow for a longer period than one time step of one month(KRAUSE AND HANISCH, 2009).

The value for parameter ETR also indicates relatively low variability among the subcatchments. But the NSE, however, was very sensitive to Tbase, TMF and LVD parameters. The remaining parameters GWK, FCA, and LVD exhibit considerably more variability among the catchments compared to the other three parameters. However, the NSE was not very sensitive to changes in GWK (or FCA and ETR) which accounts for the wide range in values. The NSE values for three of subcatchments were computed between 0.78 and 0.82 which demonstrates that J2000g simulates the observed streamflow reasonably well in the calibration period.

For the all Latyan catchment application of J2000g it was assumed that one "global" parameter set could be derived from the calibrated parameter values from the three calibration subcatchments that would result in "reasonable" estimates for the entire study area. This global set was obtained by an area-weighted mean of the parameters of the model parameters carried out for the three test catchments. To test the global parameter set it was first used in each of the three calibration subbasins for the same time period used for the calibration. The resulting NSE value (NSE (gps)) for each catchment is also shown in Table 5-7 Although there was least reduction in model performance for each subcatchment, the range of NSE (gps) values (0.68 and 0.79) is relative close to those obtained with the optimal parameter values for two of the three subcatchments.

5.2.2.2 Validation

The application of the global parameter set in the three calibration catchments resulted in the conclusion that the J2000g model is fairly robust with an acceptable degree of certainty based upon model calibration. To test if the model is also producing reliable results for other time periods and other catchments, the global parameter set derived in the calibration catchments was used in the Roodak subbasin for the longer period from October 1972 through September 2003. The simulated streamflow values were aggregated as long-term mean monthly average

values and compared to observed streamflow records of Roodak gauge. The result is shown in figure 5-5

The figure shows the observed (blue) and simulated (red) long-term monthly runoff for Roodak subbasin which is very similar to whole catchment.The plot indicates that J2000g is able to reproduce the historical 31year long-term monthly runoff values quite well for all Latyan catchment. It should be emphasised that these results were obtained with the global parameter set resulting from the calibration in three subcatchments.
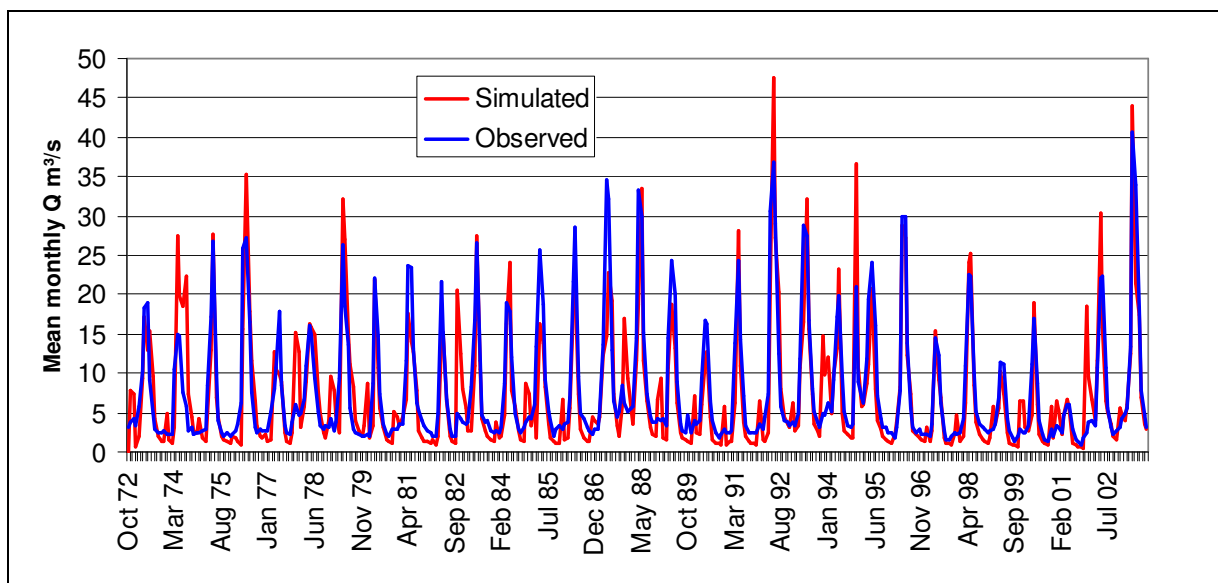

Figure 5-5: Result of the validation of J2000g for Roodak subbasin in the Latyan catchment
The plot shows the long-term monthly simulated (red line) and observed (blue line) streamflow of the period from 10/1972 to 09/2003.

Table 5-7 SubCatchment areas, J2000g parameter values from Monte-Carlo-Analysis and SCE optimisation along with best Nash-Sutcliffe efficiency (NSE) obtained and the efficiencies achieved with the global parameter set (NSE(gps)) for the calibration catchments. The last column shows the coefficient of variation (CV) of the calibrated parameter values. The values of this table were obtained with the calibration period from 10/1990 to 09/2001.

Table 5-7: SubCatchment areas, J2000g parameter values from Monte-Carlo-Analysis and SCE optimisation

CATCHMENT	ROODAK	NAJARKOLA	NARAN	gps	CV%
AREA(km²)	430.93	60.95	31.05	---	---
LVD	1.22	3.58	1.73	1.53	47
GWK	7.73	5.98	2.23	7.2	43
Tbase	- 3.07	- 2.2	-2.56	- 2.94	14
TMF	19.77	18.97	17.89	19.57	4
FCA	12.26	4.78	17.57	11.70	45
ETR	0.41	0.61	0.74	0.45	23
---	---	---	---	---	---
NSE	0.82	0.78	0.79	---	---
Log.NSE	0.80	0.65	0.76	---	---
PBIAS	- 5.6	- 2.2	7.1	---	---
r²	0.83	0.78	0.81	---	---
NSE(gps)	0.79	0.68	0.77	---	---

Additional calibration of the internal model processes was performed with measured snow water equivalent (SWE) of nine climate stations which lies inside the Latyan catchment. The measured SWE data were compared with the SWE simulated on single HRUs which had difference elevation and are located inside and around the three subcatchments. Figure shows the simulated SWE as a red line and the measured values as blue line for the ten years of the calibration period. The figure shows that the model is able to reproduce the development of the snow pack of the catchment very well. The rising limb of the snow accumulation period is captured nearly perfect despite the year 1996 as it is the maximum snow amount (despite 1996 and 1997). Obviously the snow module is defined as simplify (temperature-index) model, therefore simulated results can be accepted as good prediction. As the snow melt dynamics are responsible to a high amount for the runoff dynamics in the Latyan catchment it can be concluded that the snow modelling has a large influence on the model performance.

This is highlighted by the fact, that the four years which showed the lowest efficiencies (1997, 1999, 2000, 2001) of the validation period are also those where severe problems in the snow modelling are obvious. It is comparable that, during this time, the water table is suffering from a continuous decline as a result of the critical situation in available water resources and low flow condition and drought in Tehran as well as most parts of the Iran (JAHANI AND REYHANI, 2006).

The brief description of the case study showed that the model is able to reproduce the hydrological dynamics of a mountainous catchment quite well. This is of importance in relation to the mesoscale applications in the Latyan catchment; because it shows the transferability of the current process simplify modules to different scales. Nevertheless the relevant hydrological dynamics can be simulated by the model with a certain degree of quality as the results show.

Table 5-8, shows the estimated water balance components for the 11 year period (October 1990 to September 2001). According to this table there is no substantial difference between the model results for 3 subcatchment. Notice that for all the Latyan catchment, the snowfall constitutes almost half of the total precipitation, and consequently snowmelt has a large impact on the river discharge. The main period of precipitation occurs during late autumn till late winter, while river flow rises gradually in early spring to reach peak values in May. From the foregoing it can be concluded that the runoff occurs mainly from March till June depending upon the air temperature, indicating that most of this runoff is generated by snowmelt.

For discussion two interesting periods is selected with large and small snow accumulation and melt. The first period is from October 1992 to September 1993 for large snow and from October 2000 to September 2001 for small snow. All relevant information for these periods is given in Figure 5-6.
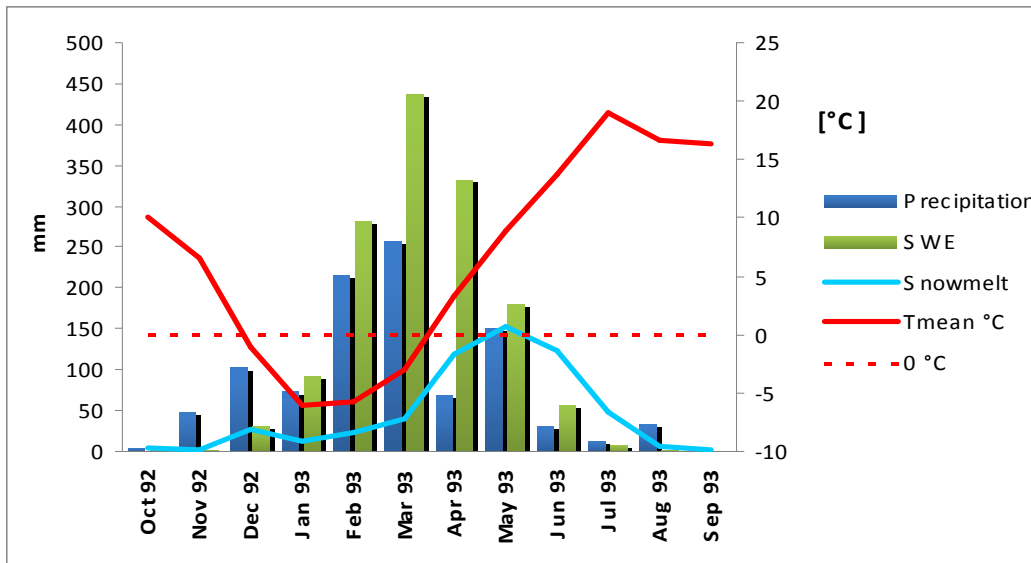
Figure 5-6: Monthly precipitation, mean air temperature, snow water equivalent and snowmelt, Roodak subbasin, J2000g model simulation, 1992-1993.

The degree day method assumes that all precipitation falls as snow when the mean temperature of the subcatchment is lower than Tbase and as rain when the temperature is higher than Tbase. The mean temperature in the catchment drops below zero from December till end March, and accordingly only snowfall occurs and the snowpack gradually builds up to reach about 438 mm of water equivalent at the first March, while there is almost no snowmelt. From end of March, the temperature becomes positive and about 119 mm of snow melts. From mid April till first May, increase temperature continues and snowmelt increase to 152 mm. Finally, at the end of July all snow has completely melted. It to be noted that, the snowmelt finish earlier July in dry years with low precipitation and high temperature.
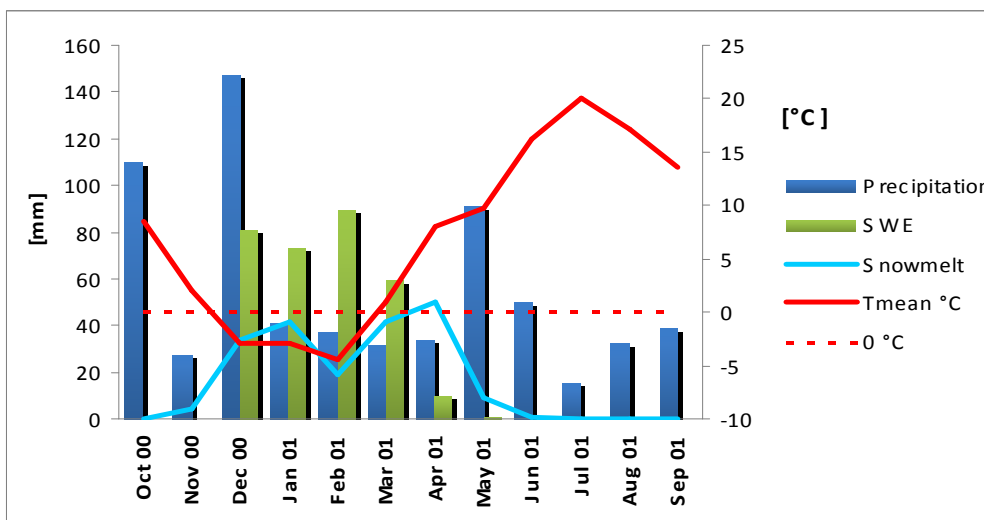
Figure 5-7: Monthly precipitation, mean air temperature, snow water equivalent and snowmelt, Roodak subbasin, J2000g model simulation, 2000-2001.

The figure 5-7 clearly showed the fluctuations of snowmelt in the dry year of 2000-2001. In this time all the study area and Tehran covered by severe drought (JAHANI and REYHANI, 2006). In addition revealed that the condition of snowmelt and SWE is not constant in the Latyan catchment and snowmelt in end of May is finished

Figure 5-8 shows a graphical comparison between observed and computed Runoff at Roodak subcatchment. In the figure the blue line represents the observed runoff and the red line represents the simulated runoff. The Parameter values used to simulate the runoff are shown in table 5-7. From the graphs of simulated and observed runoff curves, it can be seen that the model can faithfully simulated the both high and low flow. Also the model is found to simulate the recession limb very efficiently. Howevere, in all the cases NSE was moderately high (0.82) which means that the model traced very well agree with the observations.
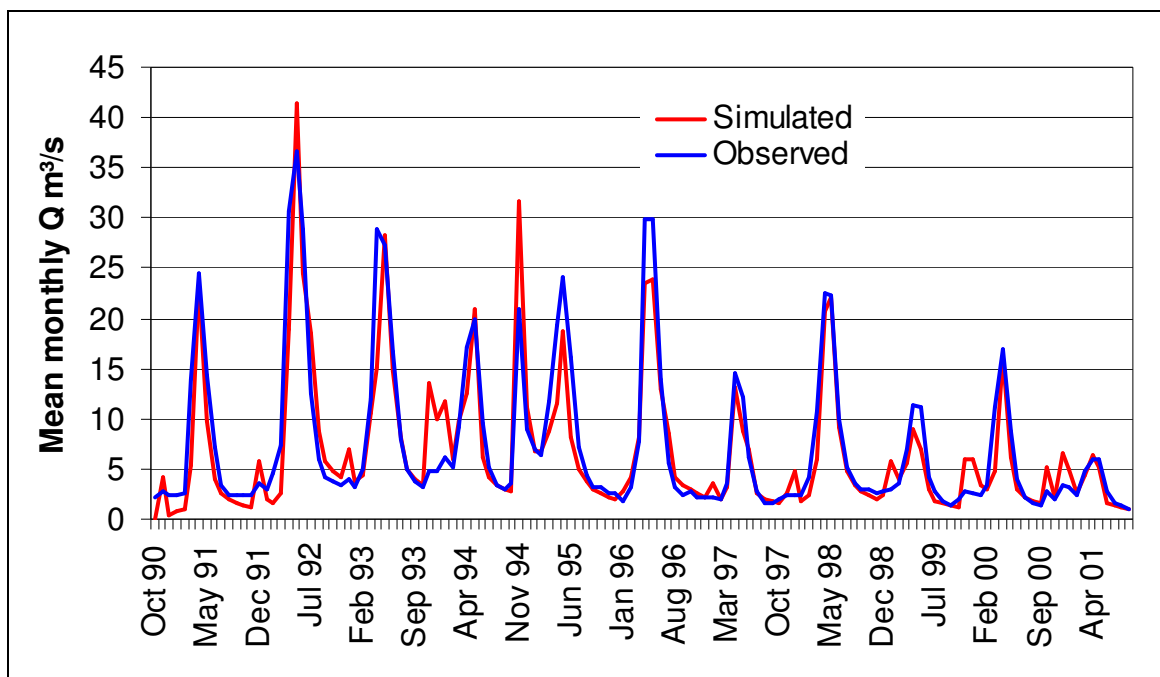

Figure5-8: Graphical comparison between simulated and observed Runoff at Roodak subcatchment in the Latyan catchment, from 10.1990 through 09.2001

5.2.2.3 Verification of the Modeling Results

The simulated snowmelt values range between 199 mm and 730 mm and, in conjunction with precipitation amounts between 557 mm to 1376 mm, which results in a snowmelt/rainfall ratio of 36 to 53 %. In other words, between 36 % and 53 % of the precipitation is falled as snow and melted. Hence, the snowmelt values are indicated that snow is important hydroclimatic factor in the catchment. Similar ranges for the percentage of snow were achieved by SHAFIEE (1999) and water and energy research institute (WEI) (2004).

SHAFIEE calculated snow ratio of the Northern part of Tehran in his research about snow hydrology. He calculated values showing that between 35 to 57 % of the winter and annual precipitation of this region is falled as snow.
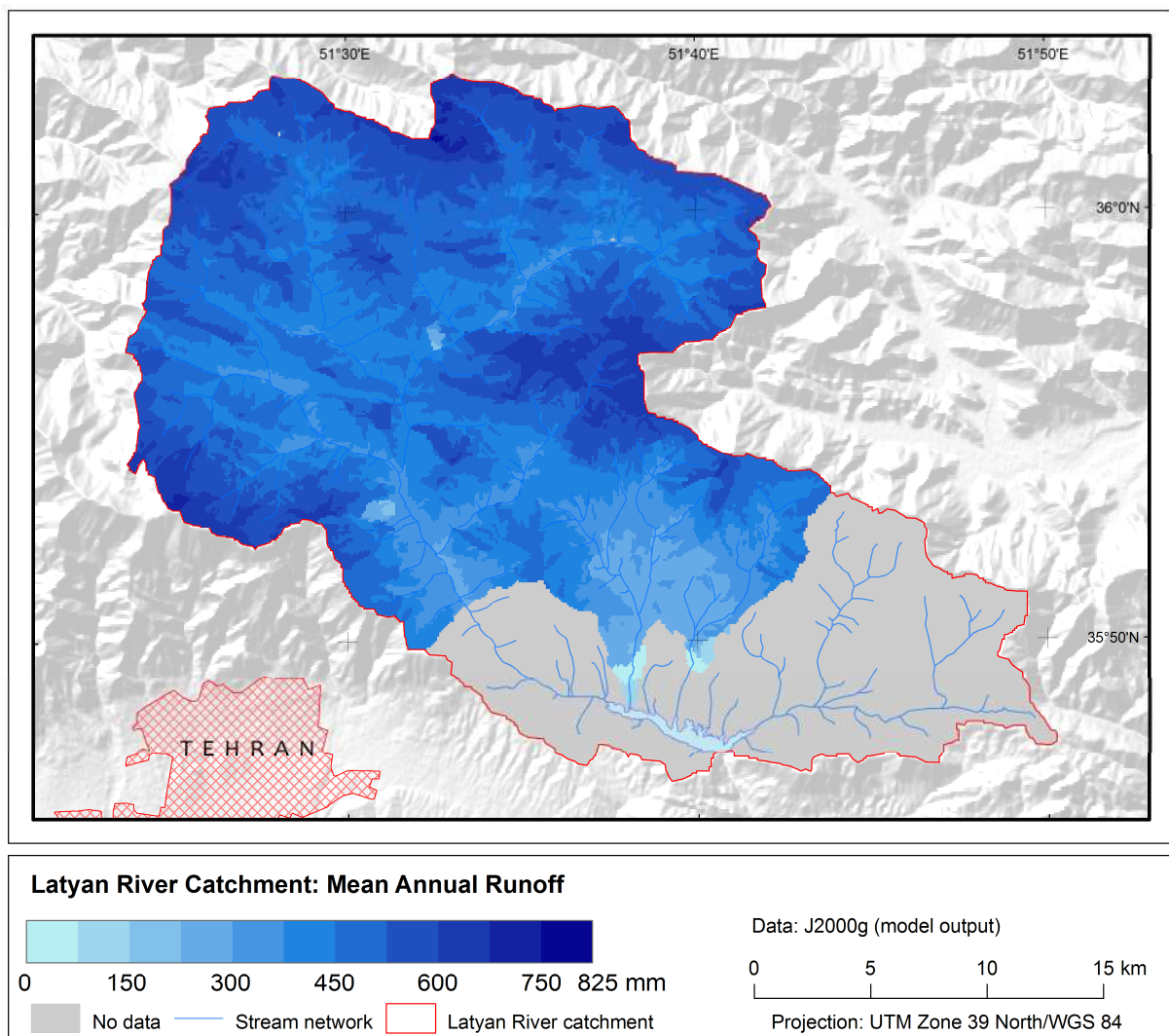

Figure 5-9: Mean Annual Runoff. Modelled using the J2000g Model

In addition computed evapotranspiration values are between 267 mm and 463 mm, which results in an evapotranspiration/rainfall ratio indicated that, between 34 % and 48 % of the precipitation water is evapotranspired. The estimated actual evapotranspiration was compared to estimated actual evapotranspiration values found in FARAMARZI ET AL., (2008). The

values of 267 mm to 463 mm for the entire modeled period are within the estimated range of 211 and 780 mm for the Tehran Province.
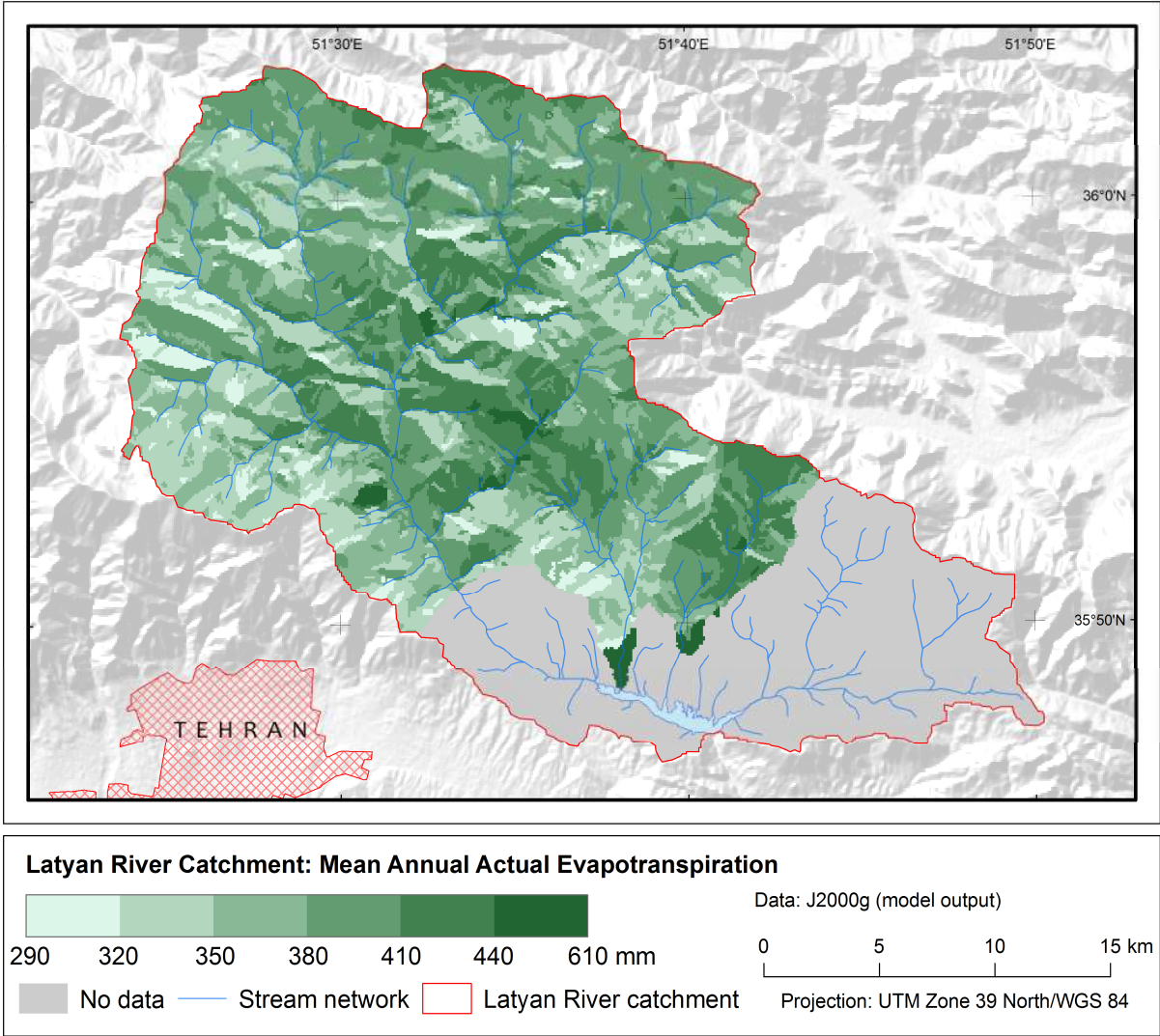
Figure 5-10: Mean Annual Actual Evapotranspiration. Modelled using the J2000g Model

Also comparison of coefficient variation(CV) between predicted and observed runoff illustrated that the variation between both values is very low and is about 1% as well as between snowmelt and precipitation were not high and is as follow about 3 and 11%.

Table xxx illustrates the computed water budget components simulated by the J2000g model time period from 1990 to 2001.

Table5-8: Water Balance Components for the Entire Modelled Period (1990-2001)

YEAR	PRECIP (MM)	POT ET (MM)	ACT ET (MM)	SNOWMELT (MM)	QSIM (MM)	QOBS (MM)
1990 - 91	719	753	356	288	329	501
1991 - 92	1376	665	425	730	802	883
1992 - 93	1000	737	401	560	661	754
1993 - 94	967	748	347	342	655	569
1994 - 95	1125	744	415	356	711	829
1995 - 96	984	707	370	470	593	659
1996 - 97	557	765	315	241	311	339
1997 - 98	988	747	463	462	485	565
1998 - 99	604	806	367	244	287	341
1999 - 00	601	782	267	311	332	368
2000 - 01	657	681	415	199	260	234
MEAN	871	739	376	382	493	549
MAX	1376	806	463	730	802	883
MIN	557	665	267	199	260	234
STDEVP	249	40	53	152	189	206
CV %	29	5	14	40	38	37

Spatial distributions of modelled snow water equivalents at the beginning of the winter and at the time of maximum snow accumulation are shown in Figure 5-11

Figures 5-9, 5-10, and 5-11 indicated that topography slopes as well as aspects played important role in the rainfall type fall, spatial distribution of snow cover, runoff generation and adjustment of evapotranspiration in the catchment. Additionally the output result also revealed the capability of the J2000g in the mountainous area for generation of runoff.Namely at the time of maximum accumulation; high elevation area and gradients seem to have dominant effect on spatial distribution of snow. Hence with increasing elevation in the catchment, the values of snow cover and SWE will increase and maximum of snowpack distribution and SWE is seen in the high altitude areas. These results comply with the knowledge of snowmelt spatial distribution in mountains. Thus, the modelled results seem to be reasonable.

Latyan River Catchment: Mean Annual Snow Water Equivalent (SWE)

Data: J2000g (model output)

| 0 | 250 | 650 | 1250 | 1850 | 2850 mm |

No data   Stream network   Latyan River catchment

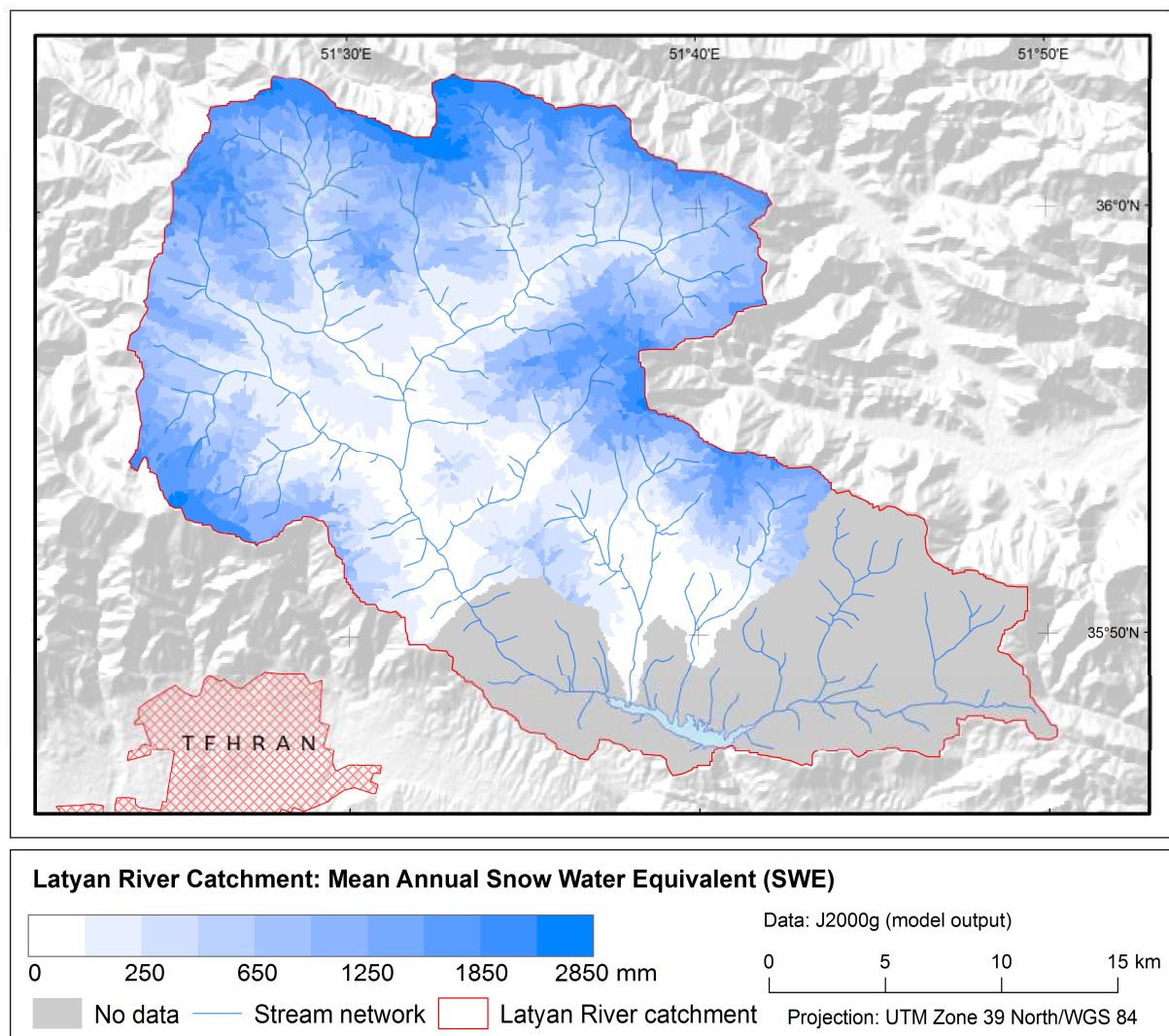0   5   10   15 km

Projection: UTM Zone 39 North/WGS 84

Figure 5-11: Mean Annual (1990-2001) Snow Water Equivalent (SWE) Modelled using the J2000g Model

In addition the various visual modelled results of the model J2000g illustrated a good relation ship between temperature, topography and, SWE and snowmelt, namely in the Latyan catchment in low elevation areas in the southern side of catchment like valleys and around lake dam average temperature is higher than northern side catchment and high altitude. Therefore the time of snow melt in valleys and lowlands of catchment begins erlier than northern of catchment. Additionally in the mentioned areas values of SWE is lower than northern of catchment. In other words, in the end of snowmelt in the southern side of Latyan, in same time in summer (July to August) the snowmelt exist and continue in the high elevations like Shemshak and Garmabdar areas. Figure 5-13 show the continuing of snowmelt on 19th august 2008 near Shemshak.

Latyan River Catchment: Mean Annual Temperature

-2 0 5 10 15 °C

No data   Stream network   Latyan River catchment

Data: J2000g (model output)

0   5   10   15 km
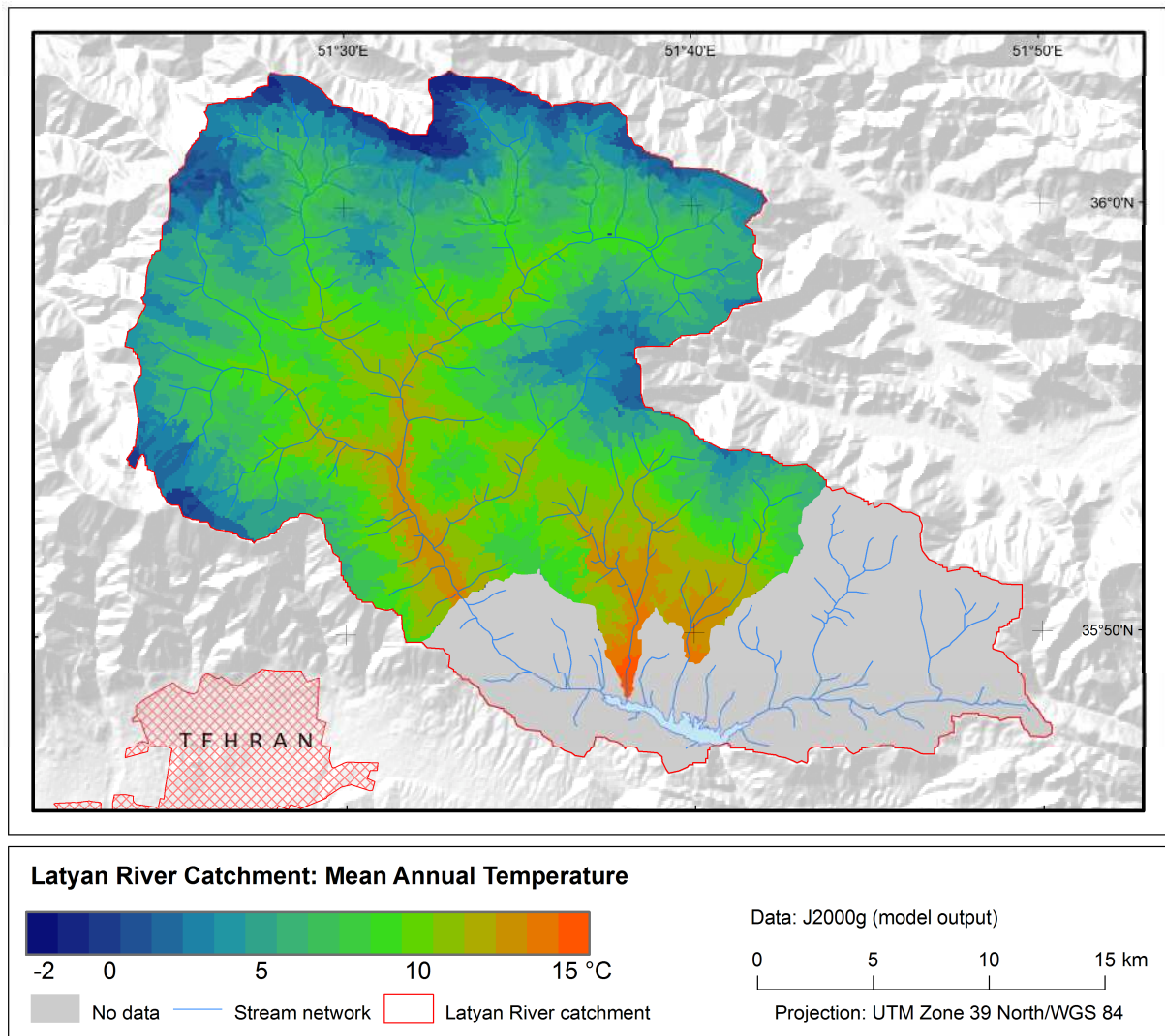
Projection: UTM Zone 39 North/WGS 84

Figure 5-12: Mean Annual Temperature (1990-2001) modelled using J2000g model in the Latyan Catchment

Figure 5-13: snowmelt in the high elevation areas of the Alborz Mountains (source: http://www.flickr.com/photos/ 2780623124_f0ff04d206_19_aug_2008.

6. CONCLUSIONS AND FUTURE RESEARCH

6.1 Conclusions and Future Research

A spatially distributed process-oriented hydrological model J2000g was developed and test in the Latyan catchment, Iran, based on simple temperature-index snow module. The model performance was tested by simulating snow accumulation and melt in the three sub catchments.

The model performance was first tested by simulating runoff as well as snowmelt and snow water equivalent (SWE) in the three subcatchments of the Latyan (Roodak, Najarkola and Naran) with various extents between 30 through 430 km², in the mountainous area in north-eastern part of the Tehran, Iran. The model was applied and calibrated with 11 years (1990-2001) of monthly observed precipitation, air temperature, sunshine duration, relative humidity and wind speed. Monthly discharge data at Roodak, Naran, and Najarkola gauge station was used for model calibration. The model calibration was performed automatically by means of Monte-Carlo-Analysis and SCE methods for extracting global parameter sets of the model only, whereas spatial model parameters (DEM, landcover and soil maps, and characteristics derived) are fixed as modelling unit's entities (HRU). The model efficiency criteria especially NSE (Nash-Sutcliffe- Efficiency) turns out to be 0.78 through 0.82. In order to show the performance of the model two interesting periods with high and low snow accumulation and melt were discussed in detail. Peak discharges as well as low flow and Drought were well predicted by the model as compared to the measured data and observed hydrographs.

The model was also developed and tested by simulating SWE separately and in the 9 snow measurement with various spatial and temporal variability inside the Latyan catchment, The model is applied for simulating SWE in single HRUs station with difference elevation and slope 0° (degree) as well as 1 m² area. Therefore the J2000g SWE module calibrated automatically using Monte-Carlo-analysis runs with 11years (1990-2000-01) of measured monthly SWE. As mentioned, seasonal measurements SWE data inside the Latyan and near three sub catchments were used for model calibration. Hence, two snow parameters (Tbase, TMF) are calibrated for the J2000g snow module. The comparison of the separate SWE models resulted in values between 0.28 - 0.68 for NSE and values between 0.53 - 0.83 for r². The resulting SWE hydrographs was good and show that the model is able to reproduce the development of the snow pack of the catchment very well despite of simply snow module components. It is concluded that the degree day method for snowmelt with calibrated parameters gives good results.

This study showed that the spatially distributed conceptual hydrological model J2000g model, for snow accumulation and melt has great potentiality to simulate the impact of snow

accumulation and melt on the hydrological behaviour of a river basin. Hence, it can be concluded that accurate snowmelt prediction is possible with a temperature-index approach with coupling HRU concept as modelling unit entities with automatically parameters calibration like Monte-Carlo-Analysis and SCE-UA methods.

This study presents very promising results for hydrological snow modelling. However, uncertainties still exist, from which key areas for further research can be derived.

• It is clear that energy and temperature variations in a snow can be more complex than assumed in the present model. However, a more comprehensive approach would need very accurate temporal and spatial observations of snow depth, water content, temperature, as well as energy fluxes, which in practice are usually not available especially in mountainous regions. Certainly such data can be achieved by satellite data and remote sensing techniques. Hence, the method presented can be a useful tool for simulating snowpack processes and snowmelt, but should be verified in the field and improved provided more comprehensive datasets become available.

• Slope and aspects played important role in the spatial distribution of snow cover at the beginning of the winter, too. At the time of maximum accumulation, elevation gradients seem to have dominant effect on spatial distribution of snow.

• Another hydrological significant output of the J2000g model is the prediction outflow from melting snow. It may help to identify the parts of the catchment which dominate in providing meltwater for overland runoff formation. High snowmelt output areas may also contribute to floods at the beginning of the snowmelt thus affecting water resource management and environmental hazards.

• Another source of error in this module could be the quality and temporal scale of input data as monthly precipitation, temperature, sunshine duration, and potential evapotranspiration, which are distributed over the watershed by the various measuring and computing. This is rather inaccurate for heterogeneous landscapes. Other methods and temporal scale data like daily data and radar data may be more reliable and could be considered in future studies.

• Elevation seems to be the most important factor influencing the spatial distribution of areas with melting snow. Much higher snowmelt occurred along the lower elevations with dense vegetations. All these results comply with the knowledge of snowmelt spatial distribution in mountains. Therefore using topological approach for routing flows to outlet catchment and downstream can increase the capability of the model.

• Certainly, residence areas have an important impact on snow accumulation and melt, although few studies have been done to show these effects. Hence, working on these areas in future can improve the model.

• Lastly, extending the model application to macroscale areas with various spatial and temporal variability and applying satellite data for evaluation of model and also simulation of impact projected climate change on the spatially distributed waterbalance, as well as more focus under sensitivity and uncertainty analysis can help the enhance applicability and capability of model And should also be performed in future research.

REFERENCES

Allen, R. G., Pereira, L., Raes, D., and Smith, M (1998): Crop evapotranspiration: Guidelines for computing crop water requirements, FAO Irrigation and Drainage Paper 56, FAO, Rome.

Anderson, E. A. (1973): National Weather Service River Forecast System-Snow Accumulation and Ablation Model, *NOAA Technical Memorandum: NWS Hydro-17*, US National Weather Service.

Anderson, E.A., (1976): A Point Energy and Mass Balance Model of Snow Cover. *NOAA Tech Pep NWS 19*, US Dept. Commerce, Washington DC.

Armstrong, R.L. and E. Brun, (2008): Snow and Climate: Physical Processes, Surface Energy Exchange and Modelling, Cambridge University Press, 219 p.

Bahremand, A., andF. De Smedt (2008): Distributed Hydrological Modeling and Sensitivity Analysis in Torysa Watershed, Slovakia. *Water Resources Management, 22*(3), 393-408.

Balazs, A. (1983): Ein kausalanalytischer Beitrag zur Quantifizierung des Bestands- und Nettoniederschlages von Waldbeständen. Verlag Beiträge zur Hydrologie, Kirchzarten.

Bathurst, J.C. (1986): Sensitivity Analysis of the Système Hydrologique Européen for an Unplanted Catchment. *Journal of Hydrology* 87, 103-123.

Baumgartner, A. and H.-J. Liebscher (1996): Lehrbuch der Hydrologie. Band 1: Allgemeine Hydrologie. Quantitative Hydrologie. 2. Aufl., Verl. Gebr. Bornträger, Berlin, Stuttgart.

Baumgartner, M.F. and A. Rango (1995): A Microcomputer-Based Alpine Snow-Cover Analysis System (ASCAS). *Photogrammetric Engineering & Remote Sensing, Vol. 61, No. 12*, 1475- 1486.

Bäse. F.; Helmschrot J.; Müller-Schmied, H.; and Flügel, W.-A. (2006, 4.-6. Oktober 2006): *The Impact of Land Use Change on the Hydrological Dynamic of the Semiarid Tsitsa Catchment in South Africa, The 2nd Göttingen GIS and Remote Sensing Days, Göttingen.*

Becker, A. (1992): Methodische Aspekte der Regionalisierung. In: Regionalisierung in der Hydrologie. Mitteilung XI der Senatskommission für Wasserforschung der DFG. Weinheim, 16-32.

Bende-Michl, U., D. Kemnitz, J. Helmschrot, P. Krause, H. Cresswell, S. Kralisch, M. Fink and W.-A. Flügel (2007): Supporting natural resources management in Tasmania through spatially distributed solute modeling with JAMS/J2000-S. In: Don Kulasiri and Les

Oxley, editors, *MODSIM 2007 International Congress on Modelling and Simulation,* Modelling and Simulation Society of Australia and New Zealand.

Bengtsson, L. and V. P. Singh (2000): Model Sophistication in Relation to Scales in Snowmelt Runoff Modeling. *Nordic Hydrology 31*, 267-286.

Bergström, S. (1975): The development of a snow routine for the HBV-2 model. *Nordic Hydrology 6*, 73-92.

Bergström, S. (1991): Principles and confidence in hydrological modelling. *Nordic Hydrology 22*, 123-136.

Bernier, P.Y. (1985): Variable source areas and storm-flow generation: An update of the concept and a simulation effort. *Journal of Hydrology* 79, 195-213.

Beven, K. J. and M.J. Kirkby (1979): A physically based, variable contributing area model of basin hydrology. *Hydrological Sciences Bulletin 24*, 43-69.

Beven, K. (2001): *Rainfall-Runoff Modelling*. Chichester [a.o.]: John Wiley & Sons.

Blöschl, G. (1990): Snowmelt simulation in rugged Terrain – The Gap between point and catchment scale approaches. *Wiener Mitt. Wasser, Abwasser, Gewässer 91*, 120 S.

Blöschl, G. (1991): The Influence of Uncertainty in Temperature and Albedo on Snowmelt. *Nordic Hydrology 22,* 95 -108.

Blöschl, G. (1996): Scale and Scaling in Hydrology. Habilitationsschrift. *Wiener MitteilungenWasser, Abwasser, Gewässer 132*, Wien.

Blöschl, G. and R. Kirnbauer (1991): Point snowmelt models with different degrees of complexity – internal processes. *Journal of Hydrology 129*, 127-147.

Blöschl, G. and R. Kirnbauer (1992): An Analysis of Snow Cover Patterns in a Small Alpine Catchment. *Hydrological Processes, Vol. 6*, 99-109.

Blöschl, G., Kirnbauer, R. and D. Gutknecht (1987): Zur Berechnung des Wärmeeintrages an einem Punkt der Schneedecke. *Deutsche Gewässerkundliche Mitteilungen 31, H. 5*, 149-155.

Blöschl, G., Kirnbauer, R. and D. Gutknecht (1990): Modelling Snowmelt in a Mountainous River Basin on Event Basis. *Journal of Hydrology 113*, 207-229.

Blöschl, G., Kirnbauer, R. and D. Gutknecht (1991a): A spatially distributed snowmelt model for application in alpine terrain. Snow, Hydrology and Forests in High Alpine Areas (Proceedings of the Vienna Symposium, August 1991), *IAHS Publication No. 205*, 51-60.

Blöschl, G., Kirnbauer, R. and D. Gutknecht (1991b): Distributed Snowmelt Simulations in an Alpine Catchment. 1. Model Evaluation on the Basis of Snow Cover Patterns. *Water Resources Research, Vol. 27, No. 12*, 3171-3179.

Blöschl, G., Kirnbauer, R. and D. Gutknecht (1991c): Distributed Snowmelt Simulations in an Alpine Catchment. 2. Parameter Study and Model Predictions. *Water Resources Research, Vol. 27, No. 12*, 3181-3188.

Blöschl, G. (2005):. Rainfall-Runoff Modeling of Ungauged Catchments. Encyclopedia of Hydrological Sciences.

Bongartz, K. (2001): Untersuchung Unterschiedlicher Flächendiskretisierungs- und Modellierungskonzepte für die Hydrologische Modellierung am Beispiel Thüringer Vorfluter Friedrich-Schiller-Universität Jena, Jena.

Bøggild, C. E. (2000): Preferential Flow and Melt Water Retention in Cold Snow Packs in West- Greenland. *Nordic Hydrology 31*, 287-300.

Braun, L.N. (1985): Simulation of Snowmelt-runoff in Lowland and Lower Alpine Regions of Switzerland. *Zürcher Geographische Schriften, Heft 21*. (ETH) Zürich

Braun, L.N. and H. Lang (1984): Vergleich von Schneeschmelzmodellen mit unterschiedlicher Komplexität in zwei voralpinen Einzugsgebieten verschiedener Größe. *DVWK-Mitteilungen 7*, 77-90.

Braun, L.N. and H. Lang (1986): Simulation of snowmelt runoff in lowland and lower Alpine Regions of Switzerland. *IAHS Publication No 155*, 125-140.

Braun, L.N. and M.B. Rohrer (1992): Schneedeckenverteilung im mikro- bis mesoskaligen Bereich. In: Kleeberg, H.-B. (Hrsg.) Regionalisierung in der Hydrologie. Ergebnisse von Rundgesprächen der DFG. DFG Mitteilung XI der Senatskommission für Wasserforschung. Weinheim. 185-199.

Buttle, J.M. and J.J. McDonnell (1987): Modelling the areal depletion of snowcover in a forested catchment. *Journal of Hydrology 90*, 43-60.

Calder, I.R. (1990): Evaporation in the Uplands.,Wiley, Chichester.

Colbeck, S.C. (1978): The physical aspects of water flow through snow. *Advances in Hydroscience 11*, 165-206.

Colbeck, S.C. (1987): A review of the metamorphism and classification of seasonal snow cover crystals, Avalanches formation, movement and effects. *IAHS Publication No. 162*, 3-34.

Colbeck, S.C.; Anderson, E.A.; Bissell, V.C.; Crook, A.G.; Male, D.H., Slaughter, C.W. and D.R. Wiesnet (1979): Snow accumulation, distribution, melt and runoff. *EOS, vol. 60, no. 21*, 465- 468.

Colbeck, S.C.; Akitaya, E.; Armstrong, R.; Gubler, H.; Lafeuille, J.; Lied, K.; McClung, D. and E. Morris (1990): The international classification for seasonal snow on the ground. IAHS, International Commission on Snow and Ice (ICSI), Wallingford.

Daly, S. F., R. Davis, E. Ochs, and T. Pangburn (2000): an approach to spatially distributed snow modeling of the Sacramento and San Joaquin basins, California, *Hydrological Processes, 14*, pp. 3257-3271.

Danish Hydraulic Institute (1986): Introduction to the SHE – Système Hydrologique Européen / European Hydrologic System. DHI, Horsholm.

Dickison, R.B.B., Daugharty, D.A. and N.B. Fredericton (1984): Influence of forest cover and forest removal on accumulation and melting of snow in an eastern Canadian catchment study. *DVWK-Mitteilungen 7,* 419-447.

Dingman, S.L. (1994): Physical Hydrology. Macmillan, New York.

Dingman, L. S. (2002): *Physical Hydrology*. Upper Saddle River: Prentice- Hall Inc.

Doorenbos, J. and W.O. Pruitt (1977): Guidelines for Predicting Crop Water Requirements. FAO Irrigation and Drainage Paper 24, Rom.

Dunn, S.M. and R.J.E. Colohan (1999): Developing the snow component of a distributed hydrological model: a step-wise approach based on multi-objective analysis. *Journal of Hydrology 223*, 1- 16.

Edwards, A.C., Scalenghe, R. and M. Freppaz (2007): Changes in the seasonal snow cover of alpine regions and its effect on soil processes: A review. *Quaternary International* (162–163): 172-181.

FAO, ISRIC, and ISSS. (2006): World Reference Base for Soil Resources 2006: A Framework for International Classification, Correlation and Communication (No. 103). Rome: FAO.

Faramarzi, M., K. Abbaspour, R. Schulin and H. Yang (2008): Modelling blue and green water resources availability in Iran, *Hydrological Processes*, Vol.23 Issue 3, pp 486-501.

Fattahi, E. (1998): A quantitative model for snowmelti, case study, Latyan dam basin, thesis (M.A.), Institute of Geography, University of Teacher training of Tehran, Iran.

Ferguson, R.I. (1986): Parametric modelling of daily and seasonal snowmelt using snowpack water equivalent as well as snow covered area. *IAHS Publication 155*, 151-161.

Ferguson, R.I. (1999): Snowmelt runoff models. *Progress in Physical Geography 23, 2*, 205- 227.

Flügel, W.-A. (1995): Delineating Hydrological Response Units by Geographical Information System Analyses for Regional Hydrological Modelling Using PRMS/MMS in the Drainage Basin of the River Broel, Germany. *Hydrological Processes*, 9(3-4), 423–436.

Flügel, W.-A. (1996): Hydrological Response Units (HRU's) as modelling entities for hydrological river basin simulation and their methodological potential for modelling complex environmental process systems, Results from the Sieg catchment. *Die Erde 127*, 42-62.

Flügel, W.-A. (2000): Systembezogene Entwicklung regionaler hydrologischer Modellsysteme. *Wasser und Boden 52/3*, 14-17.

Franz, K. J. (2006): Characterization of the comparative skill of conceptual and physically-based snow models for streamflow prediction, Phd thesis, *University of California*, Irvine, USA.

IPCC (2001): Climate Change 2001: Impacts, Adaptations, and Vulnerabilities. Contribution of Working Group II to the Third Assessment Report of the Intergovernmental Panel on Climate Change, Eds. J. J. McCarthy, O. F. Canziani, N. A. Leary D. J. Dokken, K. S. White, *Cambridge University Press*, UK

Gellens, D.; Barbieux, K.; Schädler, B.; Roulin, E.; Aschwanden, H. and F. Gellens-Meulenberghs (2000): Snow Cover Modelling as a Tool for Climate Change Assessment in a Swiss Alpine Catchment, *Nordic Hydrology 31 (2)*, 73 88.

Golterman, H.L. (2005): Reviewing the chemistry of Phosphate and Nitrogen compounds in Sediments, RMZ - *Material and Geoenvironment*, 52(1), 2005.

Gray, D.M. and D.H. Male (1981): Handbook of Snow: Principles, Processes Management and Use. Pergamon Press, Toronto.

Gray, D.M. and T.D. Prowse (1993): Snow and floating ice. In: Maidment, D.R. (ed.): *Handbook of Hydrology*, Ch.7. McGraw-Hill, New York, 7.1-7.58.

Grohman, G., Kroenung, G. and Strebeck, J. (2006): Filling SRTM Voids: The Delta Surface Fill Method. *Photogrammetic Engineering & Remote Sensing, 72*(3), 213-216.

Groebner, F.; Braun, H.; Gastinger, W.; Gralka, B.; Körner, W.; Richter, H. and J. Schramm (1980): Erläuterungen zur Standortskarte des Staatlichen Forstbetriebes Suhl. Technischer Bericht, VEB Forstprojektierung Potsdam, Betriebsteil Weimar.

Gude, M. (1997): Snow metamorphism – a review of the state of knowledge, *Proceedings of the EARSeL Workshop Remote Sensing of Land Ice and Snow*, University of Freiburg, Germany, April 1997, 1-5.

Gude, M. and D. Scherer (1998): Snowmelt and slush flows: hydrological and hazard implications. *Annuals of Glaciology 26*, 381-384.

Gupta, H. V., S. Sorooshian, and P. O. Yapo. (1999): Status of automatic calibration for hydrologic models: Comparison with multilevel expert calibration. *Journal of Hydrologic Engineering.* 4(2): 135-143.

Helmschrot, J. (2006): An Integrated, Landscape-Based Approach to Model the Formation and Hydrological Functioning of Wetlands in Semiarid Headwater Catchments of the Umzimvubu River, South Africa. Göttingen: Sierke Verlag.

Herpertz, D. (2001): Schneehydrologische Modellierung im mittellgebirgsraum, Friedrich-Schiller-Universität Jena, Jena.

Herrmann, A. and R.G. Rau (1984): Snow cover stores and winter runoff behaviour of a small basin in the German highlands. *DVWK-Mitteilungen 7*, 449-472.

Hewlett, J.D. and A.R. Hibbert (1965): Factors affecting the response of small watersheds to precipitation in humid areas. Sopper, W.E. and H.W.Lull (ed.): *Forest Hydrology.* Oxford/London, 275-290.

Heydarpour, J. (1989): Modeling Runoff in Semiarid Rangeland Watersheds. *Environmental Software, Vol. 4, No. 4*, 210-215.

Hossein, M. (1997): Hydrological Analysis of The Roodak Catchment, Iran and evaluation of a flood simulation model, thesis(M.Sc), *International Institute for Aerospace Survey and Earth Sciences* (ITC), Netherlands.

Ishii, T. and Fukushima, Y. (1994): Effects of forest coverage on snowmelt runoff. Snow and Ice covers: Interactions with the Atmosphere and Ecosystems, *IAHS Publication No. 223,* 237-245.

Jahani, H.R. and Reyhani, M., (2006): Role of groundwater in Tehran Water crisis mitigation, *Proceedings of the International Workshop*, Tehran, 29-31 October 2006.

JAMS. Jena Adaptable Modelling System Wikipage (updatable, 2010): from *http://jams.uni-jena.de/jamswiki/index.php/J2000g*Hauptseite.

James, L.D. (1991): Learning by Parametric Modeling: Hydrologic Investigations of Utah Mountain Catchments. In: Bowles, D.S. und O'Connell, P.E. (ed.): Recent Advances in the Modeling of Hydrologic Systems. *NATO ASI Series C: Mathematical and Physical Sciences,* Vol. 345, Kluwer Academic Publishers, Dordrecht/ Boston/ London, 571-587.

Johanson, R.C. et al. (1984): Hydrological Simulation Program - FORTRAN (HSPF): Users Manual For Release 8.0., *Environmental Research Laboratory, Office for Research and Development,* U.S. Environmental Protection Agency, Athens, Georgia 30613.

Karamouz, M., Zahraie, B., Torabi, S., and Shahsavarie, M. (1999): Integrated Water Resources Planning and Management for Tehran Metropolitan Area in Iran. *Proceedings of*

Water Resources Planning, Management and Development (WRPMD'99) – Preparing for the 21st Century, doi 10.1061/40430(1999)96

Karamouz, M., Zahraie, B., Araghi-Nejhad, S., Shahsavari, M. and Torabi, S., (2001): An integrated approach to water resources development of the Tehran region in Iran. *Journal of the American Water Resources Association*, 37(5), 1301-1311.

Kattelmann, R. (1998): Runoff generation during the early stages of snowmelt in the Sierra Nevada, California, U.S.A. Hydrology, Water Resources and Ecology in Headwaters. Poster Volume of the *International Conference HeadWater '98*, Meran, April 1998.

Katwijk, V.F.v.; Rango, A. and A.E. Childress (1993): Effect of Simulated Climate Change on Snowmelt Runoff Modeling in Selected Basins, *Water Resources Bulletin*, Vol. 29, No. 5, 755- 766.

Kääb, A. (2005): Combination of SRTM3 and Repeat Aster Data for Deriving Alpine Glacier Flow Velocities in the Bhutan Himalaya. *Remote Sensing of Environment, 94*(4), 463-474.

Keller, H.M.; Strobel, Th. and F. Forster (1984): Die räumlich zeitliche Variabilität der Schneedecke in einem schweizerischen Voralpental. *DVWK-Mitteilungen 7*, 257-284.

Kirnbauer, R.; Blöschl, G.; Waldhäusl, P. and F. Hochstöger (1991): An analysis of snow cover patterns as derived from oblique aerial photographs. *Snow, Hydrology and Forests in High Alpine Areas,* Proceedings of the Vienna Symposium, August 1991, *IAHS Publication No. 205*, 91-99.

Kirnbauer, R.; Blöschl, G. and D. Gutknecht (1994): Entering the era of distributed snow models. *Nordic Hydrology, 25*, 1-24.

Kitanidis, P. K. (1997): Introduction to Geostatistics. Cambridge: Cambridge University Press.

Kite, G. W. (1995): Scaling of Input Data for Macroscale Hydrological Modelling Water Resources Research, 31(11), 2769-2781.

Kralisch S. and Krause, P. (2006): JAMS – A Framework for Natural Resource Model Development and Application; *Proceedings of the International Environmental Software Society* (IEMSS), Vermont, USA (Reviewed paper)

Krause, P. (2001): Das Hydrologische Modellsystem J2000- Beschreibung und Anwendung in großen Flussgebieten (Vol. Band 29), Jülich: Forschungszentrum Jülich.

Krause, P. (2002): Quantifying the Impact of Land Use Changes on the Water Balance of Large Catchments Using the J2000 Model. *Physics and Chemistry of the Earth, 27*, 663-673.

Krause, P., Boyle, D. P., and Bäse, F. (2005): Comparison of Different Efficiency Criteria for Hydrological Model Assessment. *Advances in Geosciences, 5*, 89–97.

Krause, P., and S. Hanisch. (2009): Simulation and analysis of the impact of projected climate change on the spatially distributed waterbalance in Thuringia, Germany", *Advances in Geosciences*, in print.

Krause, P., (2010): Uncertainty analysis of the hydrological model J2000g, in review.

Kuhn, M. (1984): Physikalische Grundlagen des Energie- und Massenhaushalts der Schneedecke. *DVWK Mitteilungen 7*, 5-56.

Kustas, W.P.; Rango, A. and R. Uijlenhoet (1994): A simple energy budget algorithm for the snowmelt runoff model. *Water Resources Research*, Vol. 30, No. 5, 1515-1527.

Kuusisto, E. (1980): On the Values and Varablility of Degree-Day Melting Factor in Finland. *Nordic Hydrology, 11*, 235-242.

Lang, H. (1986): Forecasting meltwater runoff from snow-covered areas and glacier basins. *River Flow Modeling and Forecasting*, eds. D.A.Kraijenhoffand J.R. Moll, D. Reidel, Dordrecht, Holland, pp. 99-127.

Leavesley, G.H. (1989): Problems of snowmelt runoff modelling for a variety of physiographic and climatic conditions. In: *Hydrological Sciences Journal 34 (6)*, 617-634.

Leavesley, G.H., Lichty, R.W., Troutman, B.M. and L.G. Saindon (1983): Precipitation-Runoff Modeling System: User's Manual. Water-Resources Investigations Report 83-4238, Denver, Colorado.

Ludwig, R., Hellwich, O., Strunz, G., Roth, A., and Eder, K. (2000): Applications of Digital Elevation Models from SAR Interferometry for Hydrologic Modelling. *Photogrammetrie - Fernerkundung - Geoinformation (PFG), 2*, 81-94.

Lundberg, A. and H. Thunehed (2000): Snow Wetness Influence on Impulse Radar Snow Surveys, Theoretical and Laboratory Study. *Nordic Hydrology 31 (2)*, 89-106.

McCuen, R. (1973): The Role of Sensitivity Analysis and Hydrologic Modeling. *Journal of Hydrology, 18*, 37-53.

Mahmudian A. A. (2002): Atlas of Shemiran Subprovince(Persian), Gitashenasi Institute, Tehran, Iran.

Maniak, U. (1993): Hydrologie und Wasserwirtschaft. Eine Einführung für Ingenieure. Berlin, Heidelberg.

Martinec, J. (1975): Snowmelt runoff model for river flow forecasts. *Nordic Hydrology 6*, 145-154.

Martinec, J. (1980): Limitations in hydrological interpretation of snow coverage. *Nordic Hydrology 11*, 209-220.

Martinec, J. and A. Rango (1981): Areal Distribution of Snow Water Equivalent Evaluated by Snow Cover Monitoring. *Water Resources Research, Vol.* 17 (5), 1480-1488.

Martinec, J. and A. Rango (1986): Parameter values for snowmelt runoff modelling. In: *Journal of Hydrology 84*, 197-219.

Martinec, J. and A. Rango (1991): Indirect Evaluation of Snow Reserves in Mountain Basins. In: Snow Hydrology and Forests in High Alpine Areas. Proceedings of the Vienna Symposium, *IAHS Publication No.205*, 111-119.

Martinec, J.; Seidel, K.; Burkart, U. and R. Baumann (1991): Areal modelling of snow water equivalent based on remote sensing techniques. Snow Hydrology and Forests in High Alpine Areas. Proceedings of the Vienna Symposium, *IAHS-Publication No. 205*, 121-129.

Martinec, J.; Rango, A. and R. Roberts (1992): Rainfall-Snowmelt Peaks in a Warmer Climate. *Managing Water Resources During Global Change* (Am. Water Resources Ass.), November 1992, 195-202.

Martinec, J.; Rango, A. and R. Roberts (1994a): Modelling the Redistribution of Runoff Caused by Global Warming. *Effects of Human-Induced Changes on Hydrologic Systems* (Am. Water Resources Ass.), June 1994, 153-161.

Martinec, J.; Rango, A. and R. Roberts (1994b): Snowmelt Runoff Model (SRM) User's Manual (Updated Edition 1994, Version 3.2; ed. M.F. Baumgartner). Geographica Bernensia P29, Bern.

Matthäus, H.; Rachner, M. and G. Schneider (1994): Zum Extremverhalten des Niederschlagsdargebotes aus Schneeschmelze und Regen. Erste Ergebnisse. *Korrespondenz Abwasser 41, H. 10*, 1762-1764.

Michl, C. (1999): Prozeßorientierte Modellierung des Wasserhaushalts zweier Einzugsgebiete im Thüringer Wald. Dissertation an der Friedrich-Schiller-Universität zu Jena.

Micaelli, R., Behbahani, H. I. and Shafie, B., (2007): River-Valleys as an Intra-city Natural Feature, International Journal of Environ. Res., 1(3): 204-213.

Morid, S., Gosain, A.K. and Keshari, A.K., (2004): Response of different snowmelt algorithms to synthesized climatic data for runoff simulation, J. Earth & Space Physics. 30(1), 1-9

Morris, E.M. (1982): Sensitivity of the European hydrological system snow models. Hydrological aspects of Alpine and High Mountain Areas, Proceedings of the Exeter symposium. In: *IAHS Publication No. 138*, 221-231.

Morris, E.M. (1991): Physics-Based Models of Snow. In: Bowles, D.S. und O'Connell, P.E. (ed.): Recent Advances in the Modeling of Hydrologic Systems. NATO ASI Series C:

Mathematical and Physical Sciences, Vol. 345, Kluwer Academic Publishers, Dordrecht/ Boston/ London, 85-112.

Nakawo, M. and N. Hayakawa (1998): Snow and Ice Science in Hydrology, The 7th IHP (**I**nternational **H**ydrological **P**rogramme) Training Course on Snow Hydrology, Nagayo, Japan 1998 (Published by IHAS, Nagayo University and UNESCO).

Nourani, V., Singh, V.P., Alami, M.T. and Delafroz, H., (2008): Geomorphological Runoff Routing Modeling based on Linear Reservoirs Cascade, *Journal of Applied Sciences*, 8(9), 1660-1667.

Obled, Ch. and B. Rosse (1977): Mathematical models of a melting snowpack at an index plot. *Journal of Hydrology 32*, 139-163.

Parajka, J., L. Holko,and Z. Kostka, (2001): Distributed modelling of snow water equivalent - coupling a snow accummulation and melt model and GIS, Inst. Of Hydrology, Slovak Academy of Sciences, Slovakia.

Pomeroy, J.W., Parviainen, J., Hedstrom,N. and D.M. Gray (1998a): Coupled modelling of forest snow interception and sublimation. In: *Hydrological Processes 12*, 2317-2337.

Pomeroy, J.W., Gray, D.M., Shook, K.R., Toth, B., Essery, R.L.H., Pietroniro, A. and N. Hedstrom (1998b): An evaluation of snow accumulation and ablation processes for land surface modelling. In: *Hydrological Processes 12*, 2339-2367.

Pourabdullah, M. (2006): A GIS-based erosion modeling in the Latian Dam watershed using RUSLE, USDA-CSREES 2006 National Water Quality Conference, February 5-9, 2006, San Antonio, USA.

Rachner, M. and H. Matthäus (1984): Schneehydrologische Untersuchungsergebnisse in der DDR und deren Anwendung für wasserwirtschaftliche Zwecke. In: *DVWK-Mitteilungen 7*, 235-255.

Rachner, M. and H. Matthäus (1986): Project SNOW: operational estimation of snowcover development in the mountains of the German Democratic Republic. In: *IAHS-Publication No. 155*, 71-81.

Rachner, M. and G. Schneider (1992): Ermittlung extremer Werte des Niederschlagsdargebotes aus Schneeschmelze und Regen auf der Grundlage der langjährigen Potsdamer Reihe (1893 bis 1987). In: *Deutsche Gewässerkundliche Mitteilungen 36, H. 3/4*, 115-119.

Rachner, M.; Matthäus, H. and G. Schneider (1997): Echtzeitvorhersage der Schneedeckenentwicklung und der Wasserabgabe aus der Schneedecke. Erste Ergebnisse aus dem Projekt SNOW-D. In: *Deutsche Gewässerkundliche Mitteilungen 41, H.3*, 98-106.

Rango, A. (1992): Worldwide Testing of the Snowmelt Runoff Model with Applications for Predicting the Effects of Climate Change. In: *Nordic Hydrology 23*, 155-172.

Rango, A. (1995): Effects of Climate Change on Water Supplies in Mountainous Snowmelt Regions. In: *World Resource Review, Vol. 7, No. 3*, 315-325.

Rango, A. (1996): Spaceborne remote sensing for snow hydrology applications. In: *Hydrological Sciences Journal 41*, 477-494.

Rango, A. and J. Martinec (1994a): Aereal Extent of Seasonal Snow Cover in a Changed Climate. In: *Nordic Hydrology 25*, 233-246.

Rango, A. and J. Martinec (1994b): Model Accuracy in Snowmelt-Runoff Forecasts Extending from 1 to 20 Days. In: *Water Ressources Bulletin, Vol. 30, No. 3*, 463-470.

Rango, A. and J. Martinec (1995): Revisiting the Degree-Day Method for Snowmelt Computations. In: *Water Resources Bulletin, Vol. 31, No. 4*, 657-669.

Rango, A. and V.v.Katwijk (1990a): Development and Testing of a Snowmelt-Runoff Forecasting Technique. In: *Water Ressources Bulletin, Vol. 26, No. 1*, 135-144.

Rango, A. and V.v.Katwijk (1990b): Climate Change Effects on the Snowmelt Hydrology of Western North American Mountain Basins. In: *IEEE Transactions on Geoscience and Remote Sensing, Vol. 28, No. 5*, 970-974.

Rango, A.; Wergin, W.P. and E.F. Erbe (1996a): Snow cristal imaging using scanning electron microscopy: I. Precipitated snow. In: *Hydrological Sciences Journal* 41 (2), 219-233.

Rango, A.; Wergin, W.P. and E.F. Erbe (1996b): Snow cristal imaging using scanning electron microscopy: II. Metamorphosed snow. In: *Hydrological Sciences Journal* 41 (2), 235-250.

Refsgaard, J. C., and B Storm (1996): Construction, Calibration and Validation of Hydrological Models. In M. B. Abbott & J. C. Refsgaard (Eds.), *Distributed Hydrological Modelling* (pp. 41-54). Dordrecht: Kluwer Academic Publishers.

Richter, D. (1995): Ergebnisse methodischer Untersuchungen zur Korrektur des systematischen Meßfehlers des Hellmann-Niederschlagsmessers. In: *Berichte des DWD 194*.

Rohrer, M. B. and H. Lang (1990): Point modelling of snow cover water equivalent based on observed variables of the standard meteorological networks. In: *IAHS Publication No. 193*, 197- 204.

Rohrer, M.B. (1999): Die Schneedecke im Schweizer Alpenraum und ihre Modellierung. In: *Züricher Geographische Schriften, Heft 49*. Zurich.

Santeford H. S., (1974): Advanced concepts and techniques in the study of snow and ice resources: an interdisciplinary symposium; [papers] A United States contribution to the International Hydrological decade National Academy of Sciences, 789 pp.

Scheffer, F. and P. Schachtschabel (1992): Lehrbuch der Bodenkunde. Ferdinand Enke Verl., Stuttgart.

Scheffler, C., Krause, P., Flügel, W.-A., and K. Bongartz (2007): Development of a Validation Tool for Regional Distributed Models Using Macro-scale Soil Moisture Products, Case Study: Great Letaba River, South Africa. Paper presented at the MODSIM 2007-International Congress on Modelling and Simulation.

Scheffler, C (2008): Development of a Downscaling Scheme for a Coarse Scale Soil Watr Estimation method, Case Study: Great Letaba River, South Africa. Friedrich-Schiller-Universität Jena, Jena.

Schlüter, H. (1969): Vegetationskundlich-synökologische Untersuchungen zum Wasserhaushalt eines hochmontanen Quellgebiets im Thüringer Wald. Habilitation an der Martin-Luther- Universität zu Halle (unveröff.).

Schmidt, R.A. and C.A. Troendle (1989): Snowfall into Forest and Clearing. In: *Journal of Hydrology 110*, 335-348.

Schönwiese, C. D. (2000): Praktische Statistik für Meteorologen und Geowissenschaftler. Gebr. Borntraeger, Berlin, Stuttgart.

Schulze, R.E. (1992): Hydrological Models. Skript zu einer Vorlesungsreihe am *International Institute of Hydraulic, Infrastructural and Environmental Engineering, Delft*, 75 S. (unveröff.).

Schulze, R.E. (1995): Streamflow. In: Schulze, R.E.(ed.):Hydrology and Agrohydrology. A Text to Accompany the ACRU 3.00 Agrohydrological Modelling System. *Water Resaerch Commision, Pretoria, Report TT69/95*, AT19-1 bis AT10-6.

Schulze, R.E. et al. (1995): Hydrology and Agrohydrology. A Text to Accompany the ACRU 3.00 Agrohydrological Modelling System. *Water Resaerch Commision, Report TT69/95,* Pretoria.

Seidel, K. and J. Martinec.(2004): Remote sensing in snow hydrology: runoff modelling, effect of cli25 mate change, Springer-Praxis books in geophysical sciences, Springer; Praxis Pub., Berlin; New York, Chichester, UK, 150 pp.

Service, R.F. (2004): As the west goes dry, Science, 303, pp. 1124-1127.

Sevruk, B. (1982): Methods of Correction for Systematic Error in Point Precipitation measurement for Operational Use. In: *WMO No 589*, Genf.

Sevruk, B. (1983): Genauigkeit der konventionellen Regenmessung. In: *Mitteilungen des Instituts für Wasserwirtschaft, Hydrologie und landwirtschaftlichen Wasserbau der Universität Hannover 51*, 27-39.

Sevruk, B. (1984a): Karten der monatlichen Korrekturen des systematischen Niederschlagsmeßfehlers in der Schweiz. In: *DVWK-Mitteilungen 7*, 597-600.

Sevruk, B. (1984b): Assessment of snowfall proportion in monthly precipitation in CH. In: *DVWK-Mitt. 7,* 601-603.

Shafiee, R. (1999): Snow Hydrology, Case study Amirkabir Dam(Persian), Msc. Thesis, Agricultural University of Karaj, Iran

Shahid S. and H. Behrawan (09.2008): Drought risk assessment in the western part of Bangladesh, Natural Hazard, vol. 46, Nr. 03, 391-413, Springer Netherlands.

Sheshangosht, S.; Alimohammadi, A.; and Soltani, M.-J.; (2006): Evaluation of relations between DEM-Based USPED Model Output and Satellite-based spectral indices, Proceeding of Map India 2006.

Simpson, J.J.; Stitt, J.R. and M. Sienko (1998): Improved estimates of the areal extent of snow cover from AVHRR data. In: *Journal of Hydrology 204*, 1-23.

Simpson, J. J., M. D. Dettinger, F. Gehrke, T. J. McIntire, G. L. Hufford, (2004): Hydrologic scales, cloud variability, remote sensing, and models: implications for forecasting snowmelt and streamflow, *Weather and Forecasting, 19*, pp. 251-276.

Singh, V.P. (1995): Computer Models of Watershed Hydrology. Water Resources Publications 1995, Colorado, U.S.A.

Singh, P.; Spitzbart, G.; Hübl, H. and H.W. Weinmeister (1998): The role of snowpack in producing floods under heavy rainfall. In: Hydrology, Water Resources and Ecology in Headwaters. Proceedings of the HeadWater '98 Conference, Meran, April 1998, *IAHS Publication No. 248*, 89-95.

Singh P. and V.P Singh, (2001): Snow and Glacier Hydrology, Kluwer Academic Publishers, London, 742 pp.

Strasser, U., P. Etchevers, and Y. Lejeune (2002): Inter-comparison of two snow models with different complexity using data from an alpine site, *Nordic Hydrology, 33*(1), pp. 15-26.

Swedish Meteorological and Hydrological Institute (SMHI) (1996): IHMS – Integrated Hydrological Modelling System, Version 4.0, Manual. Norrköping, Schweden.

Tarboton, K.C., Schulze, R.E. et al. (1993): Distributed Hydrological Modelling System for the Mgeni Catchment. *ACRU-Report 39/WRC-Report No234 /1/92*. Pietermaritzburg.

Tarboton, D.G.: Chowdhury, T.G. and T.H. Jackson (1995): A spatially distributed energy balance snowmelt model. Biogeochemistry of Seasonally Snow-Covered Catchments Proceedings of a Boulder Symposium, July 1995, *IAHS Publication No. 228*, 141-155.

Turčan, J. (1990): Runoff modeling in mountain basins, *Hydrology of Mountainous Areas*, IAHS Publication No, 190, ed. L. Molnar, pp. 341-345.

Vehviläinen, B. (1992): Snow cover models in operational watershed forecasting. Yhteenveto: Lumimallit vesistöjen ennustemalleissa. *Publications of the Water and Environment Research Institute 11*, National Board of Waters and the Environment, Finland, Helsinki.

Wackernagel, H. (1995): Multivariate Geostatistics. Berlin: Springer.

Walter, M. Todd, E. S. Brooks, D. K. McCool, L. G. King, M. Molnau, J. Boll (2005): Process-based snowmelt modeling: does it require more input data than temperature-index modelling? *Journal of Hydrology, 300*, pp. 65-75.

Water and Energy Institute (2004): The Final Geology Report of the Latyan Catchment (Persian), Department of Civil Engineering. Sharif University of Technology. Tehran. Iran

Webster, R., and Oliver, M. A. (2001): Geostatistics for Environmental Scientists. Chichester [a.o.]: John Wiley & Sons.

Williams, M.W.; Cline, D.; Hartman, M. and T. Bardsley (1999): Data for snowmelt model development, calibration and verification at an alpine site, Colorado Front Range. *Water Resources Research, Vol. 35, No. 10*, 3205-3209.

Williams, K. S. and D. G. Tarboton (1999): The ABC's of snowmelt: a topographically factorized energy component snowmelt model, *Hydrological Processes, 13*, pp. 1905-1920.

World Meteorological Organization (1982): Methods of Correction for Systematic Error in Point Precipitation Measurement for Operational Use (ed. B. Sevruk). *Operational Hydrology Report No. 21, WMO-No. 589*, Geneva.

World Meteorological Organization (1986): Intercomparison of models of snowmelt runoff. *Operational Hydrology Report No.23, WMO-No. 646*, Geneva.

World Meteorological Organization (2000): Precipitation Estimation and Forecasting (C.G. Collier). *Operational Hydrology Report No.46, WMO-No. 887*, Geneva.

Wohlrab et al. (1992): Landschaftswasserhaushalt. Verl. Paul Parey, Hamburg, Berlin.

Wolf, M. (2009): Optimization of the Elevation Models for the Derivation of HRU Process Areas, Institute for Geography, Friedrich-Schiller-Universität Jena.

Wood, E. F., Sivapalan, M., and Beven, K. (1990): Similarity and Scale in Catchment Storm Response. *Reviews of Geophysics*, 28, 1-18.

Woo M.K. and P. Marsh. (2005): Snow, frozen soils and permafrost hydrology in Canada, 1999-2002. *Hydrological Processes,* 19, 215-229.

Zarghaami, M. and A., Salavitabar (2006): A System Dynamics Approach for Integrated Urban Water Management, *7th System Dynamics PhD Colloquium. System Dynamics Society*. Department of Civil Engineering. Sharif University of Technology. Tehran. Iran

Zeinivand, H. and F., De Smedt, (2008): Hydrological modelling of snow accumulation and melting on river basin scale. *Water Resources Management Journal*, DOI 10.1007/s11269-008-9381-2.

APPENDIX

Appendix A

The Manual of Hydrological Model J2000g

Abstract

The Model J2000g was developed as a simplified hydrological model to calculate temporally aggregated, spatially allocated hydrological target sizes. The representation and calculation of the hydrological processes is carried out one-dimensionally for an arbitrary number of points in the space. These model points enable the use of different distribution concepts (Response Units, grid cells, catchment areas) without further model adjustments.

The temporal discretization of the modeling can be carried out in daily or monthly steps. During the modeling the following processes are calculated for each time step: regionalization of punctual existing climate data to the referring model units, calculation of global and net radiation as access for the evaporation calculation, calculation of the land-cover-specific potential evaporation according to Penman-Monteith, snow accumulation and snowmelt, soil water budget, groundwater recharge, retardation in runoff (translation and retention). The individual processes are described in more detail below.

Distribution and Attribute Tables

The model J2000g is not bound to any specific distribution concept because the processes are calculated on the basis of points in the space that are independent of each other (1D-model concept). These points can represent different space units, e.g. single station positions, polygons, grid cells, catchment areas or subcatchments but also rather administrative units such as field unit or administrative districts. In the following text the term "model unit" is used for these points.

Model Unit Attribute Table

Each model unit needs to be described with specific attributes for the modeling. These are:

ID - a clear numeric ID

X - the easting of the centre (centroid) as Gauss-Krüger coordinate

Y - the northing of the centre (centroid) as Gauss-Krüger coordinate

area - the area of the model unit in m²

elevation - the mean elevation of the model unit in m above sea level(m.a.s.l)

slope - the mean slope of the model unit in degree

aspect - the aspect of the model unit in degree from North clockwise

soilID - a clear numeric ID for the soil type (serves as allocation to the soil attribute table)

landuseID - a clear numeric ID for the land use/land cover type (serves as allocation to the land use table)

hgeoID - a clear numeric ID for the hydrological unit of the model unit (serves as allocation to the hydrogeology table)

The model unit attribute table contains the attribute names in the first row. These must not be changed because they are used as variable name for the attribute generation during the model parameterization. The second row contains the minimal possible value of the referring attribute, whereas the third one contains the maximum possible value. In the fourth row the physical unit of the attribute needs to be entered. Then, as many rows as needed are given that contain the attribute values of the single model units. The table needs to be completed by a comment row which starts with the comment symbol (#). The tab (\t) has to be used to separate the rows.

Soil Attribute Table

The soil attribute table contains soil-physical characteristics for each soil unit that occurs in the area. In the current model version only the usable field capacity for each decimeter is needed. On the basis of the field capacity the maximum storage capacity of the soil water storage is calculated in dependence of the effective root depth of the vegetation on the model unit during the model parameterization.

The format of the soil attribute table is very similar to the model units attribute table. The table can be started with an arbitrary number of comment rows that need to be started with the comment symbol (#). In the first interpreted row the attribute names need to be given. The spelling is very important here. The following attributes need to be included:

SID - clear numeric ID with which the connection to the model unit table is generated

depth - depth of the soil in cm

fc_sum - entire usable field capacity of the soil in mm

fc_1 to fc_n - usable field capacity for each decimeter in mm/dm

To complete the table, a comment row must be given (introduced with #). The tab (\t) has to be used to separate the rows.

Land Use Attribute Table

The land use attribute table contains vegetation parameters that are nearly exclusively needed for the evaporation calculation according to Penman-Monteith. In the table the following attributes need to be given for each land use unit and land cover unit that occurs in the area:

LID - a clear numeric ID with which the connection to the model unit table is generated.

description - a description as text

albedo - albedo [0 ... 1]

RSC0_1 to RSC0_12 - the stomatal resistances for good water availability for the months January (RSC0_1) to December (RSC0_12) in s/m

LAI_d1 to LAI_d4 - the area leaf index in m²/m² for the Julian Days 110 (d1), 150 (d2), 250 (d3) and 280 (d4) for a terrain height of 400 m.a.s.l.

effHeight_d1 to effHeight_d4 - effective vegetation height in meter for the Julian Days 110 (d1), 150 (d2), 250 (d3) and 280 (d4) for a terrain height of 400 m.a.s.l.

rootDepth - the effective root depth in dm

To complete the table, a comment row must be given (introduced with #). The tab (\t) has to be used to separate the rows.

Hydrogeology Attribute Table

In the hydrogeology attribute table the maximum possible ground water recharge rates per time unit are set up for each hydrogeologic unit. It only contains the following two attributes:

GID - a clear numeric ID with which the connection to the model unit table is generated.

mxPerc - the maximum possible percolation rate (ground water recharge rate) per time interval in mm per time unit

To complete the table, a comment row must be given (introduced with #). The tab (\t) has to be used to separate the rows.

Input Data - Model Driver

For the model run climate time series of an arbitrary number of climate and precipitation stations are needed. The time series have to be preprocessed in the referring formatted data files. The files have the following format:

Rows 1 to 13 contain meta information about the data. They are arranged in blocks which are started with descriptions which in turn are started with the AT-symbol (@). Multiple entries per row are separated via the tab (\t).

@dataSetAttribs (attribute of the dataset)

missingDataVal - value that marks missing data

dataStart - start date of the dataset (DD.MM.JJJJ HH:MM)

dataEnd - end date of the dataset (DD.MM.JJJJ HH:MM)

tres - termporal resolution (days "d", months "m")

@statAttribVal (attributes of the climate stations)

name - the names of the climate stations

ID - a numeric, clear ID

elevation - the elevation of the station in m.a.s.l.

x - easting as Gauss-Krüger-coordinate

y - northing as Gauss-Krüger-coordinate

dataColumn - describes the column in which the data for the referring station can be found

In the following rows the actual data for each time step is listed – starting with:

@dataVal

The format is Date, Time followed by Data that is separated by the tab.

Installation and Start

Model Initialization

Regionalization

The regionalization module is used for the transfer of punctual values to the model units. The procedure was taken from the hydrological Model J2000 without any changes and is arranged in the following steps:

Calculation of a linear regression between the station values and the station heights for each time step. Thereby, the coefficient of determination (r2) and the slope of the regression line (bH) is calculated.

Definition of the n gaging stations which are nearest to the particular model unit. The number n which needs to be given during the parameterization is dependent on the density of the station net as well as on the position of the individual stations.

Via an Inverse-Distance-Weighted Method (IDW) the weightings of the n stations are defined dependently on their distances for each model unit. Via the IDW-method the horizontal variability of the station data is taken into account according to its spatial position.

Calculation of the data value for each model unit with the weightings from point 3 and an optional elevation correction for the consideration of the vertical variability. (The elevation correction is only carried out when the coefficient of determination –calculated under point 1 – goes beyond the threshold of 0.7.)

The calculation of the data value for each model unit (DWU) without elevation correction is carried out with the weightings (W(i)) and the values (MW(i)) of each n gaging station according to:

$$DW_U = \sum_{i=1}^{n} MW(i) \cdot W(i)$$

For the calculation with elevation correction the elevation difference (HD(i)) between the gaging station and the model unit as well as the slope of the regression line (bH) are taken into account. Thus, the data value for the model unit (DWU) is calculated according to:

$$DW_U = \sum_{i=1}^{n} ((HD(i) \cdot b_H + MW(i)) \cdot W(i))$$

Precipitation Correction

Precipitation values partly show a clear systematic error in measurement which is caused instrument-determined or due to the selection of the instrument position. This error in measurement has two causes: (1) the moistening error and evaporation error, which each depends on the type of the instrument and (2) the wind error which emerges due to the drifting of the precipitations. Both errors in measurement are strongly dependent on the type (rain or snow) of the precipitation amount.

For the correction of both errors a correction method according to Richter (1995) is used which is applied in the same way in the Model J2000. The procedure for the evaporation correction differs with regard to the temporal resolution of the precipitation data.

Monthly Precipitation Correction

The corrected precipitation (Pkorr) is calculated for monthly time steps on the basis of the decrease of the measured precipitation (Pm) and the percental monthly error in measurement (MFt) (see adjacent table):

$$P_{korr} = P_m + P_m \cdot \frac{MF_t}{100}$$

Daily Precipitation Correction

For the daily precipitation correction the two error terms are calculated explicitly. For this purpose, correction functions were derived on the basis of the tabled error values according to Richter (1995).

Moistening Loss and Evaporation Loss

For a continual error correction of the moistening loss and evaporation loss continual correction functions were adjusted to the tabled values by Richter (1995). They are shown in the adjacent figure. The correction functions were derived each separately for the winter half year (November till April) and summer half year (May till October). With these functions the moistening loss and evaporation loss is calculated in mm for precipitations <= 9 mm according to:

$$BV_{Som} = 0.08 \cdot \ln(N) + 0.225$$

$$BV_{Win} = 0.05 \cdot \ln(N) + 0.13$$

If the amount of precipitation is greater than 9 mm, a constant error of 0.47 mm in the summer half year and of 0.3 mm in the winter half year is assumed.

Wind Error

The calculation of the wind error of the precipitation measurement with the Hellman precipitation gauge is also carried out according to the tabled error values from Richter (1995) which was adjusted to the referring continual correction functions. For the correction it is differentiated whether the precipitation was rain or snow. The way of internal differentiation is described further below. The relative correction value is calculated as follows:

$$WK_s = 0.5424 \cdot N^{-0.211} \text{ for snow}$$

$$WK_r = 0.1421 \cdot N^{-0.519} \text{ for rain.}$$

The corrected precipitation value (PK) is finally calculated on the basis of the value (PM), the relative correction value for the wind error (WKs, WKr) as well as the moistening loss and evaporation loss (BVSom, BVWin) as follows:

$$P_K = P_M + P_M \cdot WK_{s,r} + BV_{Som,Win}$$

Radiation Calculation

For the evaporation calculation according to Penman-Monteith, the net radiation is needed as initial value and can be calculated on the basis of the global radiation. If the global radiation is not available, it can be defined approximately on the basis of the sunshine duration. For this purpose, a number of intermediate calculations are necessary. The following calculations act on the assumption of a daily modeling. When the model runs in monthly time steps, the calculations listed below are carried out on the 15th of each month. The resulting terms are then accumulated on the basis of the days per month.

Extraterrestrial Radiation

The extraterrestrial radiation (Ra) is the short-wave radiation energy flux of the sun at the upper boarder of the atmosphere. Ra is calculated for a specific place in dependence of its latitude (lat in radians), the declination of the sun (decl in radians), the solar constant (Gsc in MJ / m2min), the hour angle at sundown (ws in radians) and the inverse relative distance between earth and sun (dr in radians) according to:

$$Ra = \frac{24 \cdot 60}{\pi} \cdot Gsc \cdot dr \cdot (ws \cdot \sin(lat) \cdot \sin(decl) + \cos(lat) \cdot \cos(decl) \cdot \sin(ws))$$

The solar constant (Gsc in MJ / m2min) results from the Julian Date (jD [1... 365,366]) as follows:

$$Gsc = 0.08139 + 0.00291 \cdot \cos\left(\frac{\pi}{180} \cdot (jD - 15)\right) \text{[MJ / m2min]}$$

The relative distance between earth and sun (dr in radians) results from the Julian Date (jD [1... 365,366]) as follows:

$$dr = 1 + 0.033 \cdot \cos\left(\frac{2\pi}{365} \cdot jD\right) \text{[rad.]}$$

The declination of the sun (decl in radians) results from the Julian Date (jD [1... 365,366]) as follows:

$$decl = 0.40954 \cdot \sin(0.0172 \cdot (jD - 79.35)) \text{[rad.]}$$

The hour angle at sundown (ws in radians) results from the latitude (lat in radians) and the declination (decl in radians) as follows:

$$ws = \arccos(-1 \cdot \tan(lat) \cdot \tan(decl)) \text{[rad.]}$$

Global Radiation

The global radiation (Rg) is calculated on the basis of the extraterrestrial radiation (Ra in MJ/m²d) and the degree of cloudiness. At this, the degree of cloudiness is approximated on the basis of the relation of the measured sunshine duration (D in h/d) to the astronomic possible sunshine duration (S0 in h/d) with the help of the Angström formula. Thus, Rg is calculated as follows:

$$Rg = Ra \cdot \left(a + b \cdot \frac{S}{S_0}\right) \text{[MJ/m²d]}$$

The coefficients **a** and **b** need to be estimated for the position. Often 0.25 is used for a and 0.50 is used for b.

The maximum astronomic possible sunshine duration (S0 in h) is calculated on the basis of the hour angle at sundown (ws in radians) as follows:

$$S_0 = \frac{24}{\pi \cdot ws} \text{[h/d]}$$

Net Radiation

The net radiation (Rn in MJ/m²d) results from the single radiation components and provides the energy for the evaporation. The net radiation is calculated on the basis of the difference of the global radiation (Rg in MJ/m²d) and the effective long-wave radiation (Rl in MJ/m²d). The global radiation is reduced by the albedo (alpha) of the referring land cover.

$$Rn = (1 - \alpha) \cdot Rg - Rl$$

The effective long-wave radiation (Rl in MJ/m²d) is calculated on the basis of the Bolzmann constant (Bk = 4.903E-9 MJ/K4m²d), the absolute air temperature (Tabs in K), the actual vapor pressure of the air (ea in kPa), the actual global radiation (Rg in MJ/m²d) and the maximum global radiation for unclouded sky (Rg0 in MJ/m²d):

$$Rl = Bk \cdot Tabs^{4} \cdot (0.34 - 0.14 \cdot \sqrt{ea}) \cdot \left(1.35 \cdot \frac{Rg}{Rg0} - 0.35 \right) \quad [MJ/m²d]$$

The actual vapor pressure of the air (**ea** in kPa) is calculated on the basis of the saturation vapor pressure (**es** in kPa) and the relative humidity (U in %) according to the following equation:

$$ea = es \cdot \frac{U}{100} \quad [kPa]$$

The saturation vapor pressure of the air (es in kPa) results from the air temperature (T in °C) according to:

$$es = 0.6108 \cdot e^{\frac{17.27 \cdot T}{237.3 + T}} \quad [kPa]$$

The maximum global radiation for uncovered sky (Rg0 in MJ/m²d) results from the extraterrestrial radiation (**Ra** in MJ/m²d) and the terrain height (h in m.a.s.l.) as follows:

$$Rg0 = (0.75 + 2 \cdot 10^{-5} \cdot h) \cdot Ra \quad [MJ/m²d]$$

Evaporation Calculation

The calculation of the potential evaporation can be carried out according to Penman-Monteith or Haude. The advantage of the Penman-Monteith method is the higher physical basis. However, much more input data is needed. For the calculation according to Haude only air temperature and relative humidity are required.

Potential Evaporation according to Penman-Monteith

The calculation of the inventory evaporation according to Penman-Monteith (PET in mm/d) is calculated as follows:

$$PET = \frac{1}{L_d} \cdot \frac{s \cdot (Rn - G) + \rho \cdot c_P \cdot \frac{es - ea}{r_a}}{s + \gamma \cdot \left(1 + \frac{r_a}{r_d} \right)} \quad [mm/d]$$

with:

Ld : latent heat of evaporation [MJ/kg]

s : slope of the vapor pressure curve [kPa / K]

Rn : net radiation [MJ/m²d]

G : soil heat flux [MJ/m²d]

ρ : density of the air [kg/m³]

cP : specific heat capacity of the air (=1.031E-3 MJ/kg K]

es : saturation vapor pressure of the air [kPa]

ea : actual vapor pressure of the air [kPa]

γ : psychrometer constant [kPa / K]

ra : aerodynamic resistance of the land cover [s/m]

rs : surface resistance of the land cover [s/m]

The latent heat of evaporation (Ld in MJ/kg) results from the air temperature according to the following equation:

$$L_d = \frac{2501 - 2.361 \cdot T}{1000}$$ [MJ/kg]

The slope of the saturation vapor pressure curve (s in kPa/K) is calculated on the basis of the air temperature:

$$s = \frac{4098 \cdot 0.6018 \cdot \epsilon^{\frac{17.27 \cdot T}{T+237.3}}}{(T + 237.3)^2}$$ [kPa/K]

The soil heat flux (G in MJ/m²d) results from the net radiation (Rn in MJ/m²d):

$$G = 0.1 \cdot Rn$$ [MJ/m²d]

The density of the air (ρ in kg/m³) results from the air pressure (p in kPa) and the virtual temperature (vT in K):

$$\rho = 3.486 \cdot \frac{p}{vT}$$ [kg/m³]

If the air pressure (p in kPa) is not available as value, it can be calculated approximately on the basis of the terrain height (h in m.a.s.l.) and the absolute air temperature (Tabs in K) according to the following equation:

$$p = \frac{1013 \cdot \epsilon^{\left(-1 \cdot \frac{9.811}{8314.3 \cdot T_{abs}} \cdot h\right)}}{10}$$ [kPa]

The virtual temperature (vT in K) results from the air pressure (p in kPa), the absolute air temperature (Tabs in K) and the actual vapor pressure of the air (ea in kPa):

$$vT = \frac{Tabs}{1 - 0.378 \cdot \frac{ea}{p}}$$ [K]

The psychrometer constant (γ in kPa / K) is calculated on the basis of the specific heat capacity of the air (=1.031E-3 MJ/kg K), the air pressure (p in kPa), the relation of the

molecular weight of dry and humid air (VM = 0.622) and the latent heat of evaporation (Ld in MJ/kg):

$$\gamma = \frac{c_P \cdot p}{VM \cdot L_d}$$

The surface resistance of the land cover (rs in s/m) results from the leaf area index LAI, the stomatal resistance for the given point in time (rsc in s/m) and the surface resistance of an uncovered surface (rss = 150 s/m) as follows:

$$r_s = \frac{1}{\frac{1 - 0.7^{LAI}}{rsc} + \frac{0.7^{LAI}}{rss}}$$

The aerodynamic roughness of the land cover (ra in s/m) results from the wind speed (v in m/s) and the effective vegetation height (eH in m)

$$r_a = \frac{9.5}{v} \cdot \ln\left(\frac{2}{0.1 \cdot eH}\right)^2 \text{ [s/m] for stands with eH < 10 m}$$

$$r_a = \frac{20}{0.41^2 \cdot v} \text{ [s/m] for stands with eH >= 10 m}$$

Potential Evaporation according to Haude

The potential evaporation according to Haude is calculated on the basis of the saturation deficit of the air and an empirical, dimensionless Haude-factor (hF). The saturation deficit results from the saturation vapor pressure (es in kPa) and the relative air humidity (U in %). The Haude-factor has to be defined for different vegetation types. The calculation of the potential evaporation (PET in mm) is carried out according to:

$$PET = es \cdot \left(1 - \frac{U}{100}\right) \cdot hF$$

The saturation vapor pressure of the air (es in kPa) results from the air temperature (T in °C):

$$es = 0.6108 \cdot e^{\frac{17.27 \cdot T}{237.3 + T}} \text{[kPa]}$$

Snow Cover Calculation

The snow cover calculation is implemented as simple accumulation and snowmelt approach. The method decides on the basis of the air temperature whether water is saved as snow on a model unit or whether potentially existing snow melts and produces snowmelt runoff. For this purpose, two temperatures are calculated from the minimum temperature (Tmin), average temperature (Tavg) and maximum temperature (Tmax) of the referring time step:

The accumulation temperature as: $$T_{acc} = \frac{T_{min} + T_{avg}}{2} \text{ [°C] and}$$

the snowmelt temperature as:

$$T_{melt} = \frac{T_{avg} + T_{max}}{2} \quad [°C]$$

If the accumulation temperature (Tacc) lies on or below a threshold (Tbase) that needs to be given by the user, it is assumed that potentially occurring precipitation falls as snow. It is then saved on the model unit.

If the snowmelt temperature goes beyond the temperature threshold Tbase, the snowmelt is calculated with the help of a simple snowmelt factor (TMF). For this purpose, a potential snowmelt rate is calculated on the basis of the TMF (in mm/d K), the temperature threshold and the snowmelt temperature:

$$SM_p = TMF \cdot (T_{melt} - Tbase) \quad [mm/d]$$

This potential snowmelt rate is then compared to the actual saved snow water equivalent which is then partly or fully melted. The resulting snowmelt water is passed on as input to the following module.
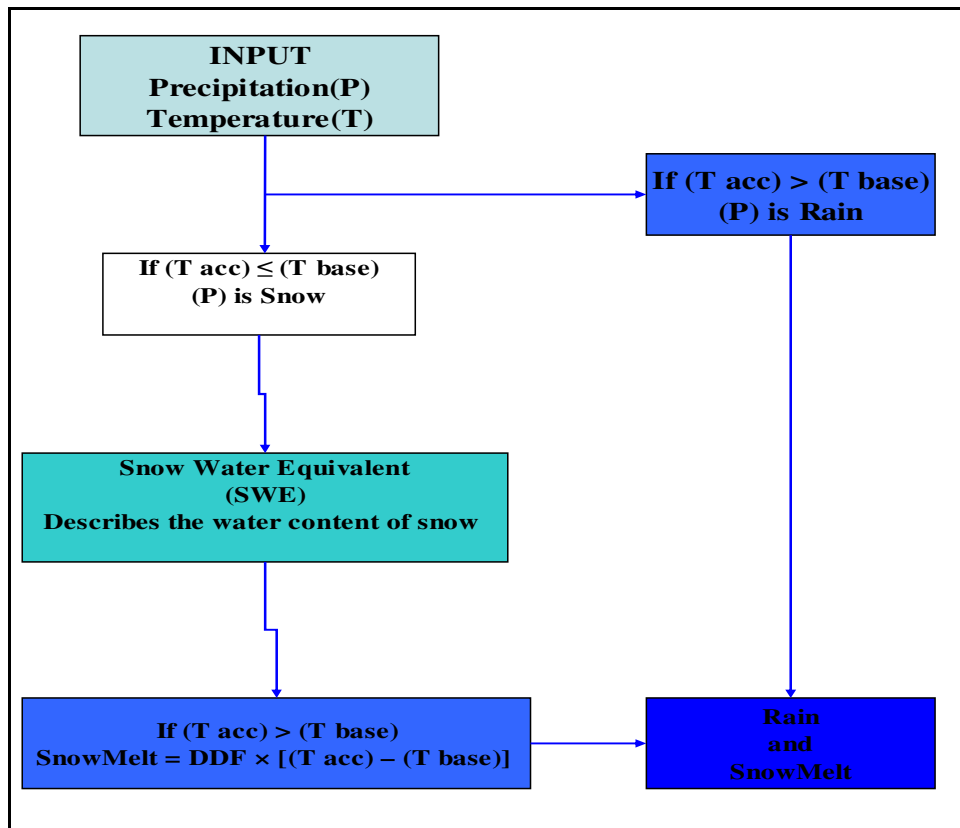
Figure A 3: The Snow module Concept of the J2000g Model

Soil Water Budget

The soil water budget module serves as allocator of the input (precipitation and snowmelt) to the output paths (evaporation, direct runoff, ground water recharge). The central element is the soil storage which is dimensioned via the usable field capacity of the rooted soil area. The maximum fill volume can be adjusted by a multiplicative user-controlled calibration parameter (FCA).

First, the input (precipitation and snowmelt) is allocated to the evaporation until the potential evaporation is reached. The surplus (inflow) is then allocated in direct runoff (SQ) and infiltration (INF), in dependence of the relative soil saturation (Θ) and a calibration parameter (DFB). The calculation is carried out as follows:

$$SQ = \Theta^{DFB} \cdot Inflow \;\; \text{[mm/d]}$$

$$INF = (1 - \Theta^{DFB}) \cdot Inflow \;\; \text{[mm/d]}$$

The infiltration (INF) is allocated to the soil storage until it is completely saturated. If there is a surplus (excess water EW), it is allocated to the two paths interflow (SSQ) and ground water recharge (GWR) in dependence of the slope (α) and a calibration parameter (LVD). The calculation is carried out according to the following equation:

$$SSQ = \tan\alpha \cdot LVD \cdot EW \;\; \text{[mm/d]}$$

$$GWR = (1 - \tan\alpha) \cdot LVD \cdot EW \;\; \text{[mm/d]}$$

The ground water recharge is seen as source for the basis runoff (BQ) now.

Runoff Concentration and Retardation in Runoff

The runoff concentration and retardation in runoff is represented as simple function of the catchment area for the three runoff components (direct runoff, SQ, intermediate runoff SSQ and basis runoff BQ). For this purpose, the generation rates of the three components are accumulated area-weighted and are lead by their own linear cascade (Nash-cascade). For each of the three cascades the user has to determine the following two parameters: number of storages (n) and retention coefficient (k).
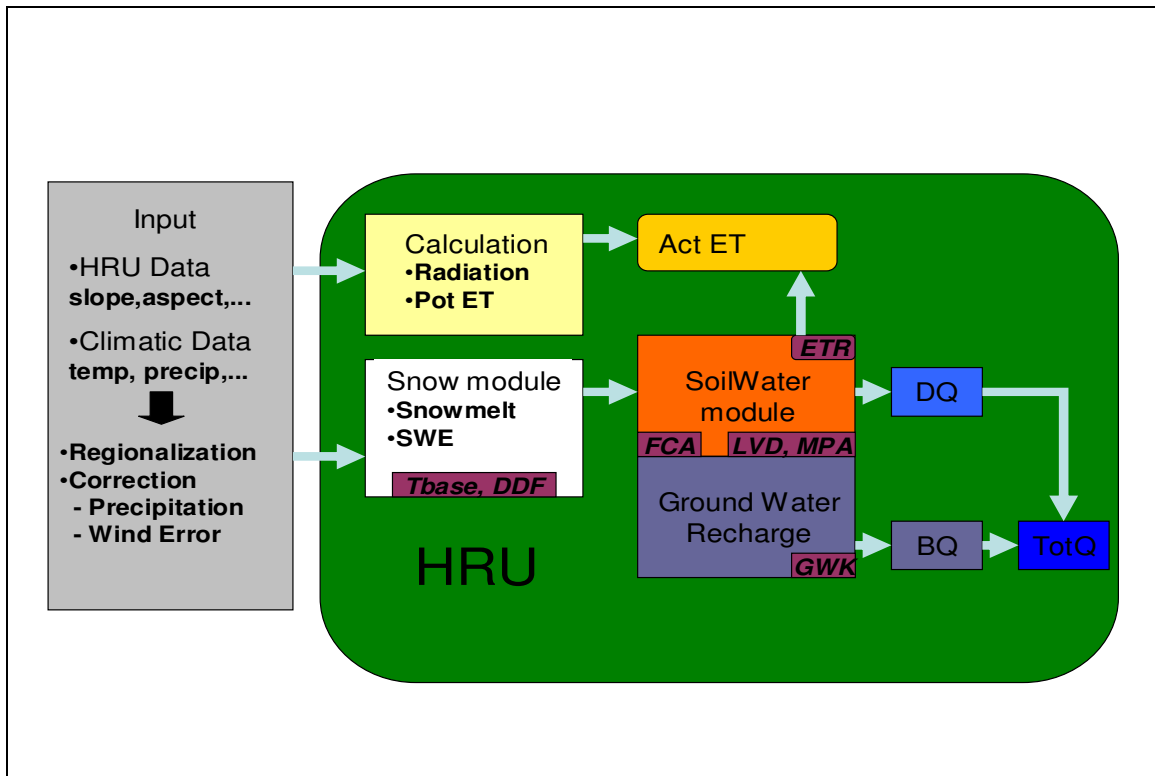
Figure A 3-1: The Modelling System Runoff Generation of the J2000g Model

Appendix B

Table B 5-4: The Landuse/Landcover Class Parameters for Evapotaranspiration and Soilwater Module in the Latyan Catchment

Landcover Class	ALBEDO [%]	Resistance Stomata Conductance [s/m]						LAI [-]		Effective Height [m]		RD [dm]
		1	2	3	4	5	6	D1	D2	D1	D2	
		7	8	9	10	11	12	D3	D4	D3	D4	
Agriculture	0.25	80	80	75	65	45	50	1	5	0.05	0.5	1.5
		50	50	50	65	80	80	3	1	0.3	0.05	
Decidous broad trees		80	80	70	65	55	55	1	8	3	10	
	0.17	55	55	60	75	80	80	8	1	10	3	20
Decidous shrubs	0.2	80	80	70	60	50	50	3	5	1.5	2.5	
		50	55	55	70	80	80	5	3	2.5	1.5	15
Grassland	0.25	80	80	70	60	40	45	2	5	0.3	0.5	
		45	45	50	60	80	80	5	2	0.5	0.3	6
Settlement (not dense)	0.1	90	90	80	70	50	55	1	1	3	5	
		55	55	60	70	90	90	1	1	5	3	3
Water		20	20	20	20	20	20	1	1	0.1	0.1	
	0.05	20	20	20	20	20	20	1	1	0.1	0.1	20

The values in the table are taken from :((Krause, (2001), and JAMSWIKI, (2010)).

Appendix C

Sensitivity analysis and Uncertainty analysis of the Hydrological model J200g in the Latyan catchments
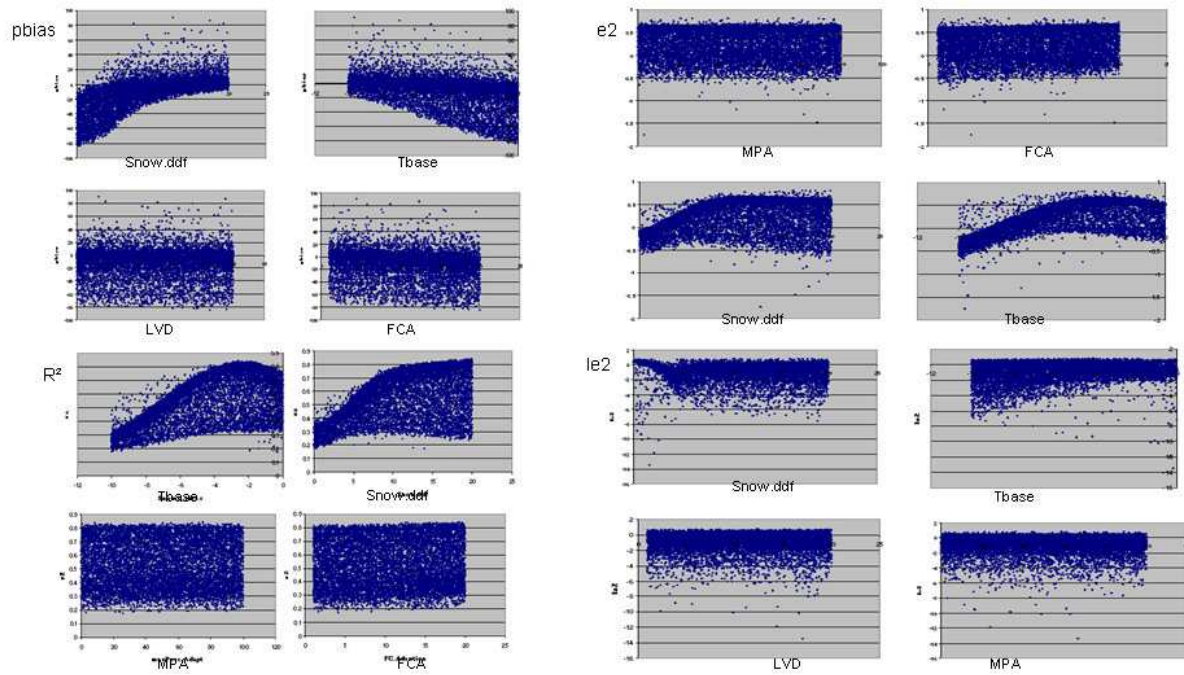
Figure C-1: Dotty plots for monthly Roodak model
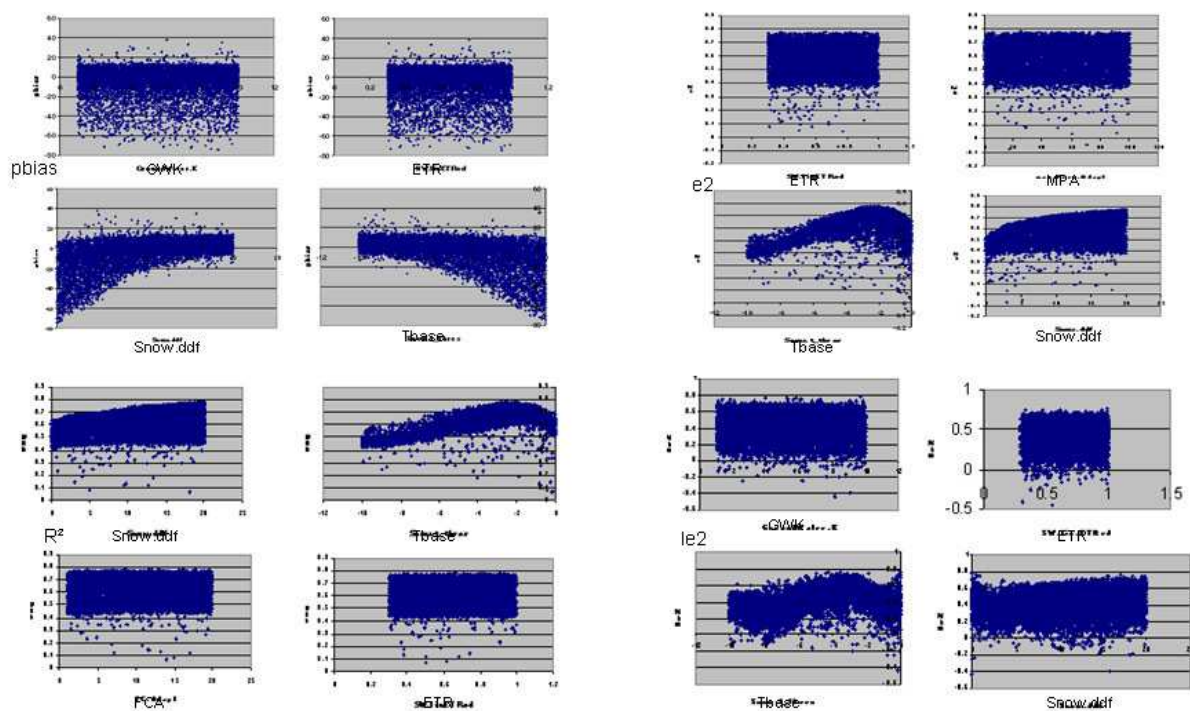
Figure C-2: Dotty plots for monthly Najarkola model
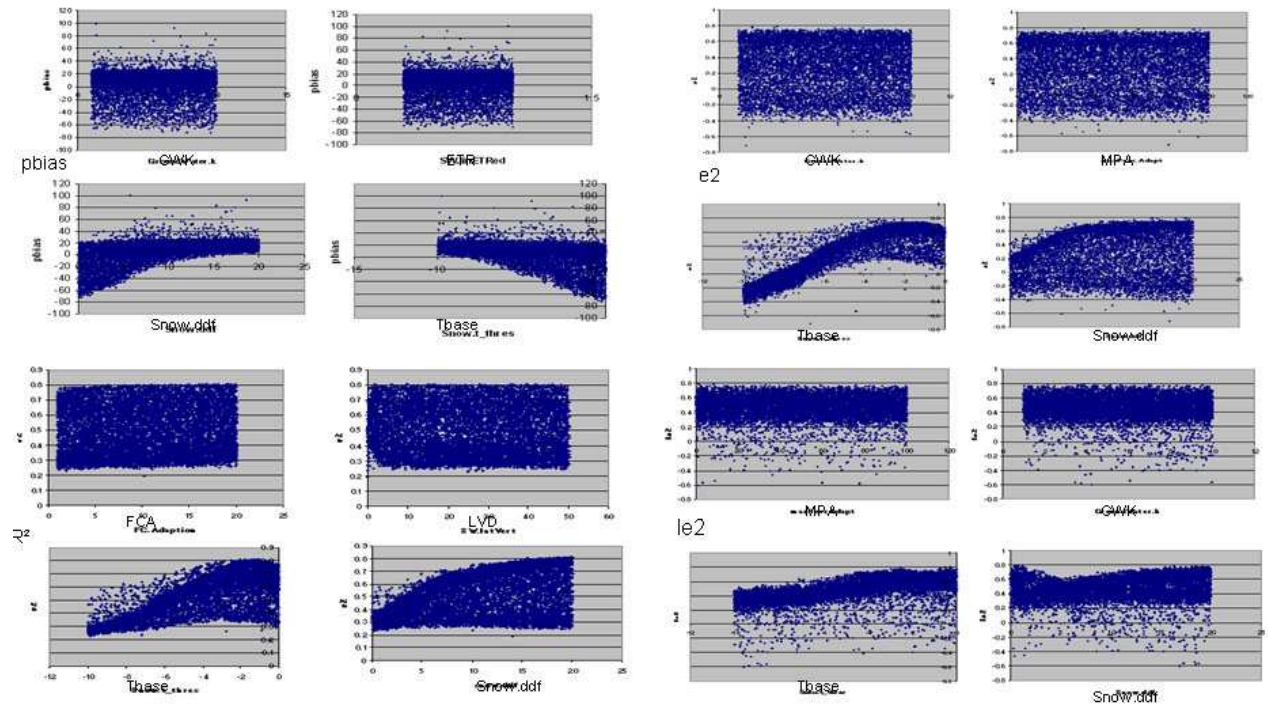
Figure C-3: Dotty plots for monthly Naran model
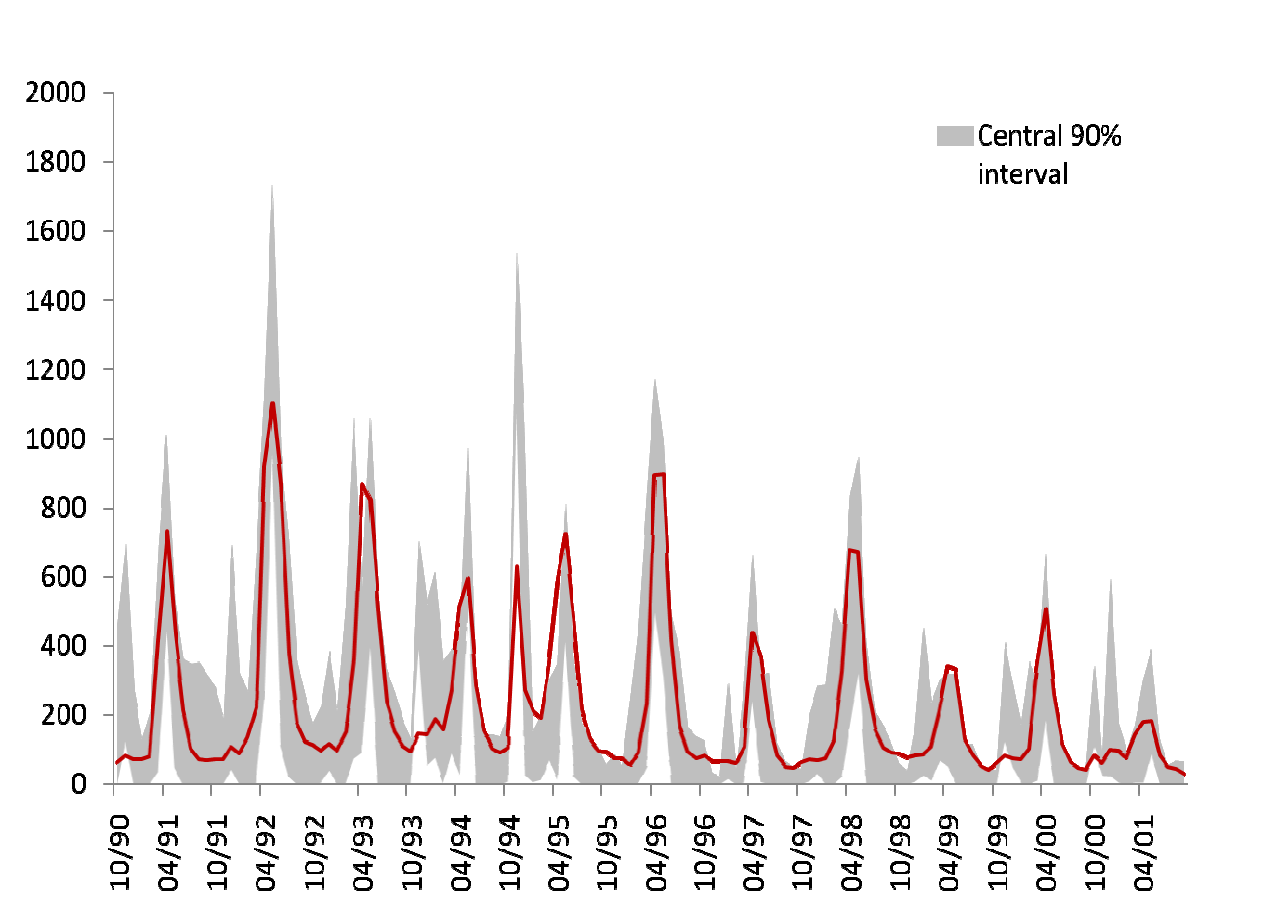
Figure C-4: Runoff ensemble from multi parameters variation of monthly Roodak model

Appendix D

The J2000g model calibration and results (Runoff, Snowmelt, SWE) for Latayan catchment
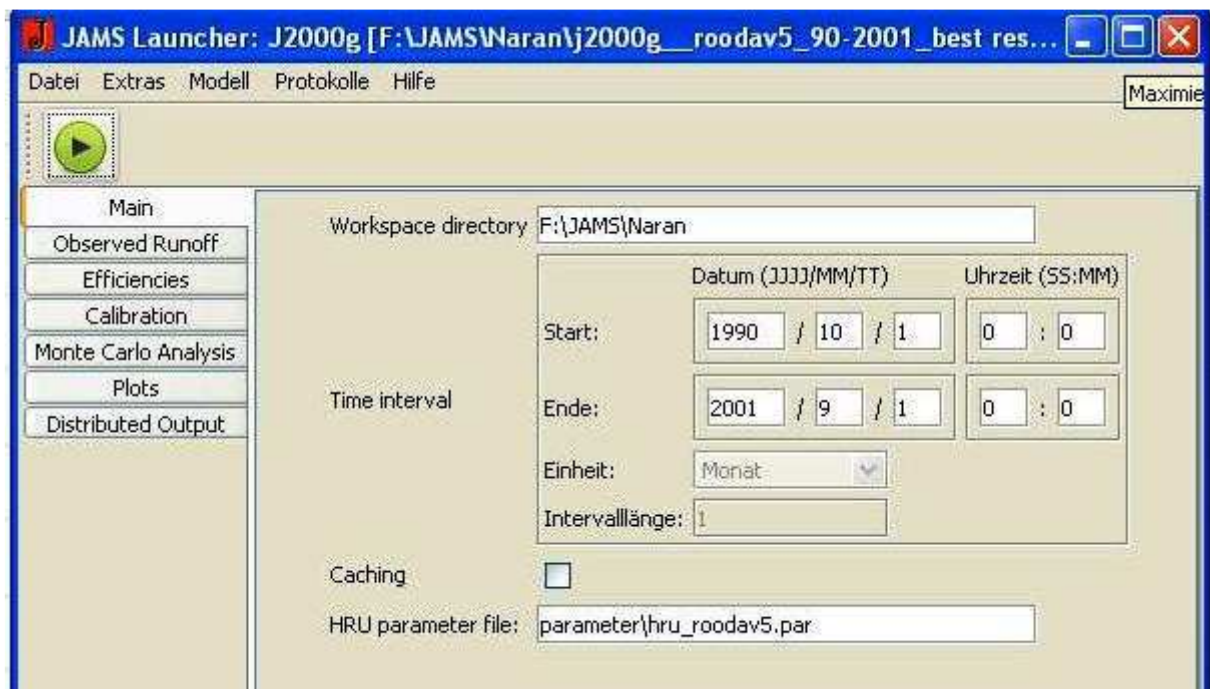
D-1: Main page of the Model
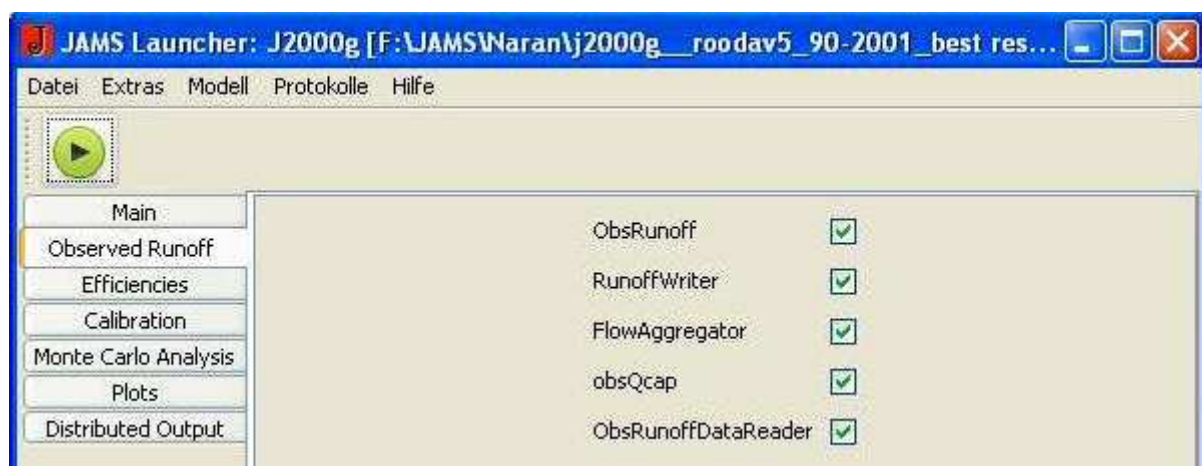
D-2: Visual availability selection of the model
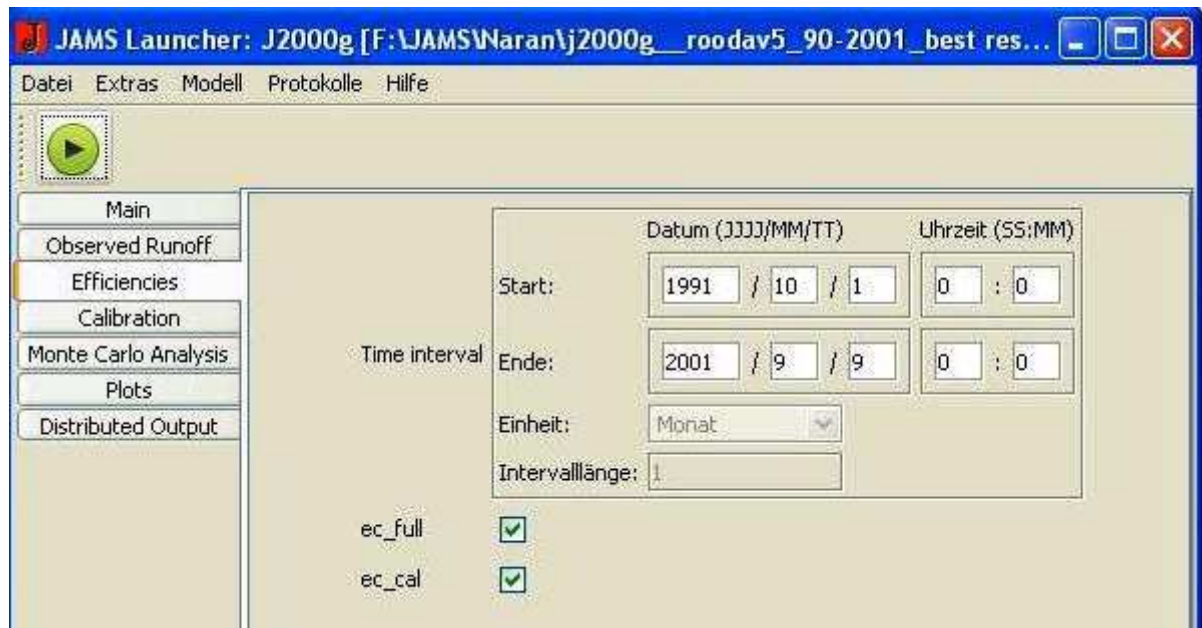
D-3: Efficiency selection of model
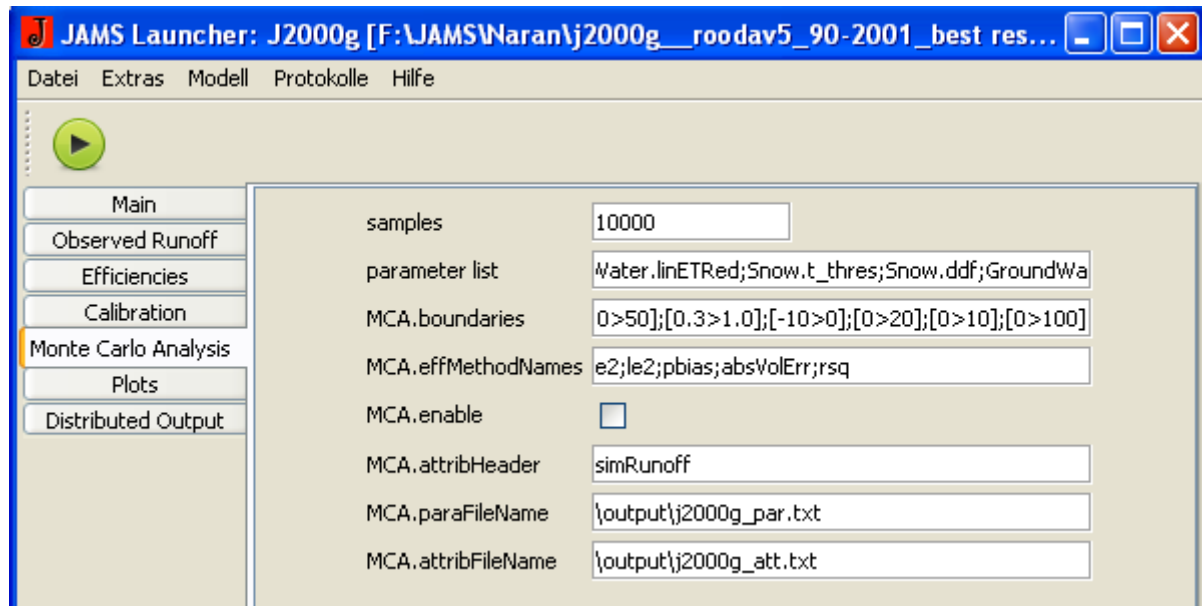
D-4: Monte Carlo Analysis method for automatically running model
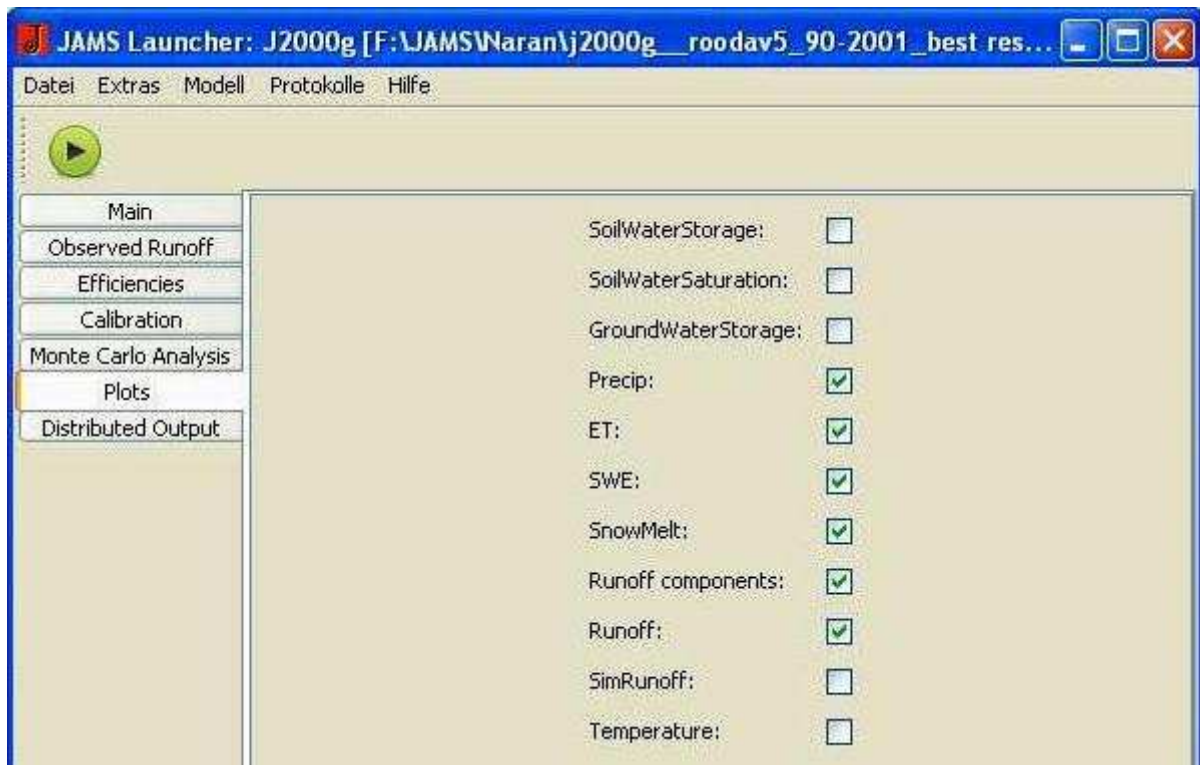
D-5: Difference visual plots of model
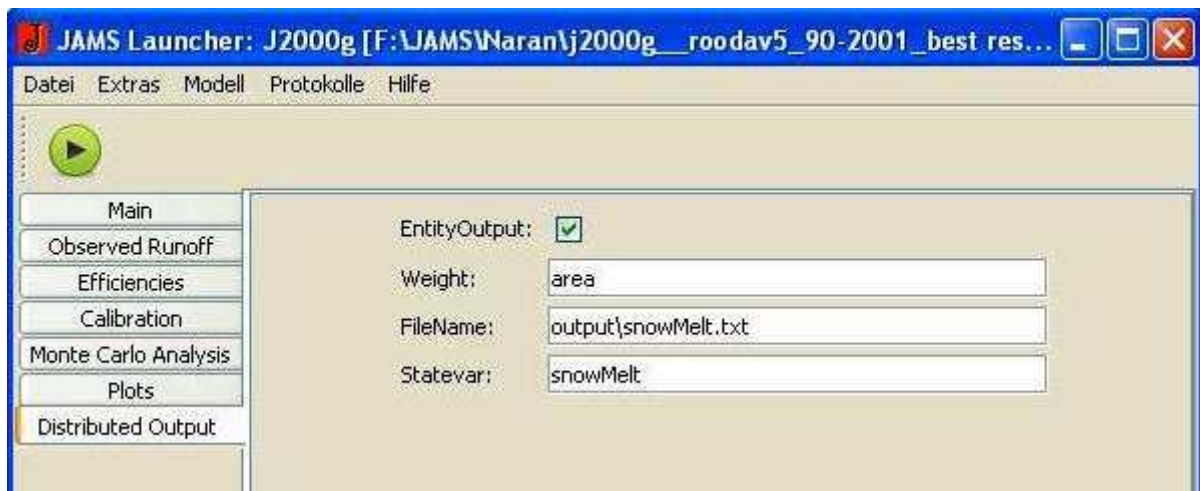
D-6: Entity output option of model for design spatial distribution of (SWE, Snowmelt, Runoff, etc.)
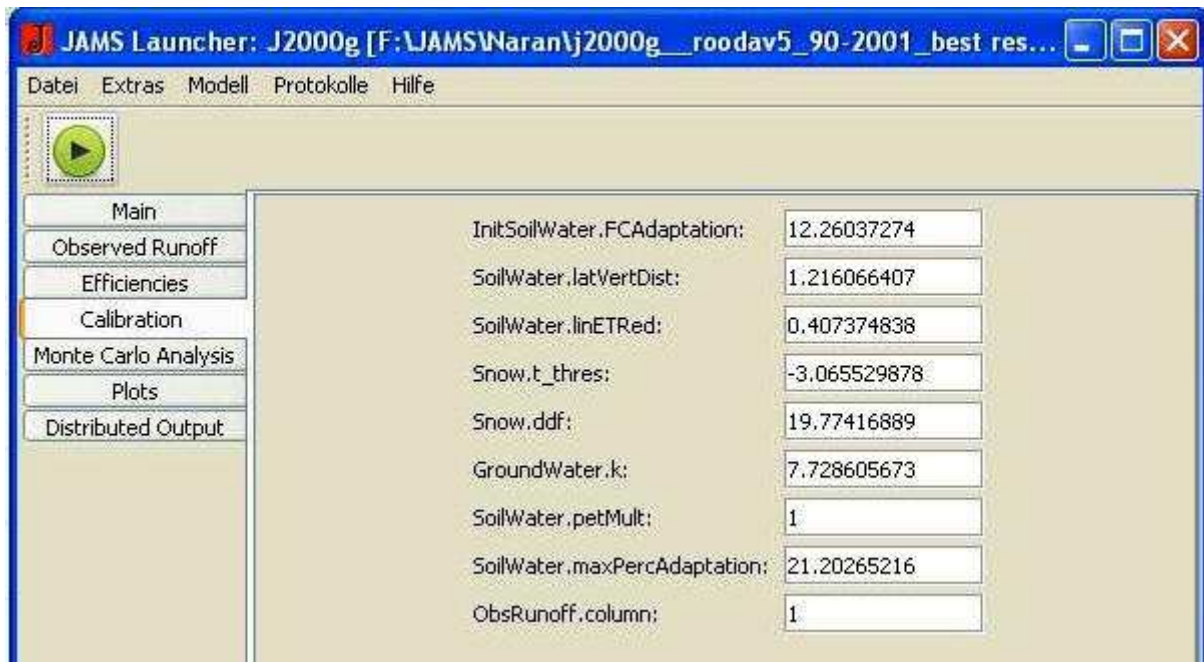
D-7: Calibration of Model Parameters for Roodak subcatchment
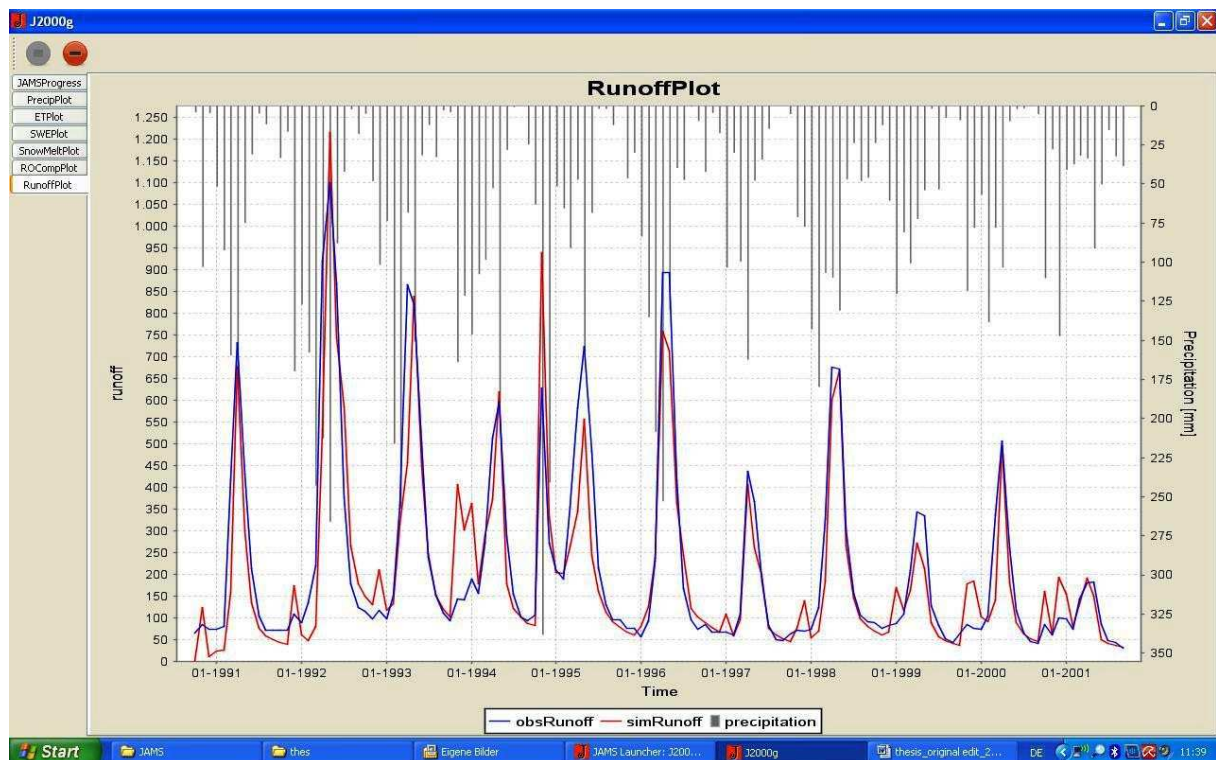
D-8: Runoff Prediction of model for Roodak subcatchment
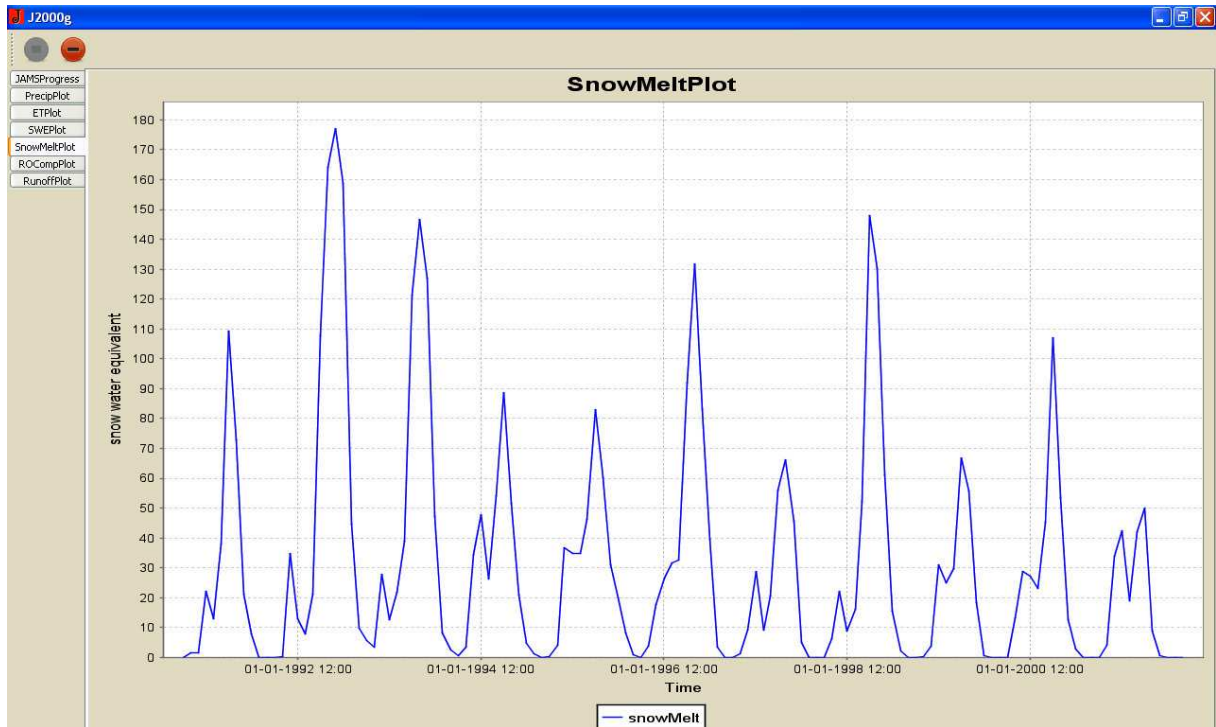
D-9: Snowmelt simulation for Roodak subcatchment
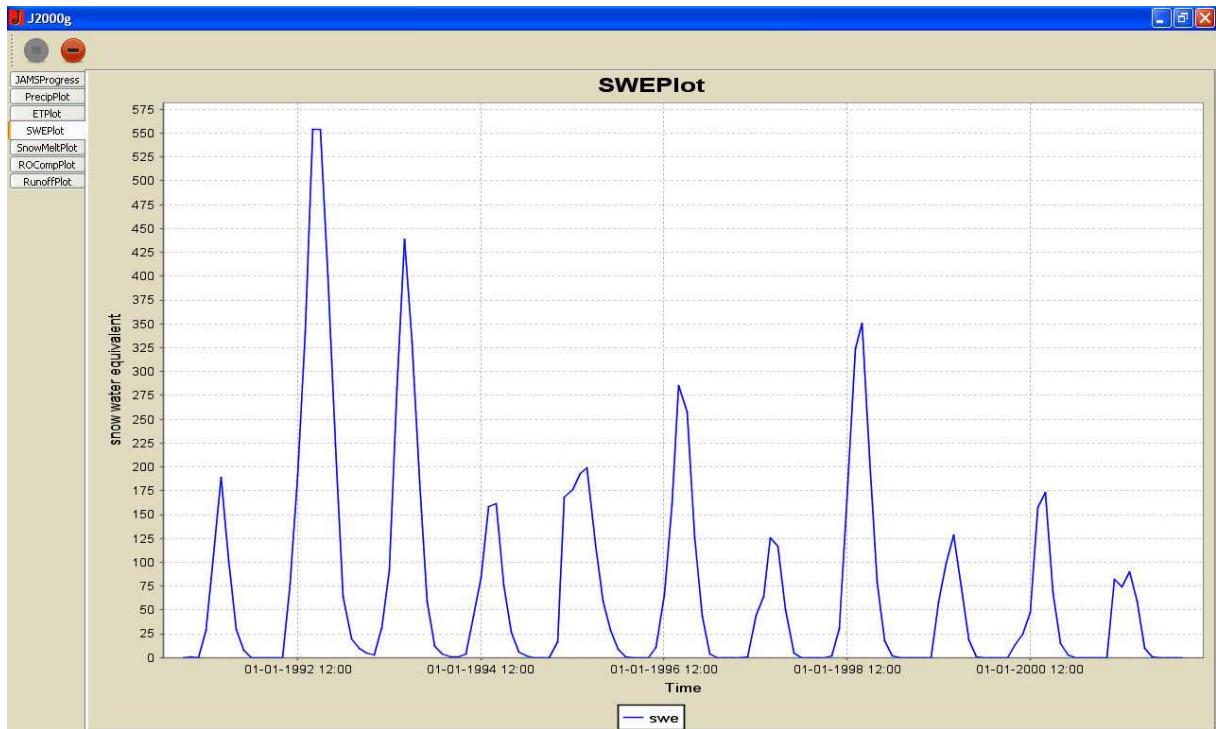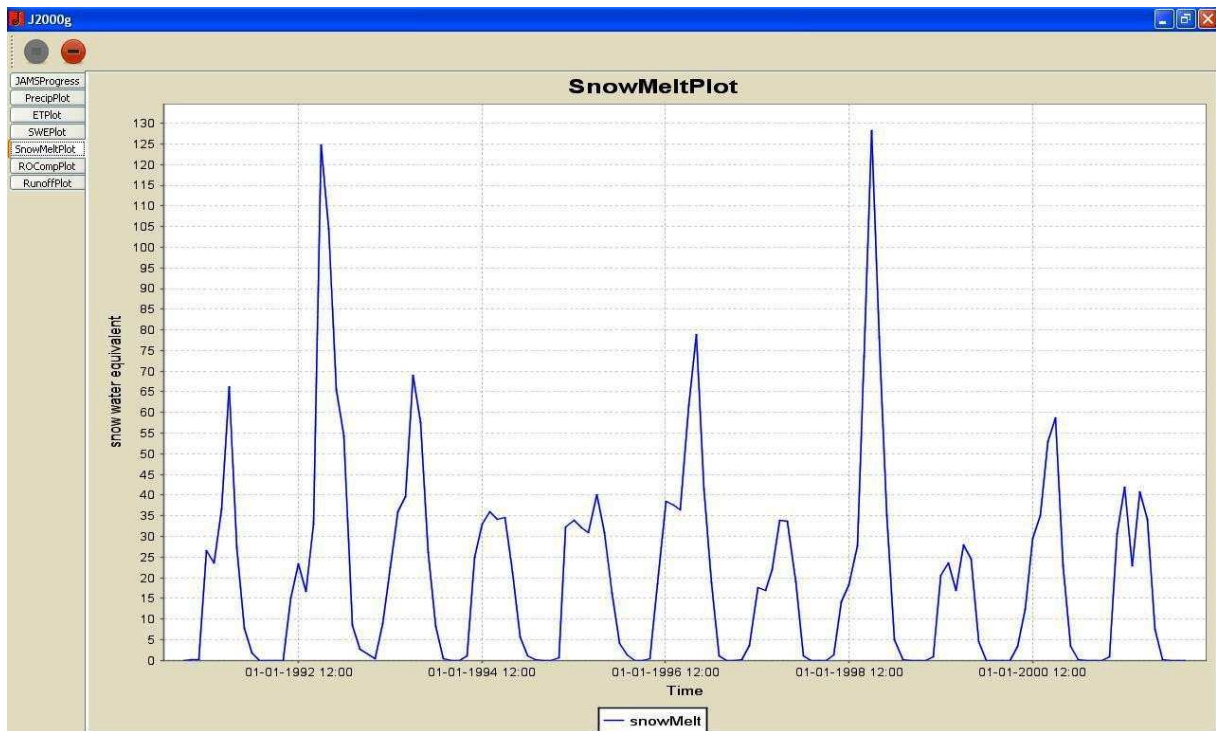

D-10: Snow Water Equivalent (SWE) simulation for Roodak subcatchment
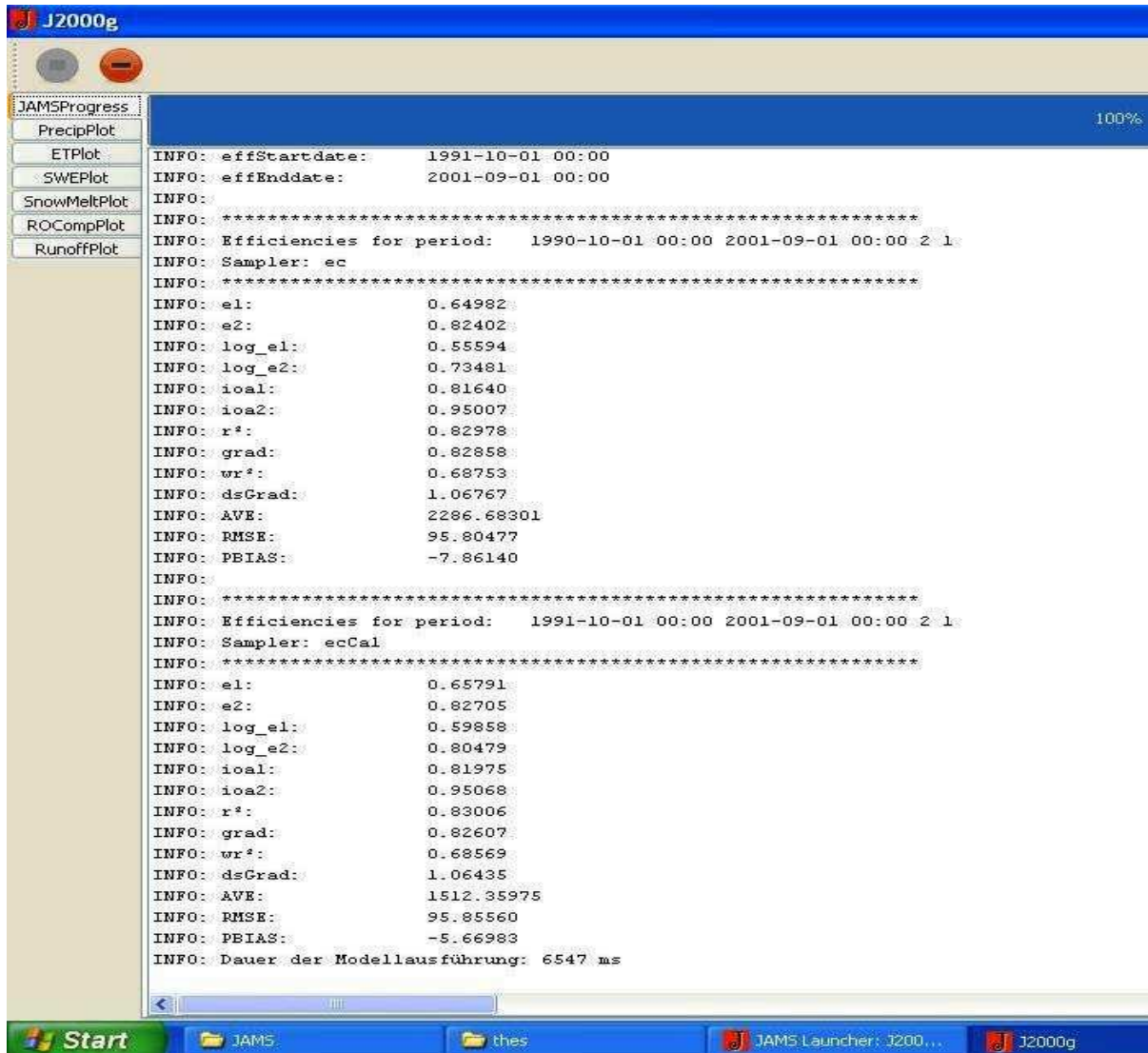
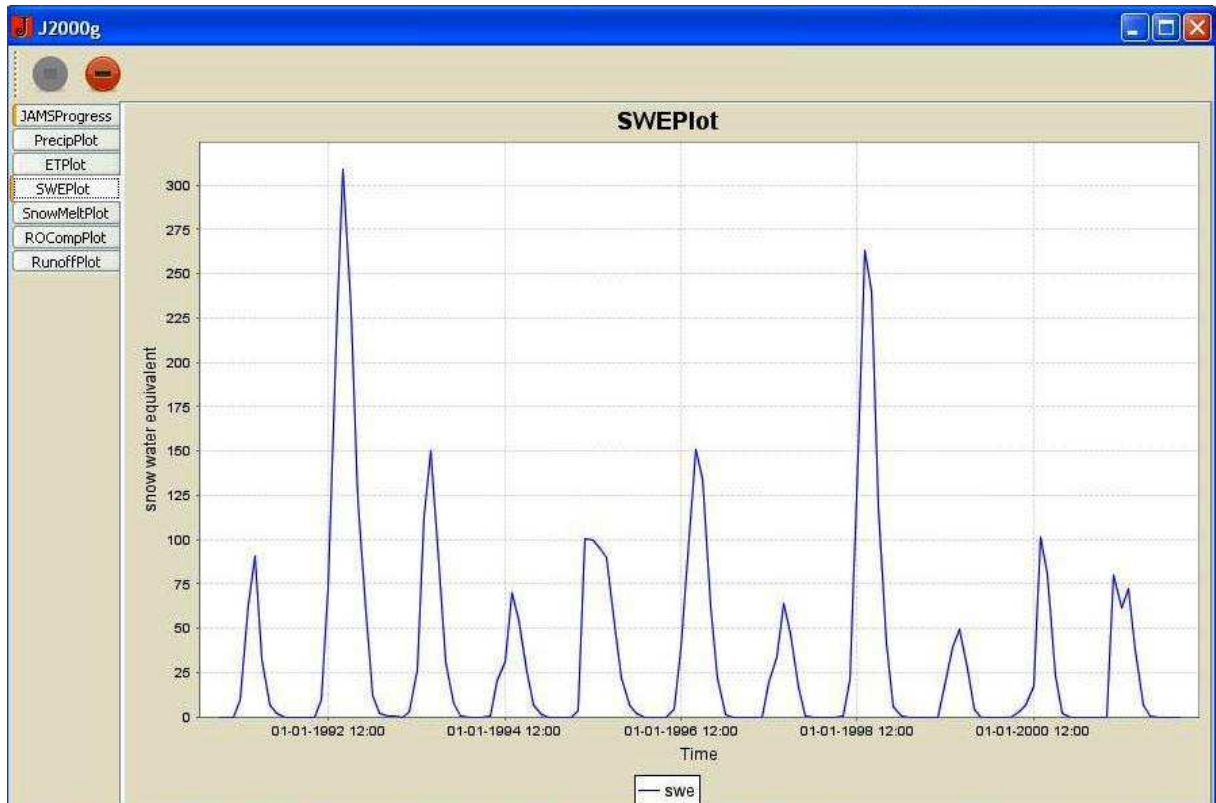D-11: Model evaluation of objective functions for Roodak subcatchment
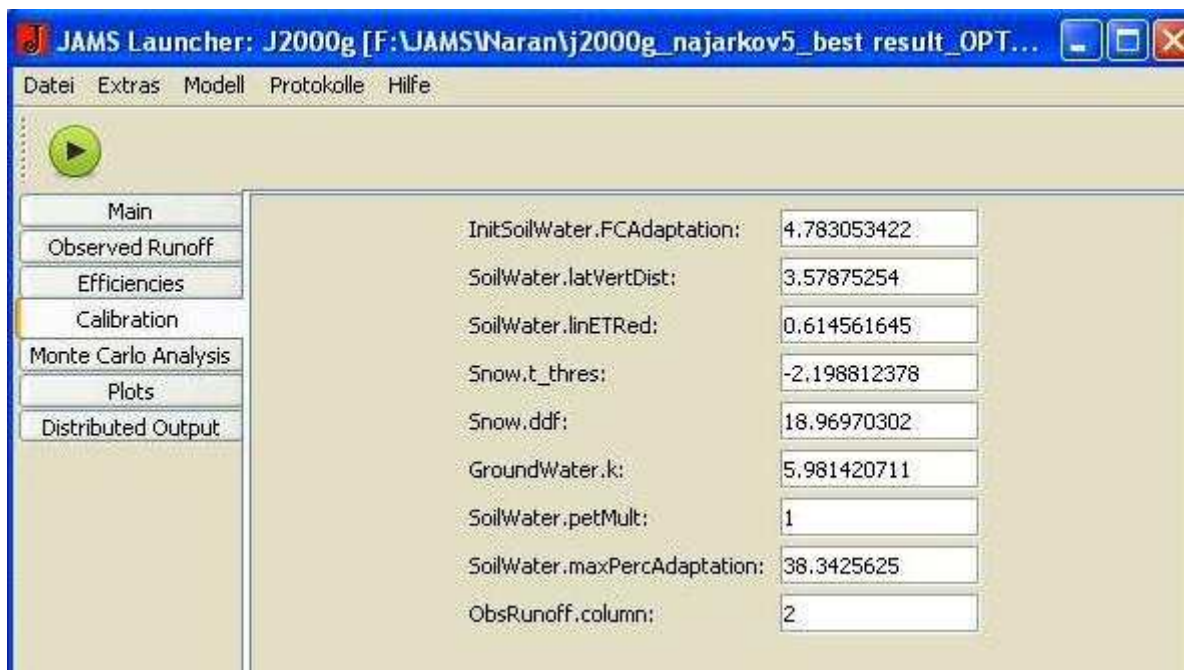
D-12: Calibration of Model Parameters for Najarkola subcatchment
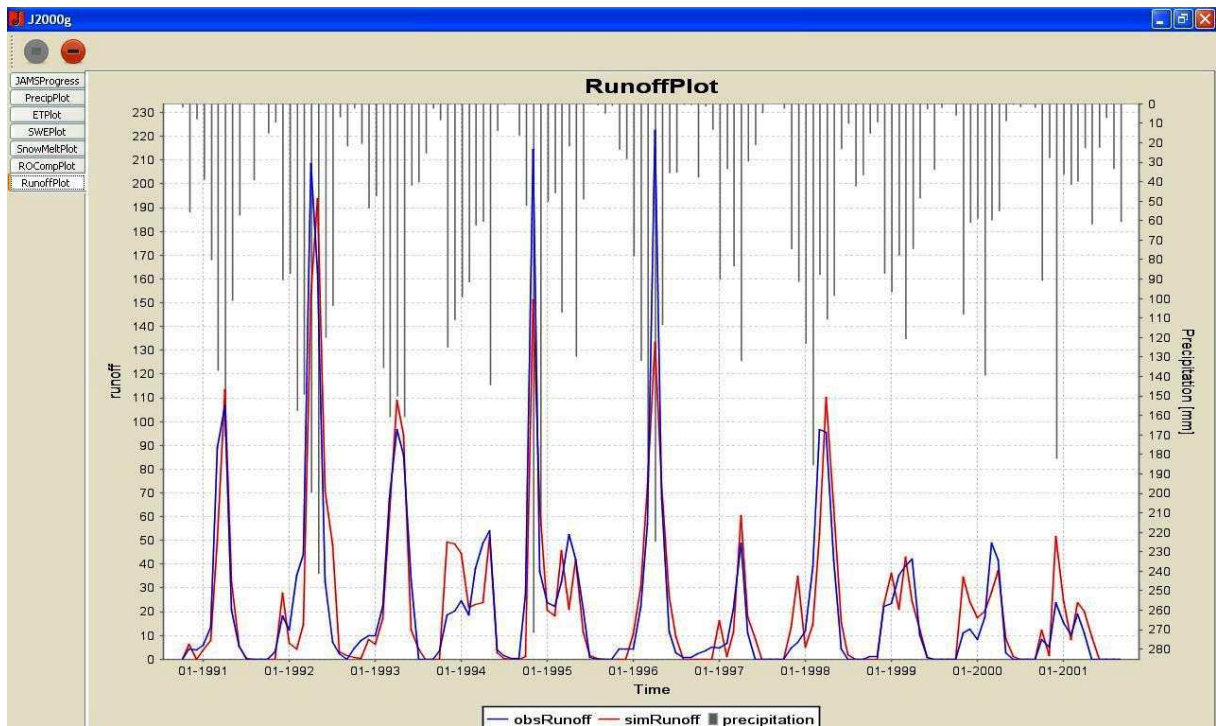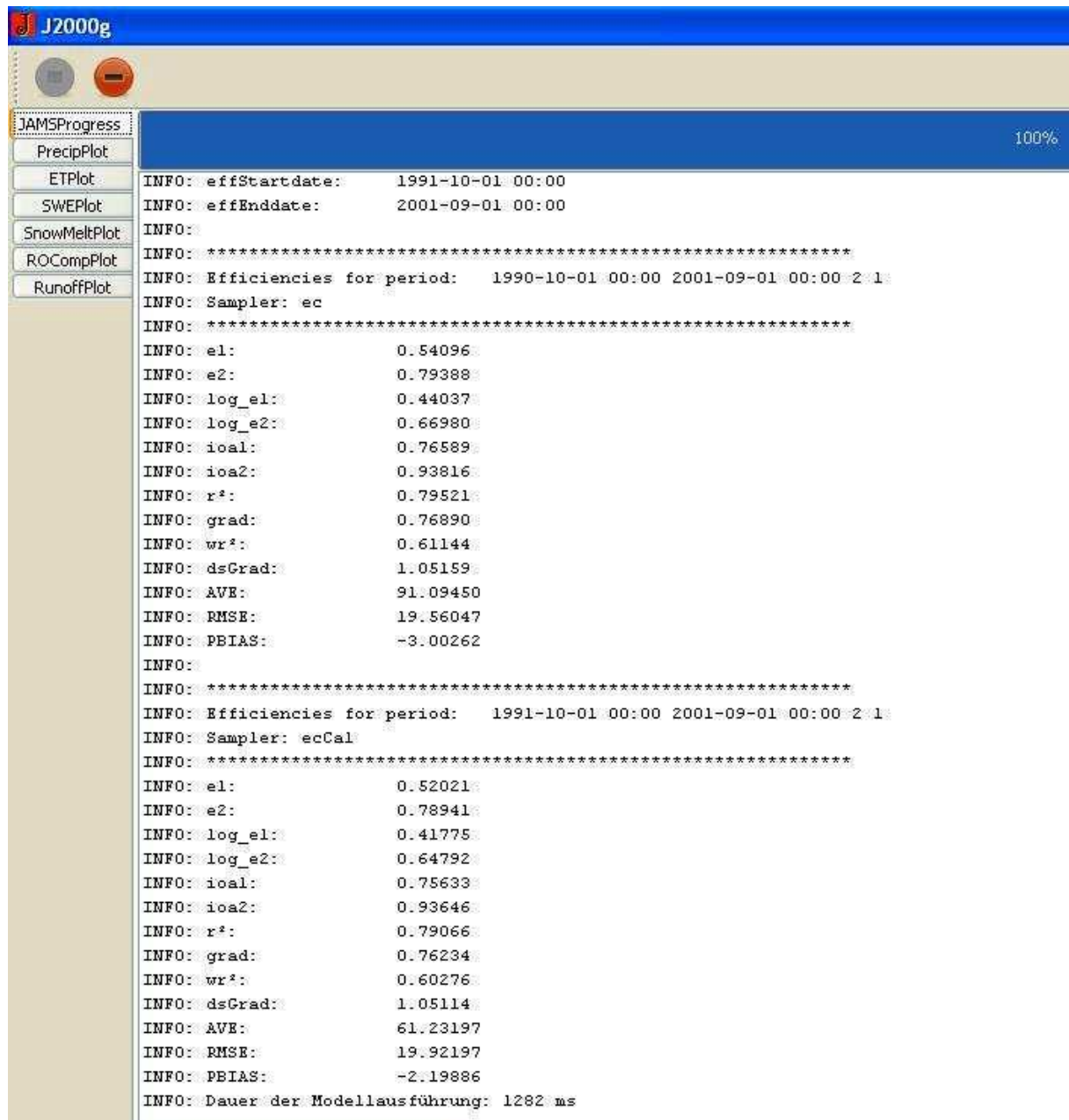
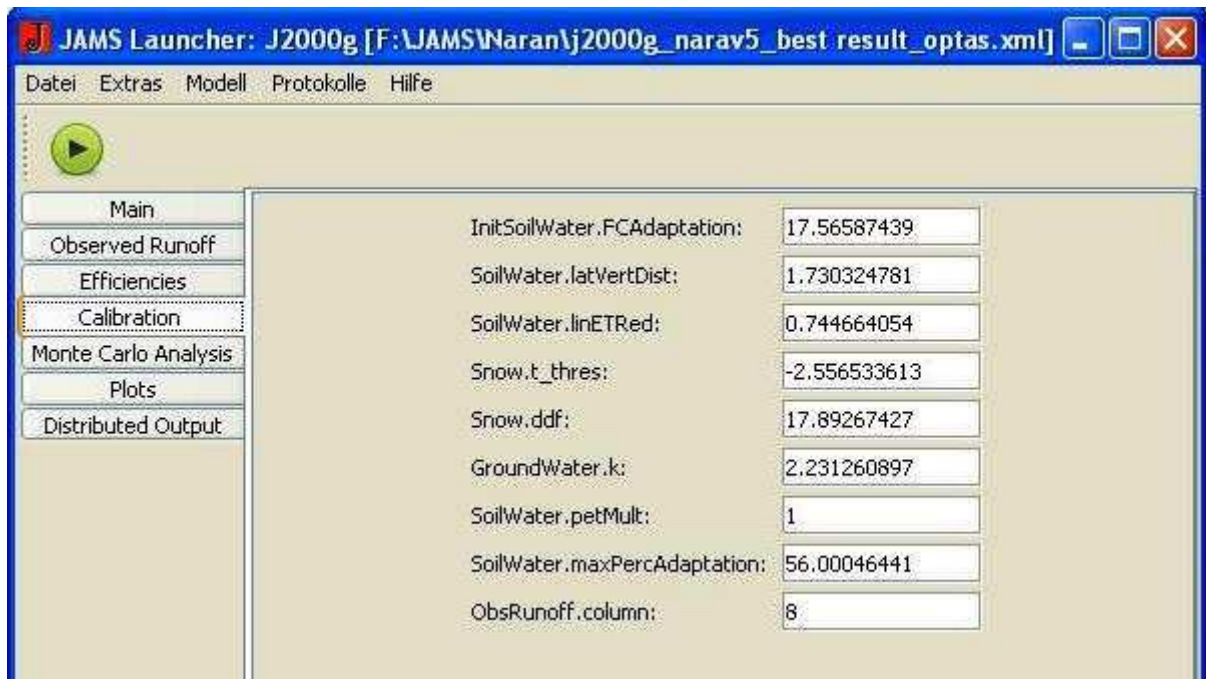D-13: Runoff Prediction of model for Najarkola subcatchment

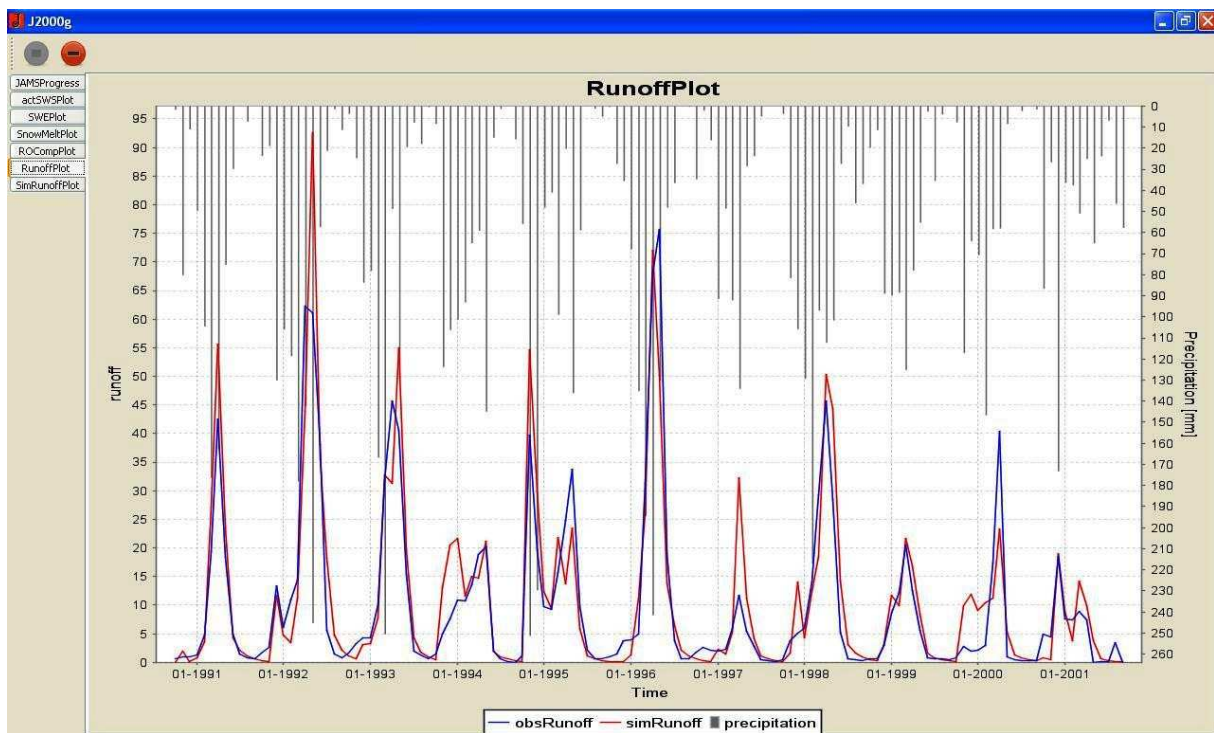D-14: Snowmelt simulation for Najarkola subcatchment

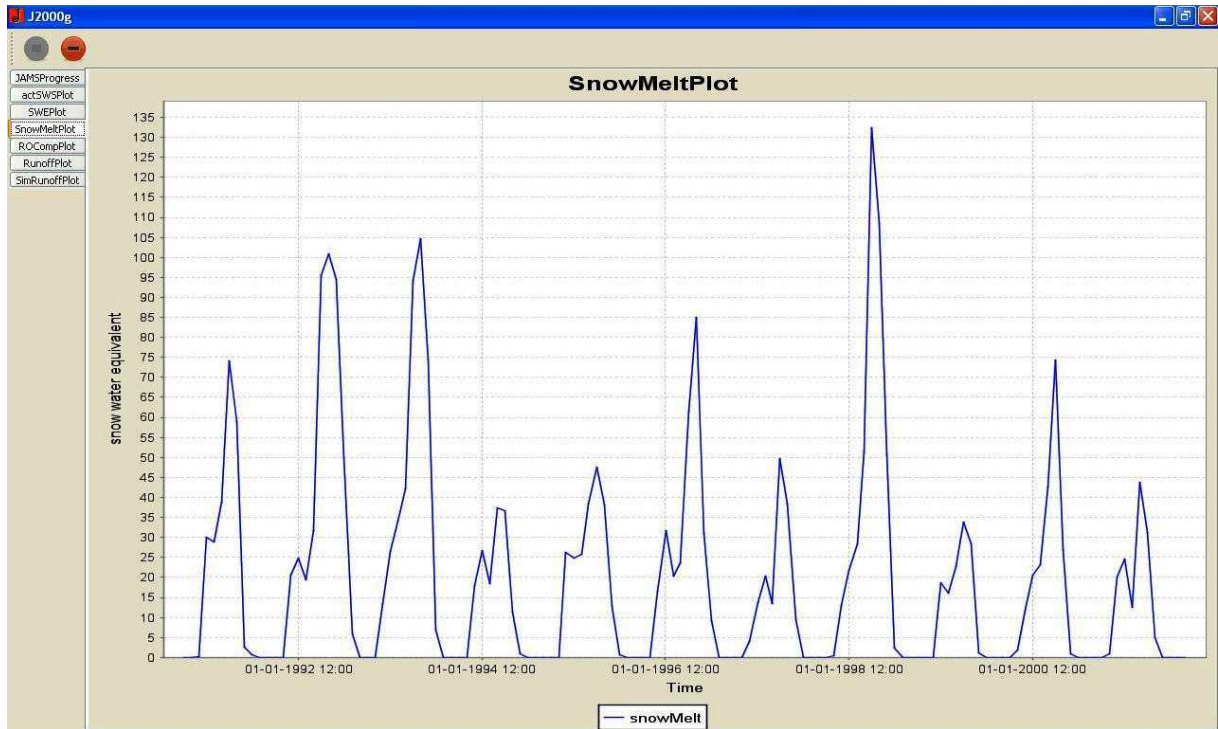D-15: Snow Water Equivalent (SWE) simulation for Najarkola subcatchment

```
J2000g

JAMSProgress
PrecipPlot
ETPlot
SWEPlot
SnowMeltPlot
ROCompPlot
RunoffPlot

                                                                              100%

INFO: effStartdate:      1991-10-01 00:00
INFO: effEnddate:        2001-09-01 00:00
INFO:
INFO: ************************************************************
INFO: Efficiencies for period:   1990-10-01 00:00 2001-09-01 00:00 2 1
INFO: Sampler: ec
INFO: ************************************************************
INFO: e1:              0.54096
INFO: e2:              0.79388
INFO: log_e1:          0.44037
INFO: log_e2:          0.66980
INFO: ioa1:            0.76589
INFO: ioa2:            0.93816
INFO: r²:              0.79521
INFO: grad:            0.76890
INFO: wr²:             0.61144
INFO: dsGrad:          1.05159
INFO: AVE:             91.09450
INFO: RMSE:            19.56047
INFO: PBIAS:           -3.00262
INFO:
INFO: ************************************************************
INFO: Efficiencies for period:   1991-10-01 00:00 2001-09-01 00:00 2 1
INFO: Sampler: ecCal
INFO: ************************************************************
INFO: e1:              0.52021
INFO: e2:              0.78941
INFO: log_e1:          0.41775
INFO: log_e2:          0.64792
INFO: ioa1:            0.75633
INFO: ioa2:            0.93646
INFO: r²:              0.79066
INFO: grad:            0.76234
INFO: wr²:             0.60276
INFO: dsGrad:          1.05114
INFO: AVE:             61.23197
INFO: RMSE:            19.92197
INFO: PBIAS:           -2.19886
INFO: Dauer der Modellausführung: 1282 ms
```

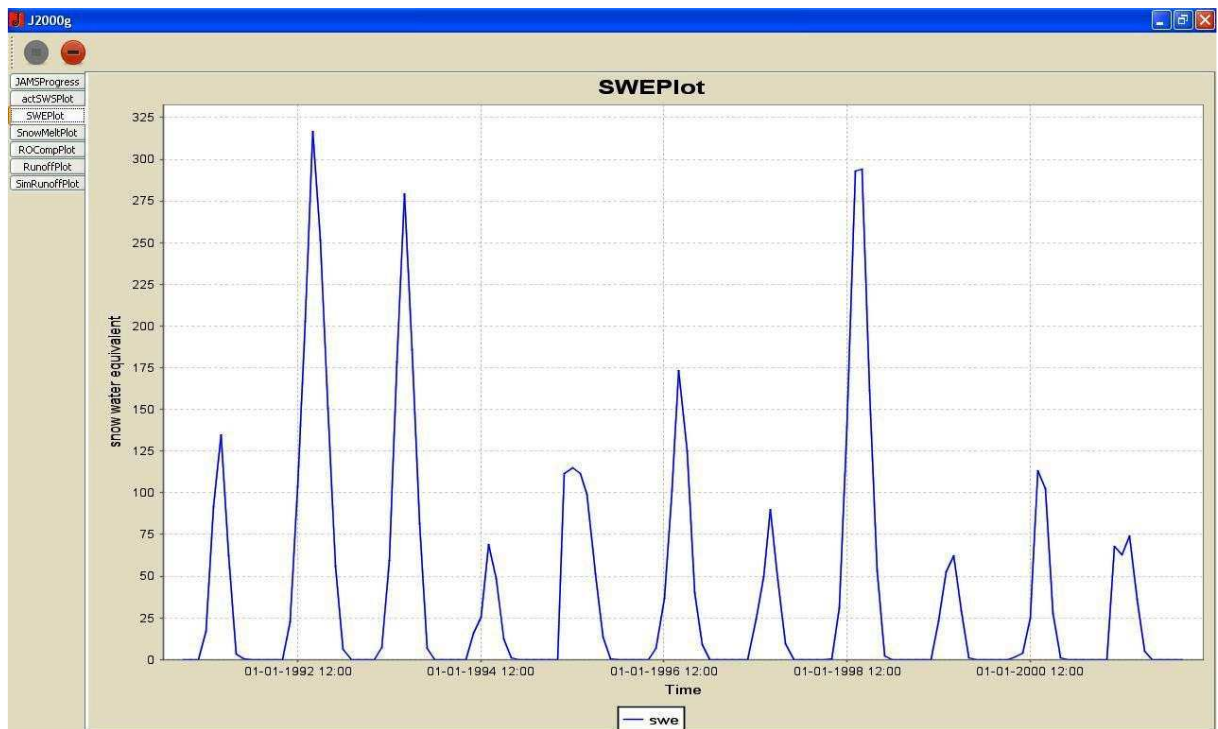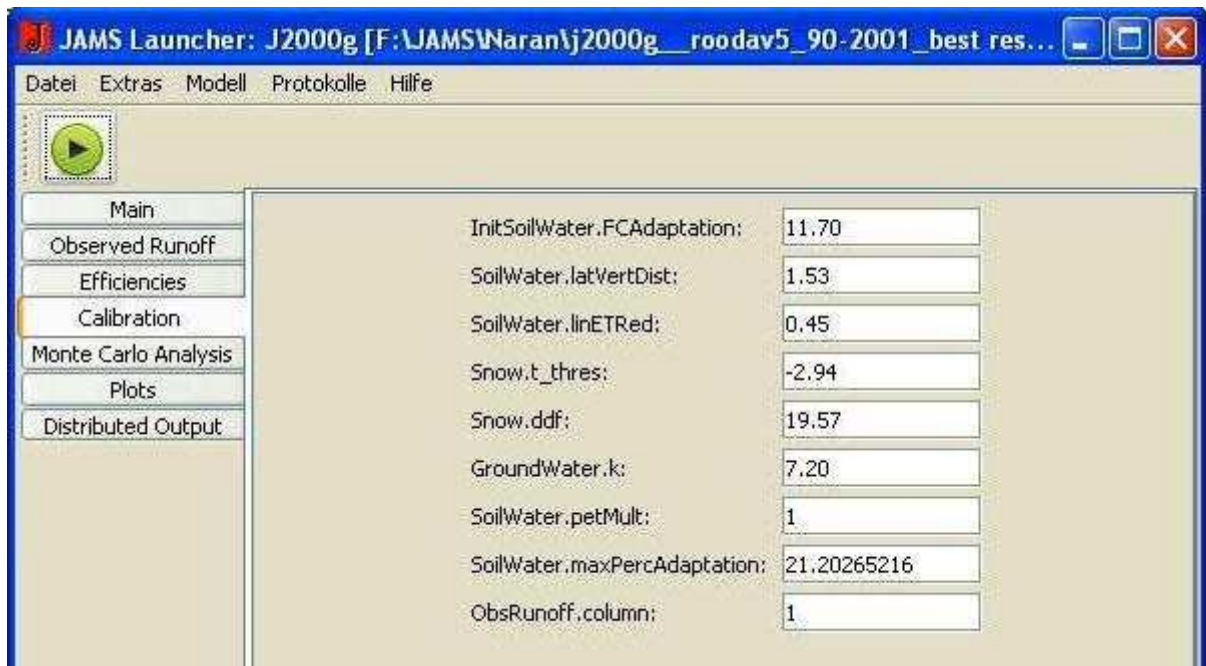D-16: Model evaluvation of objective functions for Najarkola subcatchment

D-17: Calibration of Model Parameters for Naran subcatchment

D-18: Runoff Prediction of model for Naran subcatchment

D-19: Snowmelt simulation for Naran subcatchment

D-20: Snow Water Equivalent (SWE) simulation for Naran subcatchment
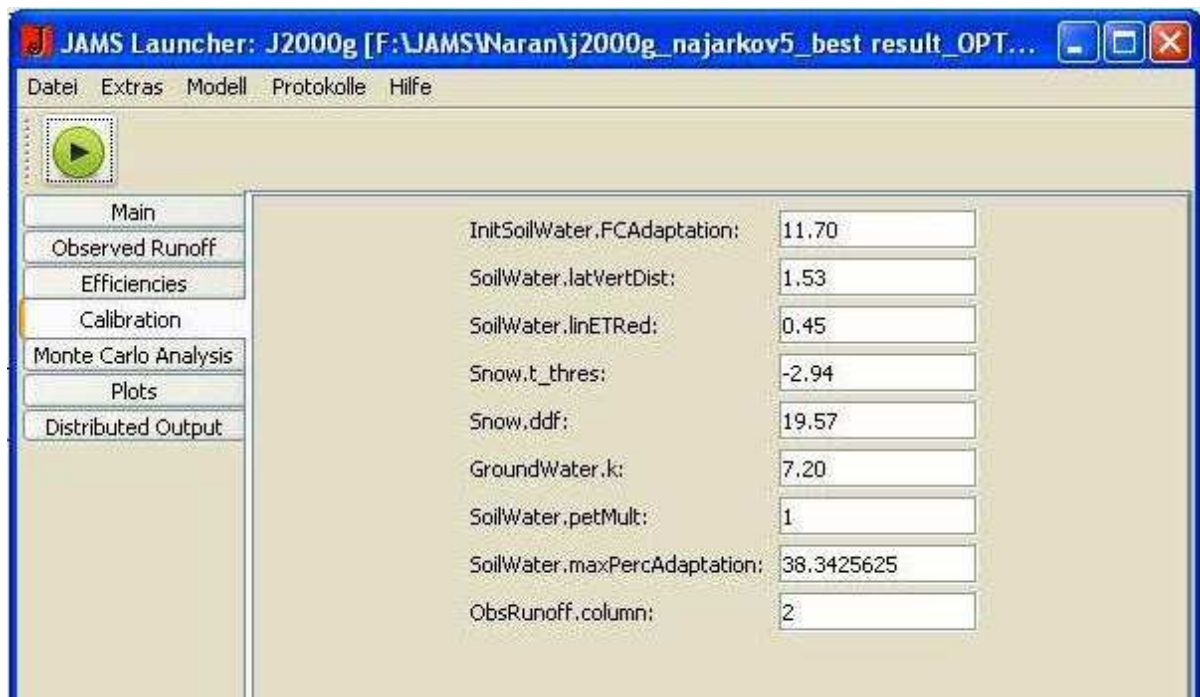
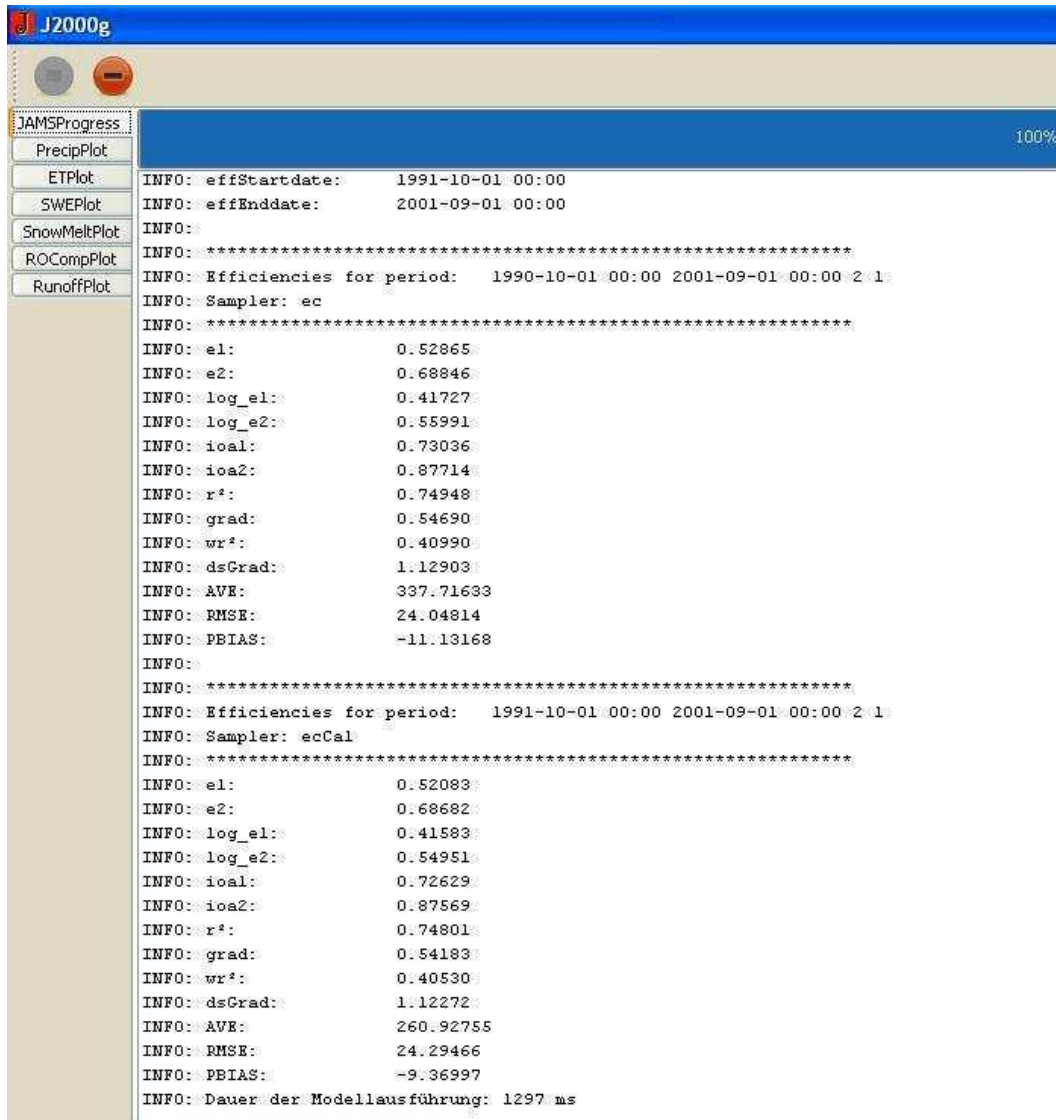D-21: Model evaluuation of objective functions for Naran subcatchment

D-22: Calibration of model with global parameter set(gps) generated using area-weighted average of parameters for Roodak
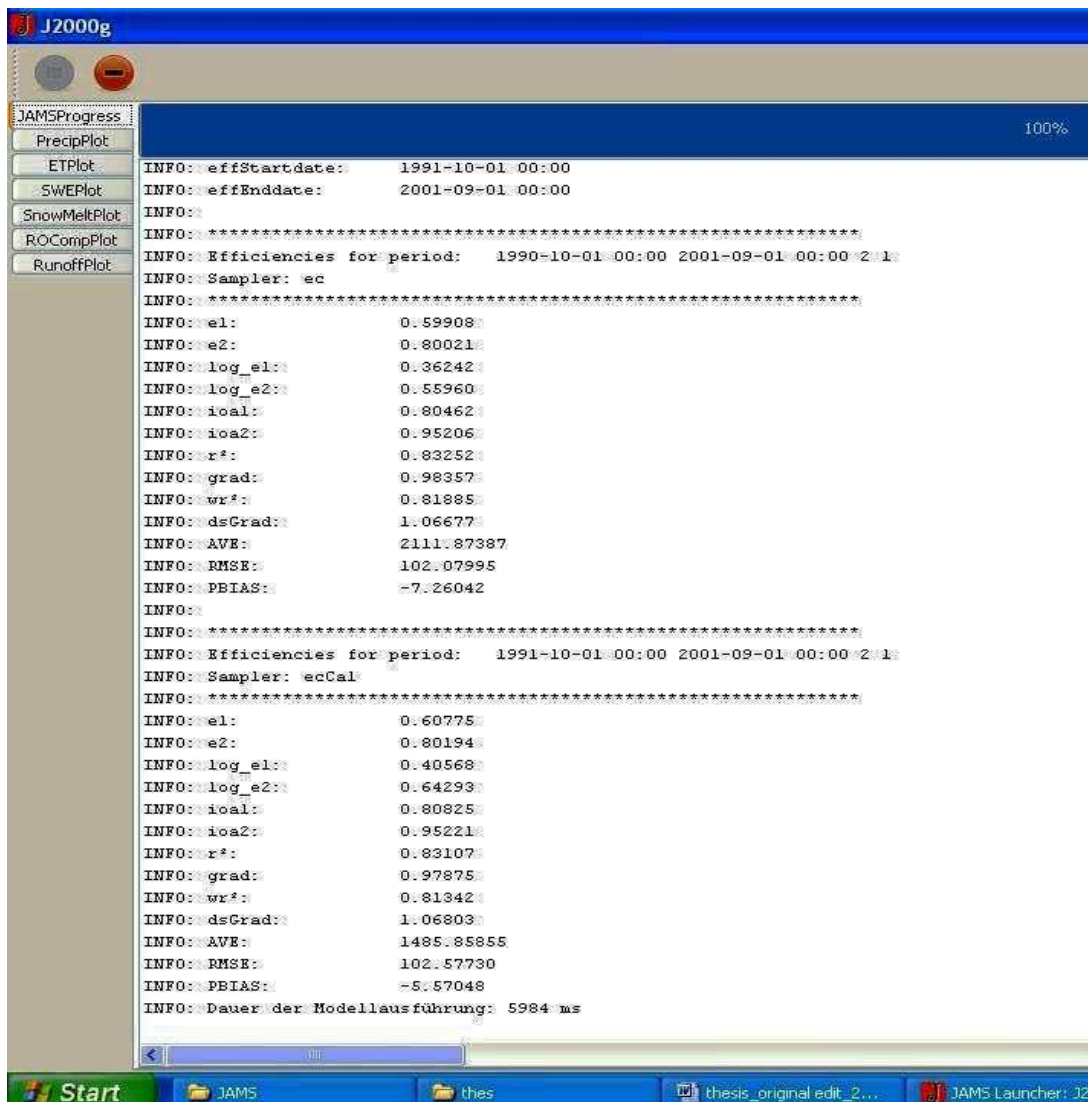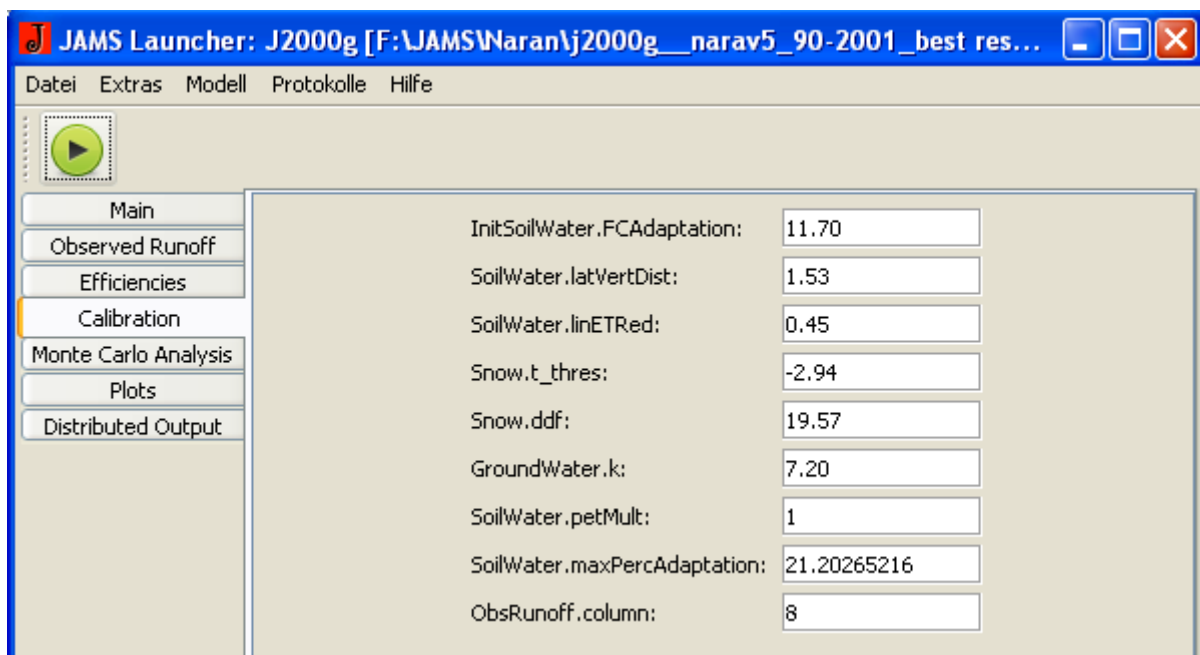
D-23: Objective function results model after calibration of model using global parameter sets (gps) for Roodak
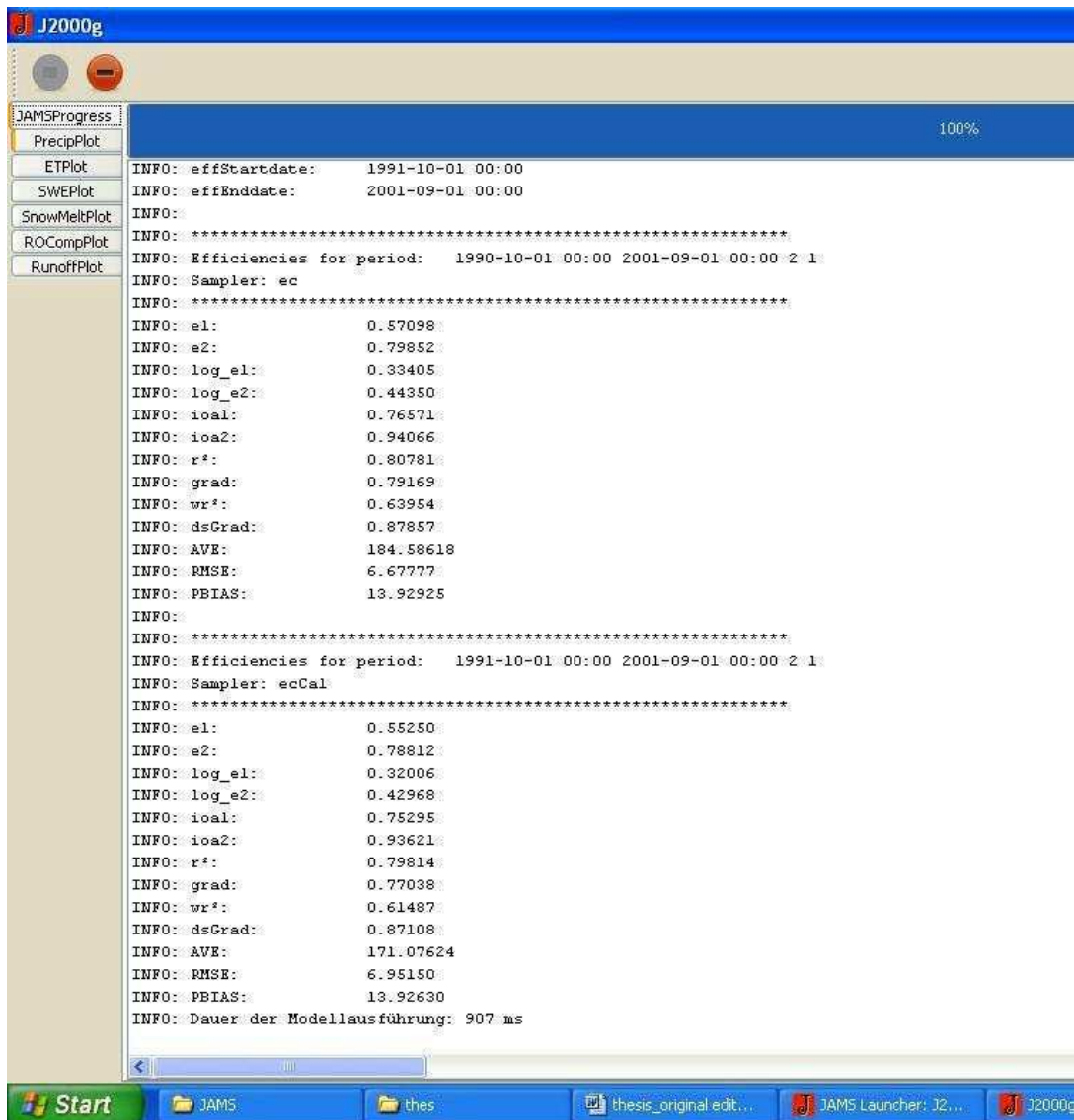

D-24: Calibration of model with global parameter set (gps) generated using area-weighted average of parameters for Najarkola

D-25: Objective function results model after calibration of model using global parameter sets (gps) for Najarkola

D-26: Calibration of model with global parameter set (gps) generated using area-weighted average of parameters for Naran


```
J2000g

JAMSProgress
PrecipPlot                                                                100%
ETPlot        INFO: effStartdate:      1991-10-01 00:00
SWEPlot       INFO: effEnddate:        2001-09-01 00:00
SnowMeltPlot  INFO:
ROCompPlot    INFO: ************************************************************
RunoffPlot    INFO: Efficiencies for period:    1990-10-01 00:00 2001-09-01 00:00 2 1
              INFO: Sampler: ec
              INFO: ************************************************************
              INFO: e1:              0.57098
              INFO: e2:              0.79852
              INFO: log_e1:          0.33405
              INFO: log_e2:          0.44350
              INFO: ioa1:            0.76571
              INFO: ioa2:            0.94066
              INFO: r²:              0.80781
              INFO: grad:            0.79169
              INFO: wr²:             0.63954
              INFO: dsGrad:          0.87857
              INFO: AVE:             184.58618
              INFO: RMSE:            6.67777
              INFO: PBIAS:           13.92925
              INFO:
              INFO: ************************************************************
              INFO: Efficiencies for period:    1991-10-01 00:00 2001-09-01 00:00 2 1
              INFO: Sampler: ecCal
              INFO: ************************************************************
              INFO: e1:              0.55250
              INFO: e2:              0.78812
              INFO: log_e1:          0.32006
              INFO: log_e2:          0.42968
              INFO: ioa1:            0.75295
              INFO: ioa2:            0.93621
              INFO: r²:              0.79814
              INFO: grad:            0.77038
              INFO: wr²:             0.61487
              INFO: dsGrad:          0.87108
              INFO: AVE:             171.07624
              INFO: RMSE:            6.95150
              INFO: PBIAS:           13.92630
              INFO: Dauer der Modellausführung: 907 ms

Start    JAMS    thes    thesis_original edit...   JAMS Launcher: J2,...   J2000g
```
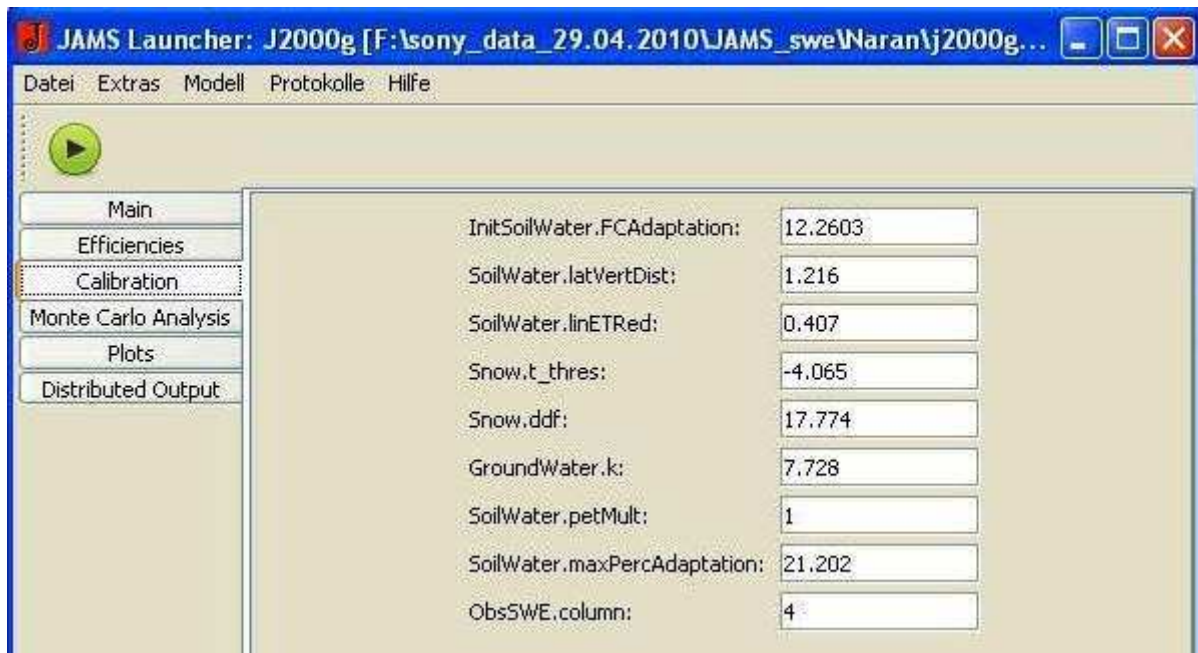
D-27: Objective function results model after calibration of model using global parameter sets (gps) for Naran
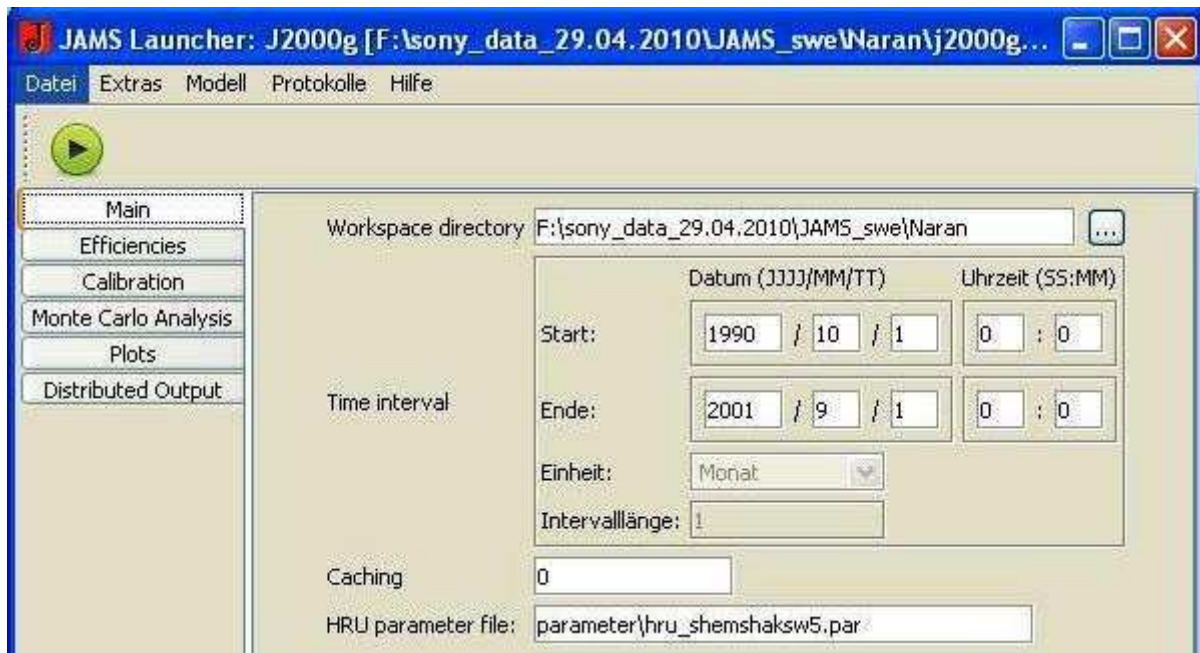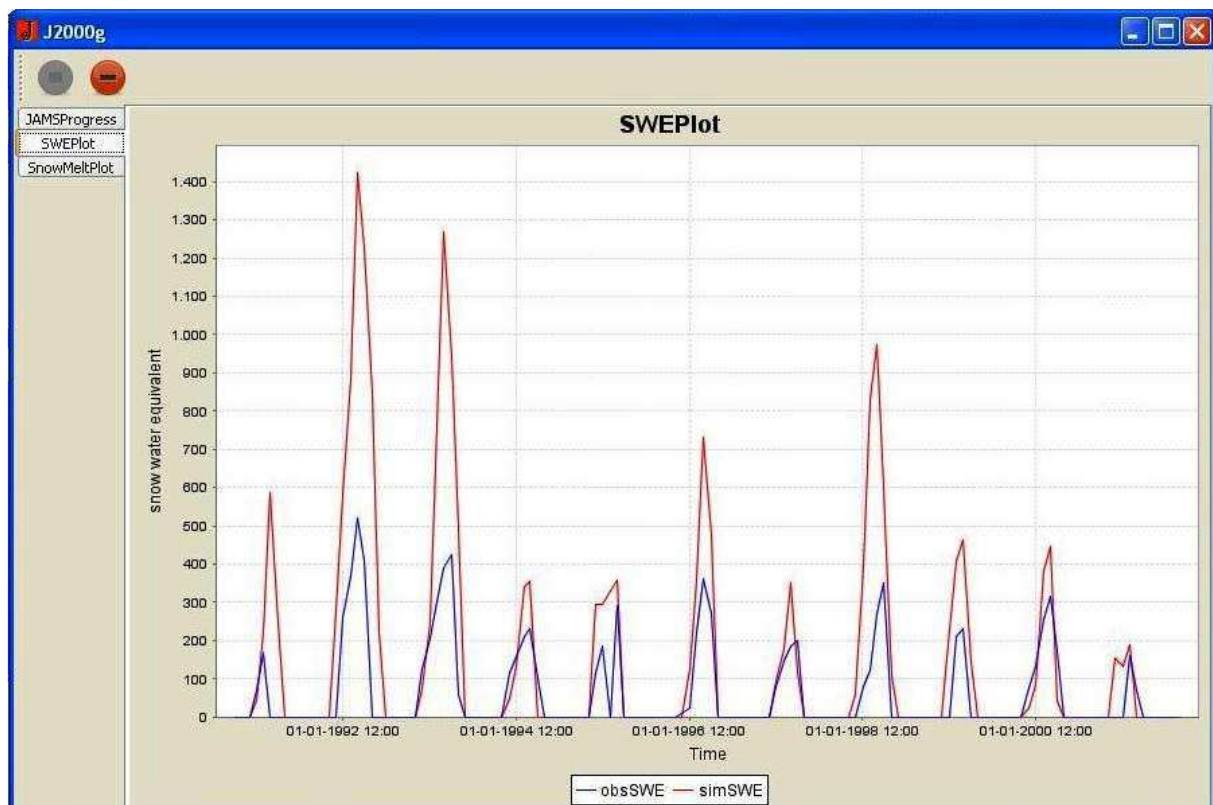
D-28: Start running the single HRU parameter model for SWE simulation in Shemshak station
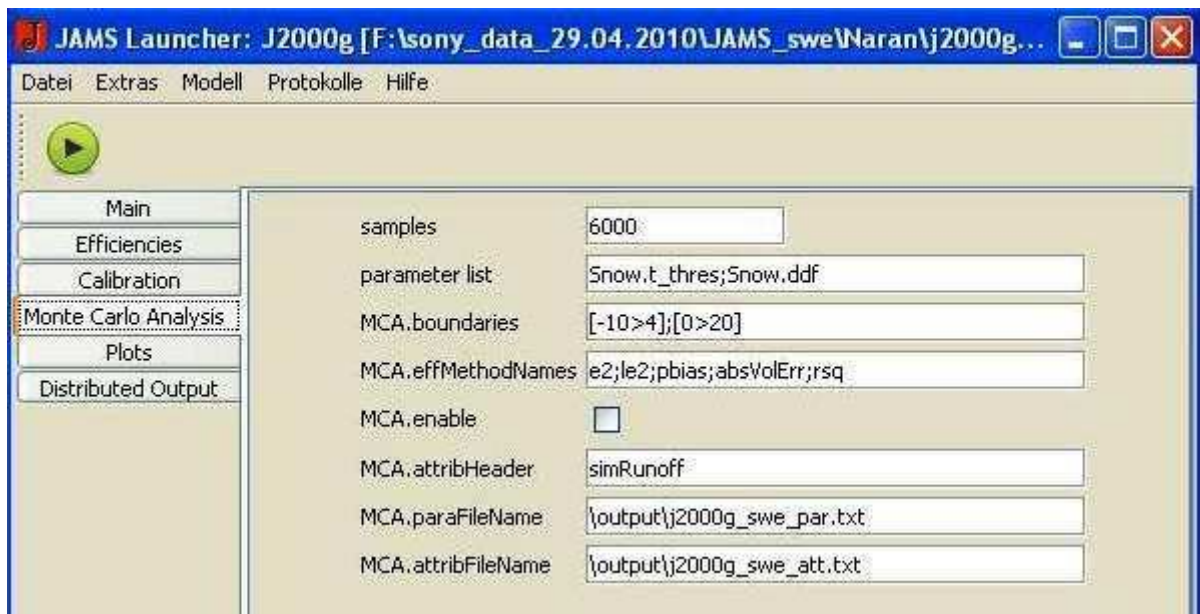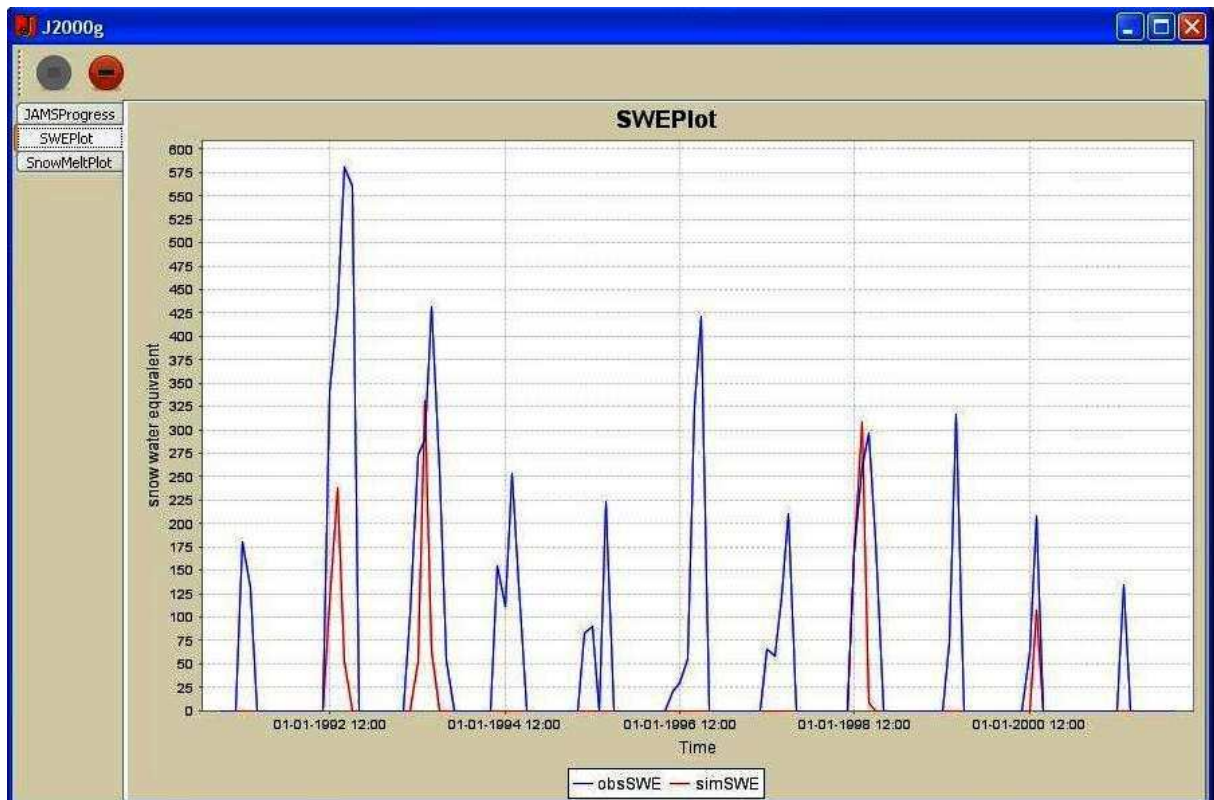

D-29: Running the model using Monte Carlo Analysis Method for generation best parameter of SWE in various snow stations in the Latyan catchment
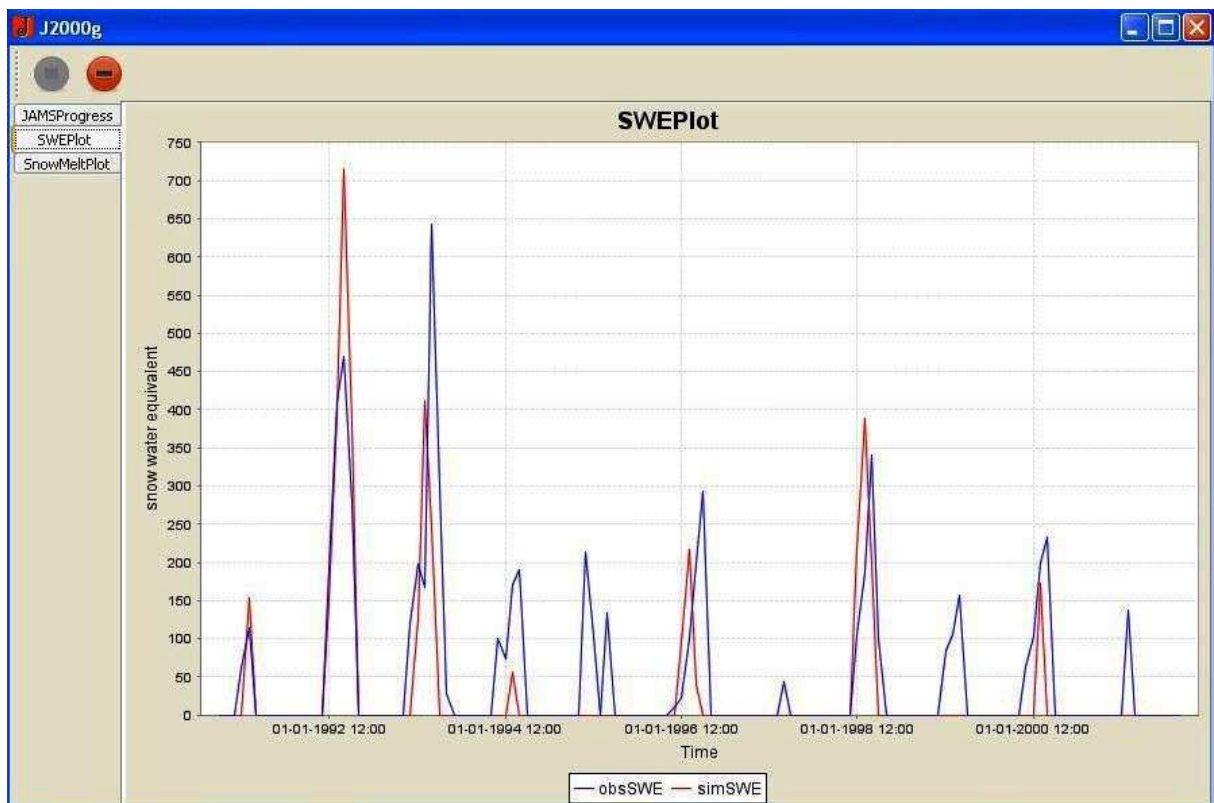
D-30: Calibration of SWE module for SWE simulation in the Shemshak snow station
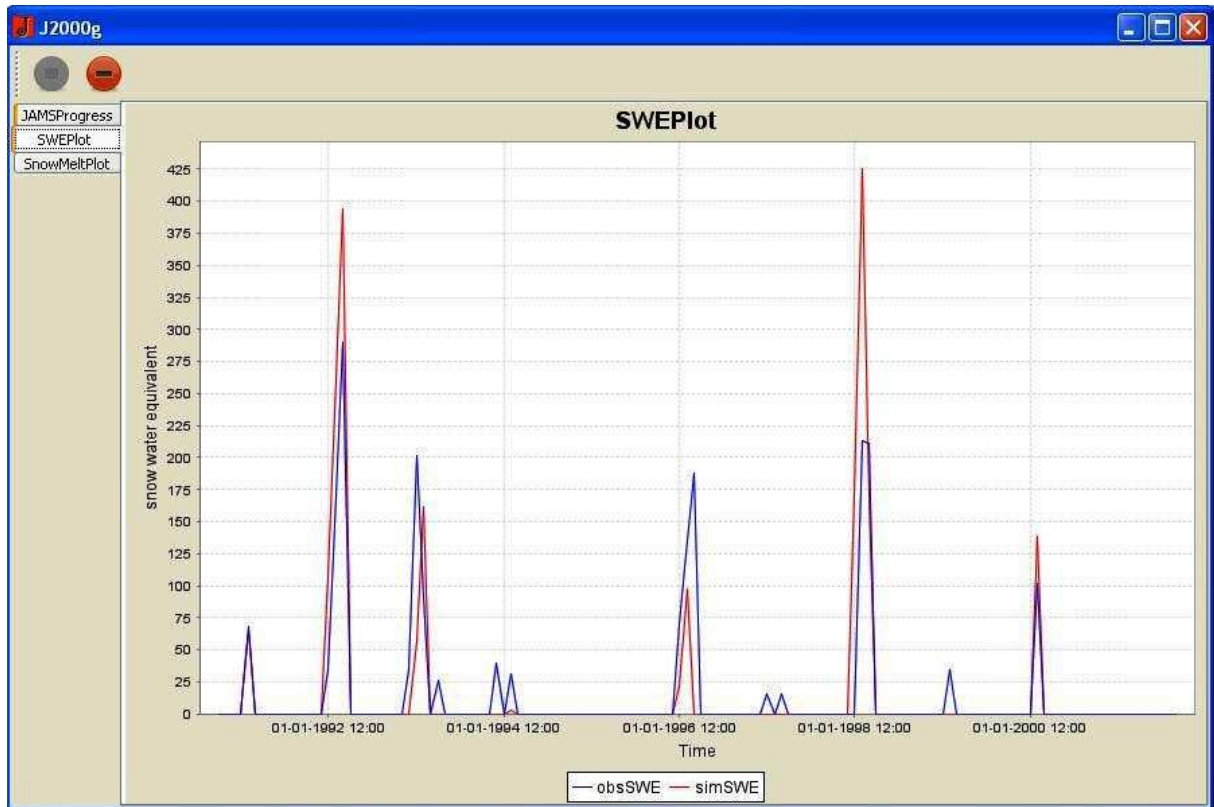

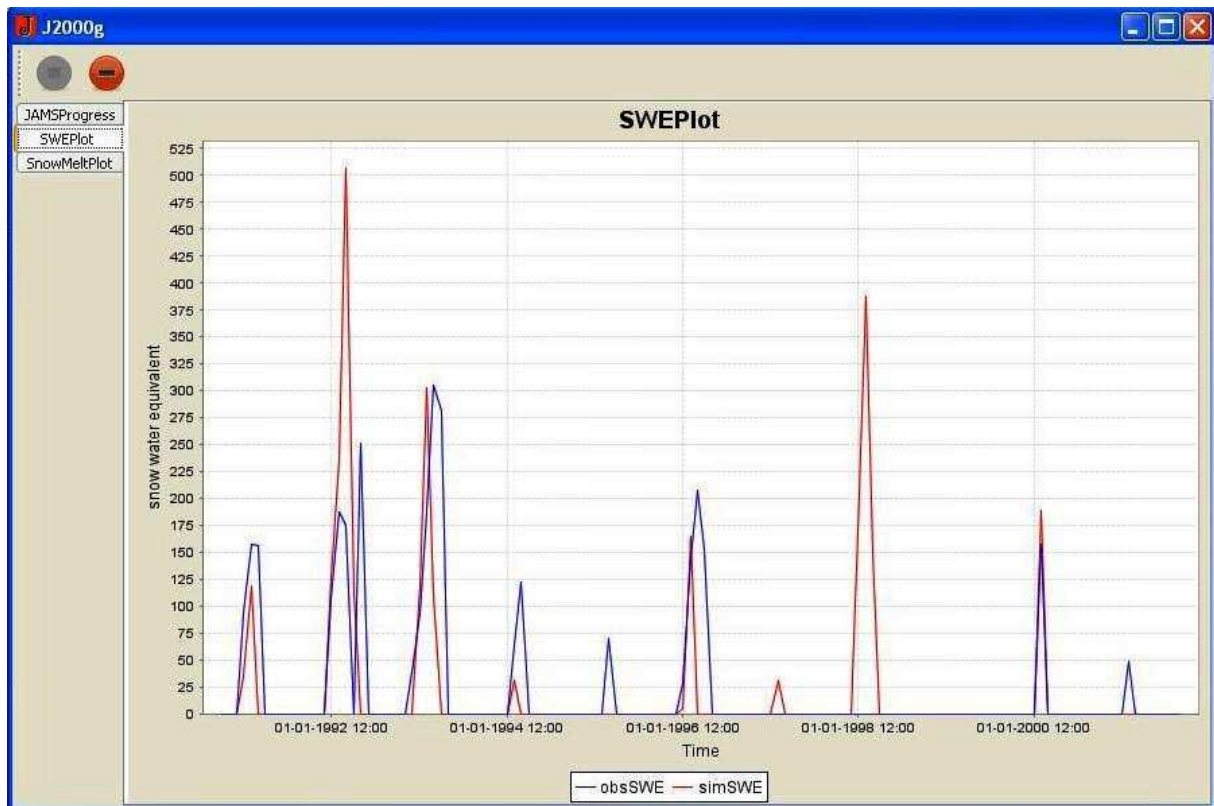D-31: SWE simulation using Single HRU in the Shemshak snow station

D-32: SWE simulation using Single HRU in the Ahar snow station

D-33: SWE simulation using Single HRU in the Garmabdar snow station

D-34: SWE simulation using Single HRU in the Konde Olya snow station

D-35: SWE simulation using Single HRU in the Lawasan snow station

Selbständigkeitserklärung

Ich erkläre, dass ich die vorliegende Arbeit selbständig und unter Verwendung der angegebenen Hilfsmittel, persönlichen Mitteilungen und Quellen angefertigt habe.

Jena, den 16.06.10   (Houshang Behrawan)